Maria Sofia Castro Henriques de Castro Fraga

Mestre em Engenharia Química e Bioquímica

CHARACTERISATION OF TRANSIENT TRANSPORT IN DENSE MEMBRANES USING ON-LINE MASS SPECTROMETRY

Dissertação para obtenção do Grau de Doutor em Engenharia Química e Bioquímica – Especialidade em Engenharia Química

Orientadora: Doutora Carla Maria Carvalho Gil Brazinha de Barros Ferreira
Investigadora de Pós-Dourotamento
FCT-UNL
Co-orientador: João Paulo Serejo Goulão Crespo
Professor Catedrático
FCT-UNL

Júri:

Presidente: Prof. Doutora Maria da Ascensão Carvalho Fernandes Miranda Reis
Arguentes: Prof. Doutor Adélio Miguel Magalhães Mendes
Prof. Doutor Thomas Schäffer

Vogais: Prof. Doutora Isabel Maria Rôla Coelhoso
Doutora Carla Maria Carvalho Gil Brazinha de Barros Ferreira

FACULDADE DE CIÊNCIAS E TECNOLOGIA
UNIVERSIDADE NOVA DE LISBOA

Janeiro, 2018

Characterisation of Transient Transport In Dense Membranes Using On-line Mass Spectrometry

ACKNOWLEDGEMENTS

Ao finalizar esta etapa tão importante na minha vida queria, antes de mais, agradecer aos meus orientadores, a Dra Carla Brazinha e o Professor Doutor João Paulo Crespo, não só por me terem proposto o presente trabalho de inegável interesse científico, como também por tudo o que fizeram para que o conseguisse levar a bom termo. Agradeço o interesse que sempre demonstraram no meu trabalho, como também pelas oportunidades que me foram dadas através da participação em colaborações científicas nacionais e internacionais que, foram, sem dúvida, uma mais-valia para a minha vida profissional e pessoal.

À Carla queria agradecer, de forma especial, por todo o apoio e acompanhamento, não só científico como também humano, ao longo destes anos permitindo-me ultrapassar todas as dificuldades. Gostava de agradecer também toda a disponibilidade, a exigência e rigor assim como a amizade sempre demonstrada. Ao Professor João agradeço a competência, a criatividade científica, clareza de raciocínio e todo o apoio dado para que, apesar das dificuldades, não caísse em desânimo, fazendo de tudo para que o trabalho fosse sempre do meu agrado. Obrigada por, através do exemplo de perfeccionismo, me ensinar a querer fazer sempre mais e melhor. Aos meus dois orientadores um grande grande obrigada!

À D. Maria José e à D. Palminha, muito obrigada por me receberem sempre com um sorriso e por tratarem de toda a parte administrativa.

Ao Professor Luis Trabucho, muito obrigada por todos os ensinamentos matemáticos e pela colaboração na elaboração de um artigo científico no qual, através dos conhecimentos em matemática, foi possível a elaboração de um modelo matemático de elevado interesse científico. Obrigada por toda a simpatia e por nos receber sempre tão bem.

À Anna Kujawska e ao Professor Wojciech Kujawski gostaria de agradecer a colaboração no estudo de membranas de PDMS, através do qual foi possível, não só um maior conhecimento deste tipo de membranas, como também a publicação de um artigo científico.

Ao Dr. John Jansen, muito obrigada pela possibilidade de ampliar os conhecimentos em relação ao *time-lag*, por todo o perfeccionismo e exigência que nos fizeram publicar um artigo de enorme interesse científico e rigor. Agradeço também por me ter recebido no seu grupo no ITM, e por toda a hospitalidade durante os dias que lá passei.

Muito obrigada à minha grupeta do almoço: a Joana, Rita, Mafalda Cadima, Mafalda Lopes e Jorge, com os quais partilhei muito bons momentos, muitas alegrias, muitas gargalhadas mas também algumas preocupações. Obrigada por terem sido sempre tão bons amigos, já tenho muitas saudades dos nossos almoços, espero que não acabem!

Muito obrigada aos restantes colegas do grupo em especial, a Carla Martins, Usman, Rita Ferreira, Claudia Galinha por toda a disponibilidade sempre demonstrada para me ajudar, por partilharem comigo conhecimentos e por toda a boa disposição

Agradeço também à Fundação para a Ciência e Tecnologia a concessão da minha bolsa (SFRH/BD/81814/2011) que me permitiu desenvolver o meu trabalho.

Um enorme e especial obrigada à minha irmã Carmo e á minha amiga Inês, por este caminho que percorremos juntas, por terem servido de suporte nas alturas em que era preciso e por terem estado sempre presentes em todas as etapas, não só do doutoramento, como também da minha vida.

Muito obrigada à minha família, pais irmãos, tios e avó, pelo interesse que sempre demonstraram no meu trabalho, pela motivação que me deram e por estarem sempre presentes na minha vida. À minha mãe um obrigada especial por todo o suporte, principalmente pelas vezes que ficou com os meus filhos para que eu pudesse investir no meu doutoramento, muito obrigada!

Por último, mas não menos importante, muito obrigada ao meu marido Nuno por me ter apoiado nesta decisão de fazer um doutoramento, e em tudo o que isso implica. Por me ajudar a rir e a descomplicar as coisas quando parece que não há solução, muito obrigada! Aos meus queridos filhos Francisco e Rosarinho queria agradecer terem servido de motivação para fazer sempre mais e melhor, por me ajudarem a desenvolver a capacidade de ser organizada de forma a fazer a melhor gestão possível do tempo entre o trabalho e vida familiar. Obrigada também pela compreensão, nesta fase final na qual tenho que conciliar um novo trabalho com a escrita. Apesar de, efetivamente, ter menos tempo para os meus filhos, nunca deixaram de sorrir e de vir dar-me beijinhos e abraços enquanto escrevo. É, de facto, maravilhoso e o melhor que se pode ter! Muito muito obrigada!

ABSTRACT

The work presented in this thesis aims at developing a new method for characterising the multi-component solute transport through dense membranes, both in the transient and in the steady state of gas separation and pervaporation systems, using a Mass Spectrometer (MS) as an on-line, real-time, monitoring tool.

The study of the transient period of mass transport through a membrane, although more complex than the steady-state period, has attracted the attention of researchers because it may offer a route for a better understanding of the membrane material under study and how it interacts with the permeating species. In fact, noticeable structural membrane adjustments may occur during the transient period, from when the solute starts permeating, impacting directly on the membrane intrinsic transport properties in a structure-transport relationship. The greater the affinity of the solute to the membrane, the greater the modification it may cause in the membrane matrix and, consequently, the greater the impact on the transport properties. Therefore, estimation of diffusion coefficients during the time-course of the whole permeation process is critical.

The goal of the work developed in this PhD thesis was to study the transport properties of different multi-component feed streams through different polymeric membrane materials and different permeation systems. This work includes a study ranging from “non-interacting” solutes, such as inert gases, to more complex systems where the solutes have strong affinity to the permeated material, such aroma compounds or water vapour. The transient behaviour of the selected membranes was followed when exposed to penetrating solvents and solutes through the on-line monitoring of the permeating species using mass spectrometry, which offers the possibility to acquire one data point per second.

The transport properties (sorption and diffusion coefficients) were assessed for mixed gas permeation systems through the development of a novel time lag measurement, where both parameters can be determined in a single step. In this system, solute-membrane interactions are not relevant and a constant diffusion coefficient can be considered during the whole permeation process, because the membrane structure is not significantly altered when in contact with these gases.

Otherwise, several phenomena may occur inside the membrane in non-ideal processes, leading to a change of the diffusivity of the permeant with its own local concentration and, consequently, the change of its diffusivity with time. From the on-line MS monitoring tool, a method for calculating time-dependent diffusion coefficients in non-ideal systems was developed, both for gas separation, humidified gas streams, and pervaporation systems, where the solute presented affinity to the membrane. Time-dependent diffusion coefficients of permeating solutes through different membranes were calculated, considering that the membrane structure is potentially modified, due to solute-membrane interactions. During solute transport in the transient period,

permeating solutes with high affinity to the membrane may extensively solubilise within the membrane structure, causing membrane rearrangements. As a consequence, longer transient periods may be observed. Finally, based on the information acquired by mass spectrometry, namely the estimation of time-dependent diffusion coefficients, a mathematical model was developed in order to obtain solute concentration profiles inside the membrane and their evolvement along time. Two case-studies were selected, corresponding to different systems, using permeating solutes with different affinities towards the membranes under study. The transport properties of two different membrane materials were compared: a polymeric membrane, which may be prone to potential material rearrangements and a ceramic membrane with a rigid structure, where material rearrangements are not anticipated.

RESUMO

O trabalho apresentado nesta tese tem como objetivo desenvolver um novo método para caracterizar o transporte de soluto, constituído por múltiplos componentes, através de membranas densas, quer no estado transiente como no estado estacionário, para sistemas de separação de gases e pervaporação, usando um Espectrómetro de Massa (MS) como ferramenta de monitorização do permeado, on-line e em tempo real.

O estudo do transporte de massa no estado transiente através de uma membrana, embora mais complexo do que no estado estacionário, tem sido alvo de estudo por muitos investigadores uma vez que pode não só ser uma via para uma melhor compreensão do material da membrana em estudo, como também para uma melhor compreensão de como esta interage com as espécies que permeiam através dela. De facto, é durante o estado transiente que podem ocorrer ajustes a nível estrutural da membrana, desde o momento em que o soluto começa a permear, com impacto diretamente nas propriedades de transporte intrínsecas da membrana, numa relação de estrutura-transporte. Quanto maior é a afinidade do soluto para a membrana, maior a modificação que este pode causar na sua matriz e, consequentemente, maior é o impacto sobre as propriedades de transporte. A estimativa do coeficiente de difusão durante todo o processo de permeação é, desta forma, preponderante.

O objetivo do trabalho desenvolvido nesta tese de doutoramento foi o de estudar as propriedades de transporte de diferentes fluxos de alimentação multi-componentes através de diferentes membranas poliméricas em diferentes sistemas de permeação. Neste contexto, no presente trabalho foram estudados sistemas em que o soluto apresenta baixa interação com a membrana, como gases inertes, até sistemas mais complexos onde o soluto tem uma grande afinidade com o material da membrana, tal como compostos aromáticos ou vapor de água. O comportamento do estado transiente das membranas em estudo foi acompanhado on-line, desde o momento em que estas foram postas em contato com solventes e solutos, através da monitorização das espécies permeantes. Desta forma, o acompanhamento do estado transiente foi realizado usando a técnica de espectrometría de massa, uma vez que esta oferece a possibilidade de aquisição de um ponto por segundo.

As propriedades de transporte (sorção e coeficiente de difusão) foram avaliadas para sistemas de permeação de misturas gasosas, através do desenvolvimento de uma modificação do método *time-lag*, através do qual os dois parâmetros podem ser determinados numa única etapa. Neste sistema, as interações membrana-soluto não são muito acentuadas, e uma vez que a membrana não é significativamente modificada em contato com os gases, o coeficiente de difusão pode ser considerado constante para todo o regime transiente .

Por outro lado, em sistemas considerados não ideais, vários fenómenos podem ocorrer no interior da membrana, levando a uma mudança na difusão do permeante com a sua

concentração local e, consequentemente, uma mudança na difusão ao longo do tempo. Neste contexto, através do sistema de monitorização com o MS; foi desenvolvido um método para o cálculo do coeficiente de difusão em função do tempo para sistemas não ideais, nos quais o soluto apresenta muita afinidade para a membrana. Assim, uma vez que a membrana é potencialmente modificada devido às interações membrana-soluto existentes, foram calculados os coeficientes de difusão em função do tempo dos permeantes através das diferentes membranas. Durante o transporte do soluto no estado transiente, os compostos com alta afinidade para a membrana podem solubilizar-se extensivamente dentro da matriz polimérica, causando, assim, rearranjos na membrana. Como consequência, podem ser observados periodos transientes mais longos, demorando mais tempo a atingir o estado estacionário. Por último, baseado na informação adquirida através do MS, nomeadamente a estimativa dos coeficientes de difusão em função do tempo, foi desenvolvido um modelo matemático com o objetivo de obter perfis de concentração do soluto ao longo do tempo no interior da membrana. Foram, desta forma, selecionados dois estudos de caso, correspondentes a dois diferentes sistemas, e usando dois solutos com diferentes afinidades para as membranas em questão. As propriedades de transporte das duas membranas de diferentes materiais foram comparadas: uma membrana polimérica, propensa a potenciais rearranjos do material, e uma membrana cerâmica, com uma estrutura rígida, onde os rearranjos não são previstos.

.

ABBREVIATIONS

$c_{i,bulk}$ - concentrations of the solute *i* in the bulk (-)

$c_{i,bl}$ - concentrations of the solute *i* in the boundary layer (-)

$c_{i(m)}^{perm}$ - concentrations of the solute *i* in the membrane in the permeate (-)

c_i^{perm} - concentrations of the solute *i* in the permeate (-)

$c^*_{i,m}$ - equilibrium concentration in the membrane (wt./wt.)

$c^*_{i,f}$ - equilibrium concentration in the liquid (wt./wt.)

$D_{i\text{-}j}$ - diffusion coefficient of the solute in the solvent calculated using the Wilke-Chang equation ($m^2\ s^{-1}$)

D_i – diffusion coefficient of the solute *i* ($m^2\ s^{-1}$)

$D_i(t)$ - time-dependent diffusion coefficient($m^2\ s^{-1}$)

$D(t=\infty)$ – diffusion coefficient of compound *i* at the steady state ($m^2\ s^{-1}$)

EF (-) – enrichment factor

EtAc – ethyl acetate

HxAc – hexyl acetate

H_i - Henry's law coefficient (Pa^{-1})

$I_i(t)$ - electrical signal intensity of the compound *i* in the instant *t* [A]

$I_i(t=\infty)$ - electrical signal intensity of the compound i at the steady state ($t=\infty$) $J_{i,bl}$ - flux across the boundary layer ($m^{-3}\ m^{-2}\ s^{-1}$)

$J_{i,m}$ - flux across the membrane ($m^{-3}\ m^{-2}\ s^{-1}$)

$J_{i,ov}$ – overall flux ($m^{-3}\ m^{-2}\ s^{-1}$)

J_i - partial flux of the compound i ($m^{-3}\ m^{-2}\ s^{-1}$)

J_T - the total flux ($m^{-3}\ m^{-2}\ s^{-1}$)

$Ji(t=\infty)$ - partial flux in the steady state ($m^{-3}\ m^{-2}\ s^{-1}$)

$k_{i,bl}$ – boundary layer mass transfer coefficient (m s^{-1})

$k_{i,ov}$ – overall mass transfer coefficient (m s^{-1})

$k_{i,m}$ - membrane mass transfer coefficient (m s^{-1})

z_{bl} - boundary layer thickness (m)

L - thickness of the membrane (m)

P - permeability of a solute i (m^2 s^{-1})

P_i^G - gas-phase permeability of compound i. (m^2 s^{-1} Pa)

p_{ifeed} - partial pressure of compound *i* in the feed liquid

Re_R – Reynolds number at the outer radius of the cell

S_i - sorption coefficient of compound *i*(-)

S_i^L - liquid-phase sorption coefficient (-)

S_i^G - gas-phase sorption coefficient (Pa^{-1})

$w_{i,permeate}$ - permeate weight fraction

$w_{i,feed}$ - feed weigh fraction

α_{i-j} - selectivity of the solute *i* in relation to the solvent (-)

β_i - enrichment factor of the pervaporation process of solute *i* (-)

CONTENTS

Acknowledgements v

Abstract vii

Resumo ix

Abbreviations xi

Contents xiii

List of Figures xix

List of Tables xxiii

1 Introduction 1

1.1 Background and Motivation 1

1.2 Research Strategy 7

1.3 Thesis Outline 9

2 A novel time lag method for the analysis of mixed gas diffusion in polymeric membranes by on-line mass spectrometry: method development and validation 11

2.1 Summary 11

2.2 Introduction 11

2.3 Materials and Methods 14

2.3.1 Materials 14

1.1 Gases 14

1.1.1 Mass flow controller calibration 14

2.3.2 Membrane preparation 15

2.3.3 Experimental set-up and operating conditions 15

2.3.4 Mass spectrometric gas analysis 20

2.4 Theoretical concepts 21

2.4.1 Time lag determination 21

2.4.2 Gas permeation on the fixed volume time lag system for pure gases 26

2.4.3 Gas permeation on the variable volume system for pure and mixed gases 26

2.5 Results and discussion 28

2.5.1 Membrane preparation 28

2.5.2 Pure gas permeation in the fixed volume time lag system 28

2.5.3 Pure and mixed gas permeation in the variable volume system using mass spectrometry 31

2.5.4 Comparison of the diffusion coefficients calculated from the different experimental set-ups used in this work 36

2.5.5 Validation experiments - Effect of the CO2 concentration on the CO2/CH4 mixed gas transport in PIM-EA(Me)-TB 37

2.6 Conclusions 39

3 Evaluation of Hybrid Polysaccharide Membranes for Gas Dehydration using On-line Mass Spectrometry 41

3.1 Summary 41

3.2 Introduction 41

3.2.1 Materials 43

3.2.2 Membrane preparation 43

3.2.3 Single and mixed gas permeation experiments under dry and humidified conditions 43

3.2.4 Calibration method 46

3.2.5 Calculation methods 46

3.3 Results and discussion 47

3.3.1 Permeability for pure gases under dry conditions 47

3.3.2 Permeability of humidified gases – effect of water vapour on the permeability of pure gases 48

3.3.3 Permeability of gas mixtures – Flue gas and biogas dehydration 52

3.3.4 Membrane Stability 54

3.4 Conclusions 55

4 Steady-state and Transient Transport Studies of Gas Permeation Through Dense Membranes Using On-line Mass Spectrometry 57

4.1 Summary 57

4.2 Introduction 57

4.3 Materials and Methods 59

4.3.1 Materials 59

4.3.2 Experimental procedure 59

4.4 Results and Discussion 64

4.4.1 Sorption coefficients of pure O_2 and pure CO_2 in dense polymers 64

4.4.2 Steady state transport of pure O_2 and pure CO_2 through dense polymers 65

4.4.3 Transient transport of pure O_2 and pure CO_2 through dense polymers 67

4.4.4 Effect of N_2 on the O_2 permeation through the pectin membrane 69

4.4.5 Effect of water vapour on gas permeation through the pectin membrane 71

4.5 Conclusions 73

5 Transport of dilute organics through dense membranes: assessing impact on membrane-solute interactions 75

5.1 Summary 75

5.2 Introduction 75

5.3 Theorical concepts 77

5.3.1 Mass transport in the feed boundary layer 77

5.3.2 Steady-state transport 79

5.3.3 Transient transport 81

5.4 Experimental....81
5.4.1 PDMS membranes preparation....81
5.4.2 Compounds....82
5.4.3 Experimental set-up....82
5.4.4 Operating conditions....83
5.4.5 Sorption experiments....84
5.4.6 Mass spectrometry monitoring....84
5.5 Results and Discussion....84
5.5.1 Effect of feed boundary layer....85
5.5.2 Determination of sorption experiments....86
5.5.3 Permeation experiments....88
5.6 Conclusions....93
6 Characterisation and modelling of transient transport through dense membranes using on-line mass spectrometry....95
6.1 Summary....95
6.2 Introduction....95
6.3 Experimental....98
6.3.1 Materials....98
6.3.2 Experimental set-up....98
6.3.3 Operating conditions....99
6.3.4 Sorption experiments....100
6.3.5 Mass Spectrometry monitoring....100
6.3.6 Off-line analysis....101
6.3.7 Calculation methods....101

6.4 Results and Discussion 101

6.4.1 Sorption experiments 101

6.4.2 Characterisation of steady state transport properties 102

6.5 Characterisation of solute permeation by on-line mass spectrometry 103

6.5.1 Development of a mathematical model for solute transient transport through a dense membrane 106

6.6 Conclusions 110

7 General Conclusions And Future Work 113

7.1 General conclusions 113

7.2 Future work 115

Bibliography 117

8 Appendix – Supporting Information 131

A1 Description of the time-lag concept 131

A2 Contribution of the tubes to the instrumental time lag 133

A3 Least squares fitting procedure with error analysis for simultaneous calculation of the diffusion coefficient from all measurements 137

A4 Mixed CO2/CH4 permeation in the membrane PIM-EA(Me)-TB 141

A5 Mathematical model to describe the concentration inside the membrane 143

A1.1. The analytical model 143

A1.2. Solution of the analytical model: Diffusion coefficient varying in the time 145

A1.3. The Analytical Solution for a constant diffusion coefficient 147

LIST OF FIGURES

Figure 1.1: Schematic representation of Mass Spectrometry operating principle. 7

Figure 2.1: Chemical structures of the polymers used in the present work 14

Figure 2.2. Scheme of the fixed volume / pressure increase time lag setup.....16

Figure 2.3. Scheme of the mixed gas permeation setup in the test mode, with quadrupole gas analyser optimized for operation with a sweeping gas at the permeate side of the membrane. In the purge mode, with the 6-way valve in the 1-position, argon purge gas flows from connection 3-4 through the feed side of the membrane cell and the feed flow is bypassed via 2-1-6-5.....18

Figure 2.4. Scheme of the mixed gas permeation setup with quadrupole gas analyser optimized for vacuum operation at the permeate side of the membrane in test mode and during purge with helium (Insert).....20

Figure 2.5. Scheme showing for both setups the contributions of the flowing gas to the total time lag of the system just after switching from purge to test mode. The feed flow (thick green arrows), permeate/sweep flow (thick red arrows) and flow through the injection port into the analyser (thick blue arrows) each contribute to the instrumental time lag given by Eq (2.9). Note the fundamental difference between the sweep gas setup with minimum volume lines in the permeate and analysis section and the vacuum operated setup with voluminous vacuum connections but with low pressure.....24

Figure 2.6. Thickness dependence of permeability (A,B) for Pebax® 2533 (left) and Hyflon® AD60X (right) with their ideal selectivity (C,D) for selected gas pairs. Determination of the diffusion coefficient for membranes with different thicknesses according to eq.(2.7) , $D=l^2/6\Theta$ (E,F).....29

Figure 2.7. (A) Determination of the instrumental time lag by an aluminium foil sample with a pinhole defect. (B) Evidence of Knudsen flux in a plot of apparent permeance versus $M_i^{-0.5}$ at different pressures according to Eq. *Error! Reference source not found.*. The apparent permeance of different gases calculated on the basis on a hypothetical active area of 2.14 cm^2.....30

Figure 2.8. A) Example of the N_2, $CO_2$and O_2 permeate flow rates as calculated by eq.(2.19) from the start of the experiment, including 10 minutes for determination of the baseline. B) Corresponding cumulative permeate volumes after switching from purge mode to test mode, as determined by eq. (2.30), allowing for the simultaneous determination of all components in the gas mixture. Gas mixture: $N_2/CO_2/O_2$ 80/10/10 vol%, Membrane: 126 μm Hyflon®AD60X dense film. Red crosses indicate the fitting interval of the tangent. 33

Figure 2.9. Determination of the instrumental time lag for membranes with different thicknesses according to the equation $\Theta_i = \Theta_0 + l^2/6D_i$ for Pebax® 2533 (A) and Hyflon® AD60X (C) in the sweeping gas setup at a sweep flow rate of 30 cm^3 min^{-1} and with gas mixture $N_2/O_2/CO_2$ 80/10/10 vol.%. Analogous results in the vacuum permeate setup (B, D) with pure CO_2 and CH_4 and in the mixture CH_4/CO_2 50/50 vol.%. Comparison with the instrumental time lag determined by an aluminium foil sample with a pinhole defect in the sweeping gas setup (E) and the vacuum setup (F), respectively. {Error bars in A an B are smaller than the symbol} 34

Figure 2.10. Dependence of the mixed gas CO_2 and CH_4 permeability and selectivity of sample PIM-EA-TB as a function of the total pressure in the sweeping gas setup (A) and as a function of the mixture composition in the vacuum setup (B) of sample PIM-EA-TB as a function of the gas mixture composition in the vacuum system. Sweeping gas system operating with mixture of 51/49 vol% CO_2/CH_4 in the pressure range from 1-6 bar(a) and vacuum system operating at a total feed pressure of 1.05 bar(a) and a composition in the range of 10-50 vol% CO_2. Concentration-dependence of CO_2 and CH_4 diffusivity and related selectivity (C) and indirectly calculated solubility (D). Filled symbols represent the runs with increasing pressure (A) or increasing CO_2 concentration (B-D) and open symbols represent the subsequently decreasing pressure or CO_2 concentration. 38

Figure 3.1: Experimental set-up for pure dry gas permeation 44

Figure 3.2Experimental set-up for permeation in test mode (position 1) of: a) humidified single gas and b) humidified mixture of gases 45

Figure 3.3:Permeation experiment with dry CO2: concentration of CO2 in the permeate when using the FucoPol+GPTMS+CaCl2 membrane, and corresponding permeability, represented against time (T=21 ºC and pperm=70 mbar) 47

Figure 3.4:Results for pure gas permeation with different gas humidity content.....48

Figure 3.5:Water permeability of the humidified gases (CO2, N2 and CH4) for the hybrid polysaccharide membrane at 22.0 ºC.(The errors are so low that not appear in the graph) 49

Figure 3.6:H2O/gas (CO2, N2 and CH4) selectivity for the dehydration process with the membrane FucoPol+GPTMS 7+CaCl2 at 22.0 ºC. (GHC corresponds to gas humidity content) 50

Figure 4.1: Schematic representation of gas permeation apparatus performed at 30 ºC. The Humidified Gas system, HGS, was used to assure the desirable humidity in the air stream, during the studies with the pectin membrane.....62

Figure 4.2: Experimental apparatus for sorption experiments of the gas in the membrane material, performed at 30ºC.....63

Figure 4.3: MS on-line monitoring of CO_2 and O_2 permeation at 30ºC and at 1.05 bar (absolute pressure) in terms of permeability (Barrer) and normalised diffusion coefficient (cm^2/s) versus time through different membranes: (a) PDMS, (b) PE and (c) Pectin + 50% glycerol 69

Figure 4.4: Evolvement of (a) the flux ($mol/(m^2.s)$), (b) the permeability (Barrer), and (c) normalised permeability (-) of pure O_2 and of O_2 in a model air mixture (20% O_2 and 80% N_2) .70

Figure 4.5: Evolvement of flux ($mol/(m^2.s)$) and permeability (Barrer) along time of: (a) O_2 (in an air mixture) in dry and humid conditions (32% relative humidity) and (b) pure CO_2, in dry and humid conditions (32% relative humidity).....71

Figure 4.6: Normalised permeabilities through the pectin membrane for (a) O_2 in an air mixture, in dry and humid conditions (32% relative humidity) and (b) pure CO_2, in dry and humid conditions (32% relative humidity).....72

Figure 5.1: Representation of solute concentration profile in a pervaporation process, adapted from [25] 77

Figure 5.2: Experimental pervaporation setup with online monitoring of the permeate stream through Mass Spectrometry (MS).....83

Figure 5.3: Ethyl acetate concentration in the membrane as a function of its concentration in solution, at 40ºC. Symbols correspond to experimental data obtained for PDMS 50.....87

Figure 5.4: Flux of water through PDMS membranes: (a) membranes prepared with different crosslinking degree; (b) effect of solute (ethyl acetate) concentration in the feed solution; (c) effect of solute type (ethyl acetate and hexyl acetate) 88

Figure 5.5: (a) Ethyl acetate diffusion coefficient and (b) normalised ethyl acetate diffusion coefficient for PDMS 25 and PDMS 50, using a feed aqueous solution of ethyl acetate with a concentration of 0.5wt.% at 40ºC. Data obtained by on-line mass spectrometry.....92

Figure 5.6: Comparison of (a) evolvement of solute diffusion coefficient and (b) evolvement of normalised diffusion coefficient of ethyl acetate in PDMS 50, when using aqueous solutions 2% wt, 0.5% wt and 300ppm of ethyl acetate, at 40ºC. 92

Figure 5.7:Evolvement of (a) the diffusion coefficient for ethyl acetate and hexyl acetate and (b) normalised diffusion coefficient, through a PDMS 50 membrane, for a concentration of solute of 300ppm in water, at 40ºC.....93

Figure 6.1: Representation of the pervaporation unit with online monitoring of the permeate stream through MS: (1) feed vessel, (2) recirculation pump, (3) pervaporation cell and (4) vacuum pump. The splitting system consists of a heated sapphire valve.....98

Figure 6.2: Sorption kinetics of water in hybrid silica, HybSi®, using a solution of water in isopropanol at 40ºC.....101

Figure 6.3: Experimental permeate partial pressures, pperm,i [Pa] and partial fluxes, Ji [m/s] obtained through on-line mass spectrometry (MS) monitoring (dots) for (a) the system of water in isopropanol and (b) the system of ethyl acetate in water and the respective fittings to the experimental data (lines).....104

Figure 6.4: Solute diffusion coefficients, Di [m2/s], obtained through on-line mass spectrometry monitoring: (a) water diffusion coefficient in the system of water in isopropanol and (b) ethyl acetate diffusion coefficient in the system of ethyl acetate in water 105

Figure 6.5: Time dependent solute weight fraction along the membrane for different periods of time (a) water concentration along HybSi® membrane and (b) ethyl acetate concentration along POMS-PEI membrane.....109

Figure 6.6: Solute weight fraction in the membrane at downstream side over time, calculated using (steady-state) constant and variable diffusion coefficients (a) for water in isopropanol using HybSi membrane and (b) ethyl acetate in water using POMS-PEI dense membrane. 110

LIST OF TABLES

Table 2.1:Average thickness (μm) of the membranes prepared and used in this work.....28

Table 2.2. Typical relative sensitivity factors for different gases and their selected fragments obtained experimentally in this work and calibrated in relation to Argon. 32

Table 2.3. Gas diffusion coefficients in Pebax® 2533 and in Hyflon® AD60X determined by different methods. 36

Table 3.1:Permeability of dry gases. 47

Table 3.2: Comparison of transport performance of different membranes referred in the literature. 51

Table 3.3: Transport performance of hybrid polysaccharide membranes for synthetic flue gas and biogas dehydration. 53

Table 4.1: Calibration factors obtained for CO_2 and O_2 in relation to N_2. 60

Table 4.2: Sorption coefficients of pure O2 and CO2 in the polymers PDMS, PE and pectin with 50% glycerol, obtained in this work at 30 ºC 65

Table 4.3: Comparison of permeability and diffusion coefficient values of O_2 and CO_2 for the polymers PDMS, PE and Pectin with 50% glycerol under steady state, obtained in this work (at 30ºC and 1.05 bar. absolute pressure) and reported in the literature. 66

Table 4.4: Permeability and ideal selectivity of CO_2 against O_2 in an air mixture, at a relative humidity of 0% and of 32%. A pectin membrane was used at 30ºC. 73

Table 5.1: Conditions of PDMS membranes preparation and resulting chosen properties. 82

Table 5.2: Transport parameters determined for 300 ppm ethyl acetate (EtAc) and 300 ppm hexyl acetate (HxAc) during pervaporative separation with PDMS 50 membrane. 86

Table 5.3: Sorption coefficient S^L_i of ethyl acetate (EtAc) and hexyl acetate (HxAc) in contact with PDMS 50 membrane. 87

Table 5.4: Impact of solute concentration on its own transport across PDMS membranes, for aqueous solutions with 2% wt, 0.5% wt and 300 ppm of ethyl acetate and 300 ppm of hexyl acetate in water at 40ºC. 90

Table 6.1: Properties of the membranes used in this work. 98

Table 6.2: Properties of the feed solution used in the pervaporation experiments at 40ºC. 100

Table 6.3: Steady-state transport properties of pervaporation for the systems water in isopropanol and ethyl acetate in water using off-line analytical methods. 102

1 INTRODUCTION

1.1 Background and Motivation

Membrane separation technologies have been established for separation and purification processes due to their potential application in different areas: chemical, petrochemical, biochemical, pharmaceutical, environmental, food, beverage and so on [1]. Membranes are increasingly competitive compared to traditional techniques due to their potential efficiency with a low energy expenditure and to the fact that they may work without the use of chemical additives in a compact modular design [2]. In membrane separation processes, the key properties that determine membrane performance are their selectivity and permeability towards the target solute(s) and their stability / lifetime under operating conditions. In the recent years there is a significant advance on the design of new membrane materials with improved transport properties for novel applications in order to respond to market needs [3].

Particularly, dense membranes are widely used industrially in processes such as pervaporation and gas separation, with the objective of reducing their operational costs maintaining or increasing the performance associated with the intended separation. In fact, it is well known that processes involving phase change are generally energy-intensive, and distillation is a notorious example of them. The energy consumption when using a pervaporation process is clearly reduced when compared to a traditional distillation process. From a thermodynamic point of view the energy required to bring a solute in solution, in the feed stream, to its vapour state in the permeate stream, is the same. However, the energy expended with the solvent and other components with a low affinity to the membrane is much lower, due to high affinity usually achieved for the solute of interest. To date, pervaporation has been proposed for applications in the following three areas: *(i)* dehydration of organic solvents (e.g., alcohols, ethers, esters, acids); *(ii)* removal of dilute organic compounds from aqueous streams (e.g., removal of volatile organic compounds, recovery of aroma, and biofuels from fermentation broth); *(iii)* organic–organic mixtures separation (e.g., methyl tert-butyl ether (MTBE)/methanol, dimethyl carbonate (DMC)/methanol). Among them, dehydration of organic solvents is best developed [4] and the only one largely used at an industrial scale.

Similarly, the membrane technology for selectively remove CO_2 gas emissions from mixtures with H_2, CO, N_2 and CH_4 is of interest for a wide variety of applications, such as syngas processing, flue gas and natural gas separations, aiming at obtaining more competitive processes in terms of their economy, reduced environmental impact and energy consumption [5,6]. However, gas streams' mixtures often comprise water vapour, a known plasticizer, which changes the behaviour of the membranes used for gas separation. The removal of water vapour from gas streams is thus an important industrial operation, particularly on the dehydration of flue gas and biogas, the drying

of compressed air and the conditioning of gas used for storage of fruits and vegetables under protective atmosphere. Water vapour is generally considered a minor component of the system in such industrial applications, however, the presence of water, even at trace concentrations, may change significantly the permeation behaviour of the other gas species present [7,8].

Adequate transport characterisation tools are required for improving strategies of membrane design. An integrated use of complementary characterisation techniques is necessary for establishing and understanding the relations between structural and morphological properties of the dense materials developed and their transport performance in terms of permeability and selectivity [9].

Nonporous/dense films have a homogeneous structure without any defined pores. However, at a molecular level, the polymer chains are arranged in such a way that dynamic free volumes should be considered. The process of permeation through dense films is classically described by the solution-diffusion model, which is based on solute-membrane interactions. The transport can be then separated into the following three steps: [10]

- sorption of the permeating species onto the membrane surface,
- diffusion of the species through the membrane,
- desorption of the species on the downstream side of the membrane.

Transport of a chemical species through a dense membrane can be described as:

$$P = S \times D \tag{1.1}$$

where the permeability (*P*) is expressed as a function of sorption (*S*) and diffusivity (*D*).

In the solution-diffusion model, because no total pressure gradient exists within the membrane, the transport can be written as the Fick's first law when the system is under steady-state:

$$J_i = -D_i \frac{dc_i}{dx} \tag{1.2}$$

where the flux, J_i, of a component through a plane is proportional to the concentration gradient *dc/dx*. The proportionality is the diffusion coefficient, D_i [10,11].

To better understand the transport properties is thus necessary to study the solubility and diffusion parameters of the permeating compounds through the membrane [12].

The concept of ideal system underlines the fact that the penetrating solute has no interaction with the membrane material. In ideal systems the diffusion coefficient can be considered constant throughout the membrane. The sorption parameter, S_i, for diluted systems can be described by

Henry's law, which assumes a linear relationship between the solute partial pressure in the contacting stream, p_i, and the concentration at the interface, inside the membrane [11]

$$c_i = S_i \times p_i \tag{1.3}$$

Sorption and desorption steps are frequently assumed to be extremely fast and, hence, they do not limit transport from a kinetic point of view when comparing with the diffusion process, which is considered the rate-determining step. In other words, the sorption equilibrium with the external phase at the membrane surface is quasi-instantaneous and not the controlling step for the transport of the penetrant component *i* from the external phase into the polymer. It is also usually assumed that the interfacial concentration of the sorbed penetrant is constant over time at the upstream side of the membrane and negligible at the downstream side of the membrane. This can be achieved either by applying vacuum conditions or by using an inert gas over the membrane downstream surface (respectively, vacuum or sweeping gas conditions at the downstream side of the membrane). As a consequence, the diffusive flux of a component *i* across the membrane is maximal and, ideally, its molecular motion within the membrane is purely diffusive. Therefore, diffusion plays a major role in determining the overall rate of permeation [13].

The change in concentration (∂c) as a function of position and time (t), when the system is under a transient regime, is given by the second Fick's law where it is assumed that the diffusion coefficient (D_i) is constant:

$$\frac{\partial c_i}{\partial t} = -D_i \frac{\partial^2 c_i}{\partial x^2} \tag{1.4}$$

with the following boundary and initial conditions:

$$c(x,0) = 0;\ \ 0 < x < L$$

$$c(x,t) = c_{i,0};\ \ t > 0$$

$$c(x,t) = c_{i,x} = 0;\ \ t > 0, x = L$$

The most common technique used to characterise mass transport through dense membranes in ideal systems is the time-lag method, originally conceived by Daynes in 1920 [14], in order to study mass transfer through an elastomeric material. This method was refined and extended by authors as Crank [15,16], and Rutherford and Do [17], applied to a large variety of materials.

The calculation method underlying the time lag technique, based on the penetrant theory, can be found in Crank et al. [16]. If a penetrant-free membrane is exposed to a penetrant at the feed side at *t=0* and the penetrant concentration is kept very low at the permeate side, then the total amount of penetrant, Q_t, passing through the membrane in time *t* is given by.

$$\frac{Q_t}{l \cdot c_i} = \frac{D \cdot t}{l^2} - \frac{1}{6} - \frac{2}{\pi^2} \sum_1^{\infty} \frac{(-1)^n}{n^2} \exp\left(- \frac{D \cdot n^2 \cdot \pi^2 \cdot t}{l^2} \right) \quad (1.5)$$

in which c_i is the penetrant concentration at the membrane interface at the feed side, l is the membrane thickness [m] and D is the diffusion coefficient [$m^2\ s^{-1}$]. When $t \to \infty$, the total amount of penetrant, Q_t [mol m^{-2}], passing through the membrane is given by:

$$Q_t = \frac{Dc_i}{l} \left(t - \frac{l^2}{6D} \right) \quad (1.6)$$

This equation has an intercept Θ_{lag} on the time-axis given by:

$$\Theta_{lag} = \frac{l^2}{6D} \quad (1.7)$$

Through the continuous monitoring of the pressure increasing rate in the permeate side of a closed membrane cell, the permeability is determined from steady state:

$$P = \frac{V_P \cdot V_m \cdot l}{RT \cdot A \cdot p_f} \cdot \frac{dp}{dt} \quad (1.8)$$

The time-lag permeation method (eq.(1.7)) is a flexible and powerful technique for studying ideal systems. This method allows for determining both equilibrium (sorption coefficient) and transport properties (diffusivity and permeability) in a single experiment [18].

Nevertheless, this technique is valid only for permeating solutes with no strong affinity to the permeated material. The standard mathematical analysis used with this technique assumes a constant diffusion coefficient throughout the transient and the steady-state permeation periods. For processes in which the diffusion coefficient cannot be assumed to be constant, the use of the time-lag technique can lead to significant errors [19], since it does not account for the concentration dependent behaviour of the diffusion coefficient (the variation of the diffusion coefficient against time, *t*, and position within the membrane, x). These changes in time and position may result from possible material rearrangements that permeating solutes may induce since the initial stage of the transient regime. For this reason, this methodology is widely used when studying “non-interacting” systems, such as some gas permeation processes through rubbery membranes and pervaporation (specifically when solute concentration inside the membrane is rather dilute). In these cases, solute-membrane interactions are less relevant and a constant diffusion coefficient can be considered during the whole permeation process. On the other hand, when the penetrant solute has a strong affinity for the membrane material, the diffusion coefficient calculated using the time-lag method proved to be underestimated since it does not account for changes induced in the polymer matrix until polymer rearrangement is stabilised and steady state achieved [18,20]

As described above, there are situations that affect transport across the membrane, deviating from the “ideal transport”. At high feed concentrations and/or when processing solutes with high affinity to the membrane, the membrane polymeric structure can be modified to an extent that its intrinsic properties are significantly altered and a strong non-ideal behaviour occurs. For understanding these interactions, as well as the polymer swelling / fluidisation, different approaches / models based on the Flory-Huggins Theory [11,21] and UNIQUAQ are often applied for a quantitative description of the interaction of the feed components with the membrane material.

The Flory-Huggins theory is based on a lattice model to describe the entropy of mixing of solutions (solute-solute, solute-polymer, and polymer-polymer). This model allows for calculating the number of combinations that are possible in order to arrange a mixture between two components based on their volume fractions. In this case, the Gibbs free energy for mixing a polymer with a solvent is described as:

$$\Delta G_m = RT\left(n_1 \ln\phi_1 + n_2 \ln\phi_2 + n_1\phi_2\chi\right) \tag{1.9}$$

with ΔG_m the Gibbs mixing energy; n_1, n_2 and ϕ_1, ϕ_2 are the number of moles and volume fraction of component 1 and 2, respectively. The Flory Huggins parameter, χ_i, is the interaction parameter, which can be adjusted for a non-ideality behaviour [11,20].

The UNIQUAC (UNIversal QUAsi-Chemical) model is widely used for the description of liquid-liquid and vapor-liquid equilibria. This model accounts for the different sizes and shapes of the molecules as well as for the different intermolecular interactions between the mixture components and the polymeric compounds [22]. Over the years, several approaches of these models have been developed to apply in the different fields describing the transport of a penetrant through the membrane in non-ideal systems [23–25].

In non-ideal processes various phenomena can occur inside the membrane, leading to a change of the diffusivity of a permeant with its own local concentration (and other permeants present). For example, a faster transport of solutes, which can be quantified by an increase of their diffusion coefficients, may result from the plasticization of the membrane [12,26–29], whereas the decrease of diffusivity can be due to solvent clustering phenomena [30]. In other words, the diffusion coefficient of a solute within a membrane may be concentration-dependent and not constant across it.

In these cases, it is common to consider a plasticisation parameter for a penetrant assuming that diffusivity varies exponentially with concentration [12,27]. The following empirical equation is commonly used for single liquids:

$$D_{i,m} = D^{0}_{i,m} \times e^{\gamma C} \quad (1.10)$$

where $D_{i,m}^{0}$ is the diffusion coefficient of species *i* in the membrane under ideal conditions, γ is the plasticisation coefficient, and C the local permeant concentration.

The models and theories presented above were developed aiming at predicting the sorption and diffusion of a solute through a polymer when non-ideal solute-polymer interactions occur at molecular level. Most time-lag work has been performed with mono-component gases [31–33] and pervaporation [12,34] systems, where data is obtained by an accurate recording of pressure in a closed receiving compartment.

Some authors calculated the concentration-dependent diffusion coefficients from transient sorption data in order to determine the plasticisation parameter of a penetrant, which diffusivity is assumed to vary exponentially with its concentration [9,26,27]. However, the treatment of data assumes a Fickian diffusion process with a constant diffusion coefficient and the model is applicable only for the transport of a single component and not in a mixture.

All these methods usually involve single gas/vapor species, which is a strong limitation when considering that in many applications individual gas species influence other species, when present as a mixture. Relatively few papers discuss mixed gas sorption, providing solubility data of individual gases in a mixture [35,36]. Mixed gas permeation measurements by the variable volume method usually uses gas chromatography (GC) for analysis of the gas composition. This is a relatively slow technique with a sampling time of several minutes per data point, for common GC, or slightly less than one minute for micro-GC, which represents a discontinuous analysis of transient phenomena [37,38]. More recently, several papers have been published using on-line mass spectrometry in order to characterise the simultaneous permeation of multiple species both in gas permeation and pervaporation processes [31,34,39,40].

The challenge still relies on the development and validation of an on-line mass spectrometry technique able to acquire composition data in the permeate compartment with a minimal time interval, in order to studying systems that undergo a fast change during the initial transient stage of species penetration in the membrane [39,40]. Additionally, the transport of vapours through dense membranes introduces a degree of complexity which results from the non-constancy of the diffusion coefficient along the time-course of permeation during the transient period [17,18], due to the progressive increase of concentration of the permeating species inside the membrane. This increase in concentration may lead to membrane swelling and rearrangement of the polymer material with impact on the permeation process and, ultimately, the diffusion coefficients of these species. Therefore, the study of the whole transient regime may contribute for the fundamental understanding of structure–transport relationships in dense membranes, aiming the designing and fabrication of new membranes for specific applications.

On-line mass spectrometry MS was proposed as an advanced analytical method for process monitoring thanks to its possibility to provide real-time information [41], while the fast analysis makes it also excellently suitable to follow the transient permeation stage in different application fields. This technique enables to follow the whole permeation process of mixtures of gases and vapours through dense films, and allows for determining permeate compositions and partial pressures, fluxes and selectivities in real-time.

Since it is a very versatile tool, mass spectrometer can be coupled to a pervaporation [39] and gas permeation system [31] by a restriction or a capillary tube in the permeate compartment in order to analyse, with a high resolution, the permeate composition leaving the membrane.

Mass spectrometry characterises compounds by their specific mass-to-electric charge (m/z) and relative abundance or intensity of electric signal, providing a characteristic mass fragments fingerprint of a specific compound. Figure 1.1 represents the Mass Spectrometry operating principle. Ions are produced in the ionization chamber by electron impact ionisation due to the potential difference between filament and electron collector. Positive ions are separated, by an electrical field in the case of the common mass filter Quadrupole, according to their mass-to-electric charge (m/z) and converted to a corresponding electric signal in the detector. Relative intensities are usually used, assuming that the highest value of ion current for a specific compound in a specific experiment is equal to 100%.

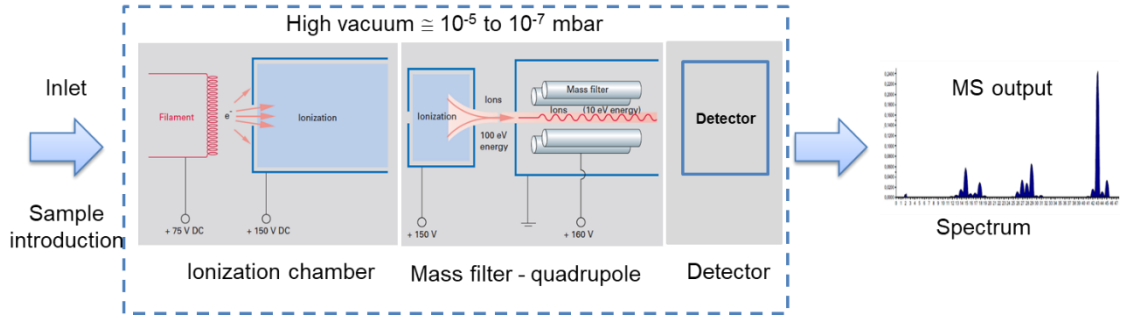

Figure 1.1: Schematic representation of Mass Spectrometry operating principle.

In addition, a sample introduction system is necessary to admit the samples to be studied to the ion source, while maintaining the high vacuum requirements (~10^{-5} to 10^{-7} mbar) of the technique. A computer is required to control the instrument, acquire and handle data, and compare spectra to reference libraries.

1.2 Research Strategy

The work presented in this PhD thesis was carried out with the objective of characterising the multi-component solute transport through dense membranes, during the whole transient and steady-state regimes, in different membrane processes: (gas separation, gas dehydration and pervaporation).

As known, before a permeation process begins, the membrane is dry and free from the target solutes. As the dense membrane is exposed to different penetrants, its structure may be gradually modified until acquiring its final steady-state conformation. The estimation of the transport parameters of permeating species through the membrane is, therefore, critical since the transport parameters may be altered due to the potential matrix rearrangement occurred during the transient period.

The extent of membrane modification is related with the interaction that the different permeating species establish with the membrane material. The greater the affinity of the solute to the membrane, the greater the modification it may cause in the membrane matrix and, consequently, the greater the impact on the transport properties.

Aiming at understanding the membrane modification during the permeation process in different applications, a mass spectrometry (MS) monitoring tool was used. The MS, used so far only as a permeate monitoring tool in pure gas permeation and pervaporation processes [12,31,39,40], will be used in this work as an instrument to characterise solute-membrane interactions. This powerful technique will enable a real-time characterisation of solute transport through dense membranes by acquiring real-time information of the transport parameters in the whole permeation process.

The strategy of this research project comprises an indirect monitoring of the interactions that the penetrating solute establishes with the membrane and, consequently, possible membrane rearrangements, both in gas permeation and pervaporation systems, through the estimation of the diffusion coefficients. The systems studied were selected due to their different affinity towards target solutes (gases, water vapour, aroma compounds or alcohols). In this way, ranging from systems where the interactions are mostly negligible, to those where the diffusion coefficient is significantly modified during the permeation process, a methodology to calculate the evolvement of the diffusion coefficient of different species through the membrane along time is proposed and assessed.

The transport studies were performed by coupling the pervaporation / gas permeation cell on-line with the Mass Spectrometer, linked by a split line to the permeate circuit. Different membranes are characterised by measuring the mass of permeating species on-line, in real-time. Through the information acquired, the purpose will be to understand how different solutes interact with different membranes and how that impacts on the membrane transport behaviour.

Mass spectrometry identifies and quantifies the target compounds. To convert the raw data (electric signal) of each compound permeating the membrane into its correspondent volumetric concentration (%v/v) or partial pressure, an innovative calibration method was implemented, both for gases and vapours. This method, based on assigning a sensitivity calibration factor of each compound to be studied in relation to the sweeping gas / internal standard used, was found to be reliable, easy and fast to implement, without the need to modify the system or perform discontinuous analyses [39,40]. The relative sensitivities of the different gases specified by the

instrument supplier or tabulated in the literature are not universal enough to be used as a standard for high precision analysis [31] as they are altered, taking into account the operating conditions used as well as the equipment. Therefore, the mass spectrometry instrument must be calibrated for each system and each permeating compound to be studied.

Finally, a mathematical model was developed in order to obtain solute concentration profiles inside the membrane and their evolvement along time. Two case-studies were selected, corresponding to different systems, using permeating solutes with different affinities towards the membranes under study. The transport properties of two different membrane materials were compared: a polymeric membrane, which may be prone to potential material reorganisations and a ceramic membrane with a rigid structure, where material rearrangements are not anticipated.

1.3 Thesis Outline

The work performed during this PhD is organised considering the relevance of solute-membrane interactions, starting from a situation where these interactions may be considered to be negligible (Chapter 2) and, therefore, the diffusion coefficient can be considered constant. In a second stage, this work addresses situations where molecular interactions become more relevant, involving solutes with a high affinity to the membrane material, which may modify its structure during the permeation process (from Chapter 3 to Chapter 5). In this second case, the transient diffusion coefficient varies significantly and was considered to be time-dependent. For the situations where the diffusion coefficient has to be considered time-dependent, a mathematical model was developed (Chapter 6) aiming to simulate the solute concentration profile inside the membrane, from the initial instants of the permeation process until reaching steady state conditions.

The present work is, thus, organised in seven chapters:

Chapter 1 describes the motivation for this PhD project, presents the research strategy, the objectives and finally describes the thesis outline.

Chapter 2 describes a new method to determine the individual diffusion coefficients of gases in a mixture during their permeation through polymeric membranes using the time-lag method. Through the monitoring of the permeate composition along time by a quadrupole mass spectrometer, the analysis of the permeation transient period after exposure of the membrane to a gas mixture was assessed. Since the gases studied have not high affinity to the membranes used, a constant diffusion coefficient was considered for all transient and steady state period.

Chapter 3 discusses an integrated gas permeation system at atmospheric pressure designed to study three different polymeric membranes when permeated by different gases under dry and humidified conditions. In this study, long transient periods were required, in order to make possible the observation of different degrees of polymer rearrangement, induced by penetration of different

solutes. The transport behaviour exhibited by the different materials, when penetrated by permeating compounds with affinity for them, is compared and discussed. To characterise the transport of each species through the membrane, time-dependent diffusion coefficients were calculated from on-line Mass Spectrometry monitoring data since diffusion coefficients were not constant throughout the permeation process.

In Chapter 4 a mass spectrometry monitoring tool is used to monitor the permeation of water vapour, pure gases (CO_2, CH_4 and N_2) and mixed gas streams, in particular flue gas and biogas, using a hybrid polysaccharide membrane. The permeation of single and mixed gases both under dry and humidified conditions through the membrane were assessed, aiming at obtaining very low gas permeabilities, and high selectivities for water in relation to each gas under study.

The characterisation and study of different solutes' permeation through dense membranes aiming at aroma recovery (ethyl acetate and hexyl acetate) and isopropanol dehydration using a pervaporation system coupled to a mass spectrometer are described in chapters 5 and 6.

Chapter 5 studies the effect of different organophilic solutes through polydimethylsiloxane PDMS membranes. The evolvement of solute transport during the transient period is assessed in this chapter, through the calculation of time dependent D(t) diffusion coefficients in the whole permeation process. Solute solubilisation within the membrane polymer matrix is noticeable in the first instants of permeation, inducing internal rearrangements that impacts not only on the transport of solutes themselves, but also on the transport of the solvent.

Chapter 6 defines and presents a methodology for characterising solute transport through pervaporation dense membranes (a ceramic membrane, where no membrane material rearrangement occurs during permeation, and a polymeric membrane). Through a real-time characterisation of transport through dense membranes, time dependent D(t) diffusion coefficients were calculated in the whole permeation process. Based on the information acquired, a mathematical model was developed in order to obtain solute concentration profiles inside the membrane and their evolvement along time.

Chapter 7 presents the overall conclusions of this work and suggestions for future work

2 A NOVEL TIME LAG METHOD FOR THE ANALYSIS OF MIXED GAS DIFFUSION IN POLYMERIC MEMBRANES BY ON-LINE MASS SPECTROMETRY: METHOD DEVELOPMENT AND VALIDATION

Submitted to Journal of Membrane Science as: S. C. Fraga, M. Monteleone, M. Lanc, E. Esposito, A. Fuoco, L. Giorno, K. Pilnacek, K. Friess, M. Carta, N. B. McKeown, P. Izak, S. Petrusova, J.C. Crespo, C.Brazinha, J.C. Jansen

The author was directly involved in planning all the experiments related with the gas permeation experiments coupled to the Mass Spectrometry under vacuum conditions, as well as on the data elaboration, discussion and interpretation.

2.1 Summary

The present manuscript describes a novel method to determine the individual diffusion coefficients of gases in a mixture during their permeation through polymeric membranes. The method was designed and validated in two independent laboratories, using rubbery Pebax® and glassy Hyflon®AD membrane samples for the method development and the Trögers base derived Polymer of Intrinsic Microporosity, PIM-EA-TB, for validation. Monitoring of the permeate composition in real time by a quadrupole mass spectrometer allowed the analysis of the permeation transient after exposure of the membrane to a gas mixture. Two operation modes are compared, using either vacuum in the permeate with a heated restriction connected to the mass spectrometer, or using a sweeping gas with a heated capillary sample inlet. Excellent agreement between the data obtained for Pebax® and Hyflon®AD in the mixed gas setup and a traditional time lag setup demonstrates the suitability of the method and confirms that no anomalous transport occurs in these two polymers. The manuscript gives a complete overview of the method development, identification of the critical parameters, calibration of the instruments, elaboration of the data and estimation of the experimental accuracy. Validation of the method with the Trögers base containing polymer of intrinsic microporosity, PIM-EA-TB, shows that it can successfully detect pressure and concentration dependency of the transport properties, such as dual mode sorption and pressure dependent diffusion.

2.2 Introduction

In the search for more competitive technologies in terms of process economy, reduced environmental impact or energy consumption [42], membrane separations are emerging in various fields, like natural gas sweetening, biogas upgrading or carbon capture from flue gas or

industrial waste gas. Increasingly challenging separation problems, involving particularly difficult olefin/paraffin separations or particularly voluminous flue gas and natural gas streams, has spurred the development of novel materials with improved selectivity and/or permeability.[43] Materials that have received considerable attention in the last 1-2 decades include glassy perfluoropolymers [44–46], polymers of intrinsic microporosity (PIMs) [47–51], microporous organic polymers (MOP),[51] thermally rearranged (TR) polymers [52–54], ionic liquids and poly(ionic liquid)s [55–57]. The development of such sophisticated novel membrane materials inevitably requires the development of improved methods to study their transport properties.

Since the transport in dense polymeric membranes is governed by the solution-diffusion mechanism, the most common approach to study their transport properties, is the use of the so-called time lag method, which allows the determination of both the permeability coefficient and the diffusion coefficient of pure gases in the polymeric matrix, and indirectly, the solubility coefficient.[15,16] This is one of the simplest and most versatile methods for determination of the diffusion coefficient, with solutions also for porous media exhibiting surface diffusion or glassy polymers with strongly nonlinear sorption behaviour[17]. The feed pressure decay in pseudo-steady state conditions[58] or the simultaneous measurement of the feed pressure decay and the permeate pressure increase[59] were proposed to study the transport properties of materials with concentration dependent diffusion or with a strongly nonlinear sorption isotherm, respectively. Complex problems like cluster formation may require different solutions, assuming for instance the simultaneous existence of different diffusion coefficients.[60,61] Despite the simplicity of the time lag method, a problem for highly condensable vapours like water is that sorption of the vapour at the wall of the permeate compartment may lead to a dramatic underestimation of the permeability and an error in the diffusion coefficient.[19] In such cases, gravimetric sorption kinetics studies may provide a better method for the determination of the diffusion coefficient, while the equilibrium sorption yields the solubility.

All the above methods usually involve single gas or vapour species, which is a strong limitation when considering that in many applications the individual gas species influence each other in a mixture. Relatively few papers discuss mixed gas sorption, providing solubility data of the individual gases in a mixture, *e.g.* [62–64]. Mixed gas permeation measurements are not straightforward because of complications in the analysis itself, and in interaction between the species in the gas mixture, especially when dealing with polymers with nonlinear sorption behaviour, strong physical aging or slow dilation.[50] Normally, these measurements are carried out in a cross-flow cell configuration by the variable volume method, using gas chromatographic analysis of the gas composition. This is a relatively slow technique with a sampling time of several minutes per point for normal GC or slightly less than a minute for micro-GC, which may yield steady state permeation data but it does not allow the analysis of transient phenomena of 'fast' materials, and thus the determination of the mixed gas diffusion coefficient. A combination of ^{1}H and ^{13}C NMR spectroscopy and pulsed-field gradient NMR, studied for this purpose, allowed the

determination of the solubility and diffusion coefficients of pure carbon dioxide and its mixtures with other gases.[65] However, this method is not suitable for routine analysis.

Instead, on-line mass spectrometry was proposed as an advanced on-line analytical method for process monitoring and control thanks to its high analysis speed and the possibility to provide real-time information on the process parameters.[41] The fast analysis makes it also excellently suitable to follow Isotopic-Transient Kinetics (ITK) in chemical reactions.[66] Interestingly, both flat and hollow fibre membranes are proposed as an alternative for the direct capillary inlet to the MS,[41] not taking into account the dynamics of the membrane itself in the mass transport. Indeed, membrane introduction mass spectrometry (MIMS) is considered as a special technique, where the high permeability of the membrane should guarantee a quick response and its selectivity should enhance the sensitivity towards specific species, in particular vapours[67] or dissolved gases.[68] Instead of using membranes for the sake of the analysis, Schäfer *et al.* proposed to follow the mass transport in pervaporation membranes on-line by MS analysis[39], while Zhang *et al.* determined the relative humidity dependence of H_2 and O_2 permeation in ionomer membranes for polymer electrolyte fuel cells.[69] Isotopic-transient permeation experiments under the steady-state pervaporation (PV) operation of rubbery polymer membranes allow the determination of concentration-dependent diffusion coefficients of penetrants.[12] Recently, the group of Crespo discussed the transient phenomena related to the membrane transport by on-line, quantitative monitoring of the organophilic pervaporation processes.[40,70] and gas separation processes [71]. Some of the present authors also used the Mass Spectrometric Residual Gas Analyser (MS-RGA) for analysis of the permeate under steady state permeation conditions of various Polymers of Intrinsic Microporosity (PIMs).[72–74] Tremblay *et al.* already described a novel method based on a MS-RGA for the analysis of permeability and diffusivity of pure He, N_2, CO_2 and CH_4 in four different rubbers, but the much lower CO_2 permeability and CO_2/N_2 selectivity, in for instance PDMS, as compared to the literature values raises serious concerns about the accuracy of their method.[31]

The scope of the present paper is therefore to set up a reliable method to study the transient phenomena during mixed gas membrane permeation and to determine the permeability and diffusion coefficient of the individual components in the mixture. We will discuss the use of MS-RGA for the continuous online analysis of the permeate gas composition, identifying all relevant instrumental and operational parameters and comparing the mixed gas transport data with those obtained with the classical time lag method in a fixed volume setup for pure gases. Development of the technique for two different membrane materials (Pebax® rubbery polymer and Hyflon® glassy perfluoropolymer), followed by its validation with the glassy PIM-EA-TB (Figure 2.1), will demonstrate its wide applicability for permeability and diffusivity measurements and the capacity to identify fundamental trends, such as absolute and partial pressure and gas composition dependence of the transport parameters. Finally, analysis of the experimental error will show that the method can be used to calculate the gas diffusion coefficient with a reasonably small error for membranes with a time lag of some ten seconds or higher.

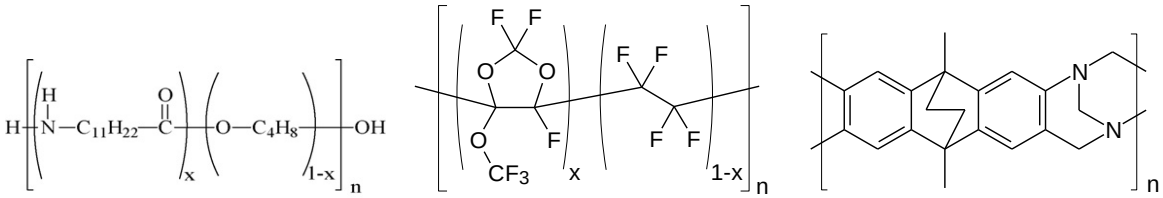

Pebax®2533 **Hyflon®AD60X** **PIM-EA-TB**

Figure 2.1: Chemical structures of the polymers used in the present work

2.3 Materials and Methods

2.3.1 Materials

Ethanol, absolute AnalaR NORMAPUR® ACS was supplied by VWR Chemicals (Italy). 1-Methoxy-perfluorobutane (HFE7100) was purchased from 3M. Hyflon® AD60X was purchased from Solvay-Solexis (Italy) and Pebax® 2533 was kindly provided by Arkema (Italy). All products were used without further purification, unless specified otherwise.

The Tröger's base containing polymer of intrinsic microporosity, PIM-EA-TB, was synthesized as described previously [72] and the membrane was prepared in the form of a dense self-standing film prepared by solvent casting and very slow evaporation of the solvent. Since PIMs are known to undergo strong physical aging, a well-aged sample was used during the permeation tests to minimize the effect of the variable time on the performance.

1.1 Gases

Pure gases were supplied by Pirossigeno (Italy) at a minimum purity of 99.9995% and by Praxair (Portugal) at a minimum purity of 99.99%. Certified gas mixtures were supplied by Sapio (Italy) at a purity of ±0.01% from the certified concentration (CO_2/CH_4 mixture with 47.89 mol.% CH_4 and $N_2/CO_2/O_2$ mixture with 10.10 mol.% CO_2 and 10.02 mol.% O_2).

1.1.1 Mass flow controller calibration

Custom-made gas mixtures were prepared in-line by mixing of the pure gases using calibrated EL-Flow electronic mass flow controllers (Bronkhorst, STV Portugal). For optimum accuracy, the MFCs were calibrated periodically to check for deviations from the factory standard and to guarantee precise gas dosage. The gas flow rates were determined at ca. 10 different flow rates in the range used for the future measurements. The measurement of the flow rate was performed

with a bubble flow meter or with a digital flow meter (ADM2000 Universal Gas Flowmeter, Agilent Technologies, USA), appropriately correcting for atmospheric temperature and pressure.

2.3.2 Membrane preparation

Hyflon® AD60X membranes were prepared as described previously, dissolving 5 wt.% of the polymer in HFE 7100 under magnetic stirring for 24 h at room temperature, normally 23±2 °C [75,76]. The homogenous solution was filtered through a 0.45 µm Teflon PTFE syringe filter and poured into a stainless steel casting ring resting on a glass plate and partially covered with a petri dish to slow down the evaporation. Dense membranes were obtained by solvent evaporation for 72 h at room temperature and the membranes were used as such for the permeation tests.

Pebax® 2533 membranes were prepared according to the procedure reported previously,[77] dissolving Pebax® 2533 at a concentration of 10 wt.% in ethanol under slight reflux, while magnetically stirring for at least 2 h. The solution was cast into a stainless steel casting ring placed on a Teflon plate and covered with a Petri dish to slow down evaporation. The solution was left for 48 h to allow complete solvent evaporation at room temperature. After this time, self standing dense membranes were obtained.

A PIM-EA-TB membrane was cast from chloroform, dried in air and then methanol treated to remove residual solvent and to reset the casting history as described previously [72]. The sample was stored for several months to allow significant initial aging and reach a more stable and time-independent performance [74].

For all membranes, a proportionally larger amount of solution was used to obtain thicker films.

2.3.3 Experimental set-up and operating conditions

2.3.3.1 Fixed volume time lag system for pure gases

All gas permeability measurements were performed at 25±0.5 °C and at 1 bar, unless specified otherwise, comparing three different instruments, based on either the fixed volume or the variable volume method. The fixed volume-pressure increase instrument, constructed by ESSR (Germany) is an improved version of the instrument described previously [76] and is schematically displayed in Figure 2.2. The instrument is equipped with a fixed feed volume of about 2 litres, a fixed permeate volume. The permeate volume is expandable from 91.6 cm^3 to 260 cm^3 if it is necessary to reduce the pressure increase rate and to prolong the time available to reach steady state. A set of two membrane pumps and a turbo molecular pump (Pfeiffer), guarantee a high and clean vacuum (< 10^{-3} mbar) for effective degassing of the samples without the risk of contamination of the membrane samples with vacuum oil.

Up to eight gas cylinders are connected simultaneously to the instrument and an additional liquid flask can be connected for vapour transport measurements. A feed pressure up to 2 bar can be used and the actual value is read with a resolution of 0.1 mbar; the permeate pressure is measured in the range of 0 to 13.3 mbar with a resolution of 10^{-4} mbar. The membrane cell diameter is 75 mm and the effective area can be reduced by the use of appropriate aluminium masks on the membrane. The feed gas pressure is set by pneumatic valves and the gases can be alternated automatically. The entire system is computer controlled, guaranteeing extremely short response times. The crucial parts of the setup are placed in a thermostatic chamber, which allows measurements according to a previously chosen temperature program. Feed pressure, permeate pressure and temperature are continuously monitored during each measurement run and the diffusivity, permeance and permeability are automatically calculated and exported to a data file. The final calculations correct appropriately for the presence of a baseline slope in the case of desorption of volatile species or Knudsen flux through pinhole defects, or for nonlinearity in the final pressure increase curve due to strong dual mode sorption behaviour.

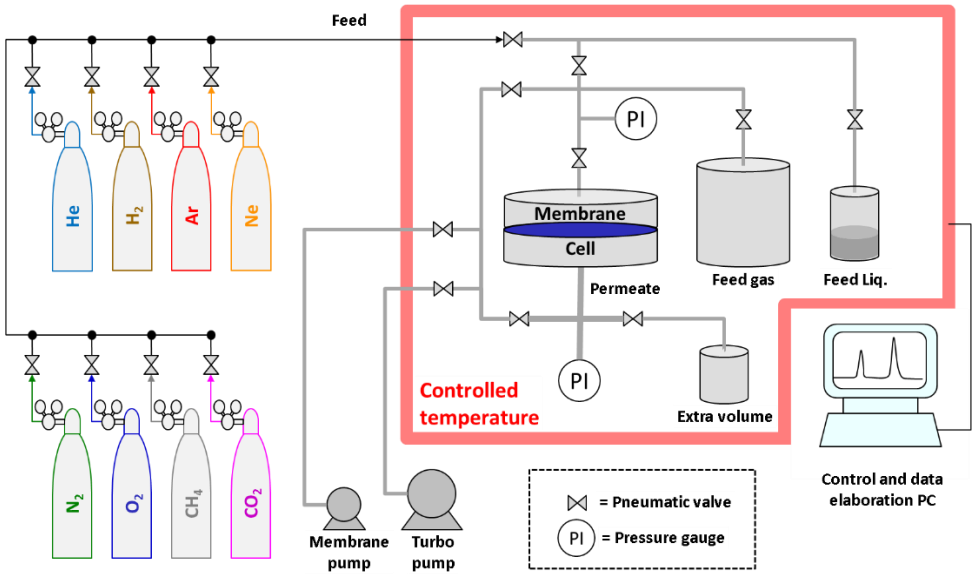

Figure 2.2. Scheme of the fixed volume / pressure increase time lag setup.

The measurement is carried out on circular membranes, typically with an effective exposed area between 13.84 cm^2 and 1.77 cm^2, depending on the need to mask the samples to reduce the effective area or to prevent cracking under the sealing ring. Before the first measurement, each membrane is evacuated inside the permeation cell for at least 1 h to remove all absorbed species, until the baseline drift is significantly below the steady state pressure increase rate of the species to be tested.[76] Between two subsequent measurements, the system is evacuated for a period of at least 10 times the time lag of the previous species in order to guarantee the complete removal of the penetrant from the membrane. The entire permeation curve is determined, including the

initial transient, to allow the determination of the diffusion coefficients of the penetrants by the time lag method (section2.4.1), and the determination of the permeability coefficient from the steady state pressure increase rate. At the standard measurement pressure of 1 bar none of the gases causes plasticization of the polymer matrix and Henry-type sorption occurs, which means that the simplest form of the solution-diffusion model can be used, in which the permeability, solubility and diffusion coefficients are all constant.

2.3.3.2 Variable volume system using mass spectrometry for pure and mixed gases with the permeate under sweeping gas conditions.

The instrumental setup for the measurements with sweeping gas is displayed in Figure 2.3. The core of the system is a mass spectrometric residual gas analyser (Hiden Analytical, HPR-20 QIC Benchtop residual gas analysis system) equipped with a quadrupole mass filter (max. 200 AMU) and a heated sampling capillary with a typical flow rate of ca. 10-20 $cm^3 min^{-1}$ at ambient pressure, depending on the gas sampled. The electron ionization energy is 70 eV and the gases are generally detected with the Secondary Electron Multiplier (SEM) ion detector at low partial pressures, or the Faraday detector at high partial pressures.

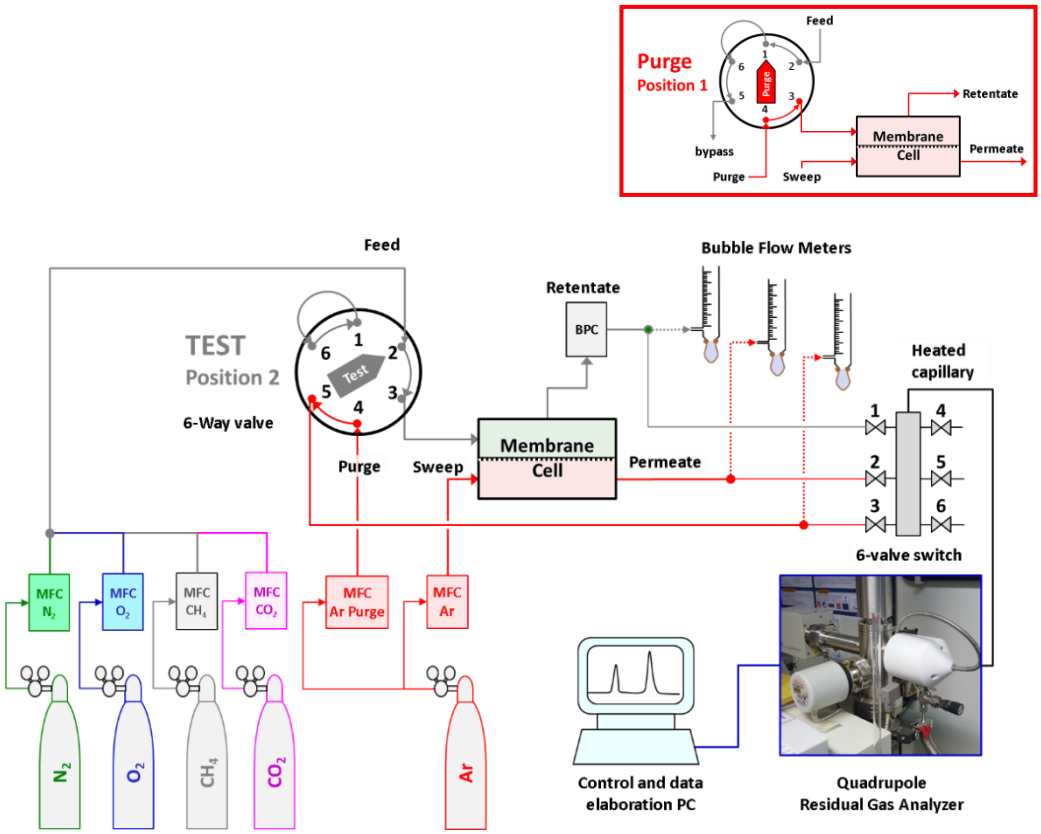

Figure 2.3. Scheme of the mixed gas permeation setup in the test mode, with quadrupole gas analyser optimized for operation with a sweeping gas at the permeate side of the membrane. In the purge mode, with the 6-way valve in the 1-position, argon purge gas flows from connection 3-4 through the feed side of the membrane cell and the feed flow is bypassed via 2-1-6-5

The mass spectrometer is connected to a custom made constant pressure / variable volume instrument, equipped with a modified Millipore permeation cell (diameter 47 mm). The cell is fed with the pure and mixed gases by means of EL-FLOW electronic mass flow controllers (Bronkhorst, NL) for each gas, and the pressure is controlled with an EL-PRESS electronic back pressure controller (0-5 bar(g)) in the retentate line. Two independent mass flow controllers provide the argon sweep gas continuously to the permeate side of the cell, and the same gas to the feed side of the cell, when in purge mode between to subsequent measurements. The measurement cell and part of the connections are located in a thermostated chamber to guarantee operation at controlled temperature. The gas is sampled with a heated capillary from the permeate side of the membrane, which is flushed with a known excess of sweeping gas at atmospheric pressure.

Two glass bubble flow meters in the retentate line and in the permeate line serve for regular checking of the flow rate or for the calibration of the mass flow controllers, when necessary. The actual temperature and pressure are recorded to convert the measured bubble flow rates to standard temperature and pressure conditions (STP, 1 atm at 0 °C).

Mixed gas permeation experiments were carried out on the described constant pressure / variable volume instrument. The experiments were carried out at a feed flow rate of 100-200 cm^3 min^{-1} and a controlled feed pressure of 0-5 bar(g). Argon was used as the sweeping gas at ambient pressure, normally at a flow rate of 30 cm^3 min^{-1}. The permeate composition was determined via Mass Spectrometric analysis of the permeate/sweep composition. The ^{36}Ar signal was used as the internal standard for calculation of the gas flow rate of the permeating species based on their relative concentrations in the sweep/permeate stream. Since too high humidity is known to affect severely the other signals by chemical reactions taking place at the filament, and thus reduce the sensitivity to detect other gases, only high purity dry argon is used.[78] Highly permeable samples were masked with an adhesive aluminium tape with a smaller aperture to limit the total permeate flow rate and to keep the stage cut close to or below 1%.

Before each analysis, the membrane was flushed for at least 1 hour at both sides with two independent argon streams until the MS signal was sufficiently stable, and this signal was taken as the background. Subsequently, the argon flux at the feed side was instantaneously replaced by the pure gas or the gas mixture at atmospheric pressure (absolute pressure 1 bar(a)) via the 6-way valve, and the gas concentrations in the permeate were followed as a function of time. Thus, the time lag (section 2.4.1) and the time needed to reach steady state permeation were determined. If desired, in a second experiment, the feed pressure was stepwise changed from 1 to 5 bar(g) and back, with sufficiently long time intervals to reach steady state permeation in each step. The background signals were determined just before switching from argon to the gas or gas mixture at the feed side, and were subtracted from the measured signal during data processing.

2.3.3.3 Variable volume system using mass spectrometry for pure and mixed gases with the permeate under vacuum conditions.

The setup for performing pure and mixed gases separation experiments with mass-spectrometric analysis of the permeate under vacuum conditions is displayed in Figure 2.4. The main difference compared to the sweeping gas setup is its direct connection of the permeate side with the mass spectrometer with a restriction. The permeate side is kept at very low pressure using a dry and oil-free diaphragm vacuum pump (Pfeiffer vacuum, MVP 015) and a constant low argon flux is used (1 cm^3 min^{-1}) as an internal standard. The unit comprises a membrane cell with the membrane, pressure and mass flow controllers (EL-FLOW electronic mass flow controllers, Bronkhorst, NL) for each gas, and the pressure is controlled with an EL-PRESS electronic back pressure controller (Bronkhorst, NL), to control the gas flow and pressure of inlet and outlet streams of the membrane cell. The permeate composition is monitored on-line each second using a mass spectrometer (MS) connected directly to the permeate. The mass spectrometer (Prisma Plus QMG 220 M2, Pfeiffeir Vacuum, Germany) was used in an axial beam ion source, emission current 1mA, electron energy 70 eV, single quadrupole, secondary electron multiplier SEM detection. In each permeation experiment with a defined feed gas / mixture of gases, the following operating parameters were controlled and measured: the feed pressure of gas was maintained

at 1.05 bar (absolute values of pressure), the total flow rate of the inlet feed stream was 50 cm^3 min^{-1} of the gas / mixture of gases and a flow rate of 1 cm^3min^{-1} of ^{40}Ar (internal standard) was fed directly to the permeate. The temperature of the system was kept at 17±1 °C.

Before each permeation experiment, the feed side of the membrane cell is purged with helium in order to clean the membrane and the system from other gases (purge mode, position 2). Following the concentrations of all gases under study in the permeate through the MS, and ensuring that all of them are at the noise level, the gas under study is introduced into the feed side, using a 4-way valve (*test mode, position 1*) and the permeation of each gas / mixture of gases through the membrane is monitored in the permeate compartment over the time in terms of electrical signal, volume fraction concentration and partial pressure.

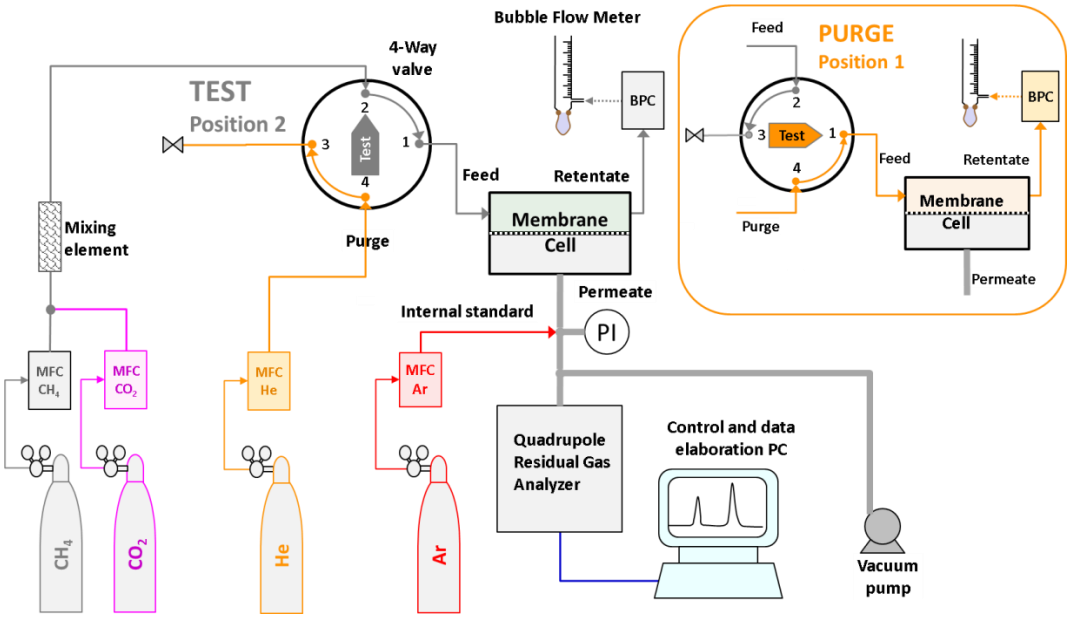

Figure 2.4. Scheme of the mixed gas permeation setup with quadrupole gas analyser optimized for vacuum operation at the permeate side of the membrane in test mode and during purge with helium (Insert).

2.3.4 Mass spectrometric gas analysis

The mass spectrometer characterises compounds according to their specific mass to charge ratio (m/z) after ionization, and to the intensity of the electric signal, providing a characteristic mass spectrum of a specific compound. In the absence of hydrocarbons, nitrogen is detected at m/z = 14 atomic mass unit (AMU), to avoid overlap of N_2 with the CO fragments from CO_2 at m/z = 28 AMU in CO_2/N_2 mixtures; methane is detected at m/z = 15 AMU (as CH_3) to avoid overlap of the molecular CH_4 peak with the O fragment from CO_2 at m/z= 16 AMU in the case of CO_2/CH_4 mixtures. All sensitivity ratios are calibrated against the weaker ^{36}Ar isotope at m/z= 36 AMU (ca.

0.3% abundancy) for the sweeping gas system, and ^{40}Ar m/z=40 AMU for the vacuum system, both used as internal standards.

In the first step, the background signal, I_{BG}, measured while purging the membrane with argon at the feed and permeate side, is subtracted from the raw data signal:

$$I_i = I_{raw,i} - I_{BG,i} \tag{2.1}$$

All measurements in the unit working under sweeping gas conditions were recorded with the MASsoft software package supplied with the mass spectrometer (Hiden), while the FlowPlot software (Bronkhorst) supplied with the pressure and mass flow controllers registered the pressure and gas flow rates. The raw partial pressure data were elaborated by a macro in MS Excel after synchronization of the time scales of the two sources of data.

Multiplication with the relative sensitivity, RS_i, yields the partial pressure in the gas analyser, $p_{MS,I}$,

$$p_{MS,i} = I_i \cdot RS_i \tag{2.2}$$

And for a system open to the air, normalization for the atmospheric pressure and all gases present yields the partial pressure in the permeate/sweep stream:

$$p_{P,i} = p_{Atm} \cdot \frac{p_{MS,i}}{\sum_i p_{MS,i}} \tag{2.3}$$

The measurements in the unit working under vacuum conditions were recorded using QUADERA software provided with the mass spectrometer and the pressure and flow rates were acquired with FlowPlot software provided with the pressure and flow controllers. The output of the mass spectrometer is the electrical signal, I_i (A), the volume concentration of each gas y_i (%vol), and the partial pressure of each gas p_i (mbar) which are calculated from the total pressure in the permeate, p_{total} (mbar):

$$y_i = y_{Ar} \cdot RS_i \frac{I_i}{I_{Ar}} \tag{2.4}$$

$$p_i = y_i \cdot p_{total} \tag{2.5}$$

2.4 Theoretical concepts

2.4.1 Time lag determination

In the present work, the diffusion coefficient was determined by the time lag procedure, well-known for pure gases and based on the penetration theory.[15,16]. A detailed description of the

calculation procedure is given in Annex A1. If a penetrant-free membrane is exposed to the penetrant at the feed side at t=0 and the penetrant concentration is kept very low at the permeate side, then the total amount of penetrant, Q_t [mol m^{-2}], passing through the membrane for long periods of time is given by: [16]

$$Q_t = \frac{D \cdot c_i}{l} \cdot \left(t - \frac{l^2}{6D} \right) \tag{2.6}$$

in which c_i (mol m^{-3}) is the penetrant concentration at the membrane interface at the feed side, l is the membrane thickness [m] and D is the diffusion coefficient [m^2 s^{-1}]. The intercept with the time axis, resulting from the plot of Q_t versus time is defined as the time lag, Θ, (s):

$$\Theta = \frac{l^2}{6D} \tag{2.7}$$

For ideal gases, where the membrane is the only resistance in the system and where the permeate is measured by a pressure transducer without significant delay, for instance in a fixed volume pressure increase setup, Θ is measured directly from the permeation curve of permeate pressure *versus* time. However, the response of any other gas analyser depends not only on the time lag of the membrane itself, but there is an additional instrumental time lag, representing the total residence time of the permeating gas in the system before reaching the analyser. The measured time lag is then given by:

$$\Theta_i = \Theta_0 + \Theta_{Mem,i} \tag{2.8}$$

Where Θ_0 is the instrumental time lag and $\Theta_{Mem,I}$ is the time lag induced by the diffusive transport across the membrane itself for each gas species i. The value of Θ_0 is very low for the classical time lag setup, where a pressure sensor registers the permeate pressure. For constant pressure variable volume systems, subject of the present work, the total residence time of the permeating gas in the system, and thus Θ_0, may not be negligible. Substituting eq. (2.7) in eq.(2.8) yields:

$$\Theta_i = \Theta_0 + \frac{l^2}{6D_i} \tag{2.9}$$

Thus, for a set of membranes with different thicknesses, a plot of Θ *vs.* l^2 should yield a straight line with slope 1/6D, intersecting the vertical axis at the value Θ_0. Once the value of Θ_0 is known, the diffusion coefficient can be determined by a single measurement, after subtraction of the instrumental time lag from the overall time lag:

$$D_i = \frac{l^2}{6\left(\Theta_i - \Theta_0\right)} \tag{2.10}$$

2.4.1.1 Instrumental time lag in the mixed gas system

As anticipated above, in contrast to the fixed volume setup, the variable volume setup has a non-negligible residence time of the gas in the analyser and in all tubing, and this residence time contributes to the overall time lag. The individual sections contributing to the residence time are highlighted in Figure 2.5. Only the sections directly after the six-way valve or four-way valve (respectively on the sweep gas and in the vacuum setups) are relevant for Θ_0, because the feed stream is already flowing before switching this valve from the purge position to the test position. To optimize the method, each part of the system should have a minimum residence time, and thus thin tubes, so that Θ_0 remains small. On the other hand, the pressure drop in the lines should be low too, which prohibits the use of very thin tubes. For the given system, 1/8" tubes offer the best compromise between small volume and low pressure drop (See A1). Under the operation conditions generally used, namely a sweep flow rate from 30 $cm^3\ min^{-1}$ up to 50 $cm^3\ min^{-1}$ and a feed flow rate of ca. 200 $cm^3\ min^{-1}$, the flow regime is laminar. This means that the transient related to the gas permeation through the membrane is further widened in the tubes. However, the time lag can still be determined by the tangent method as for the pure gas permeation in the fixed volume setup.

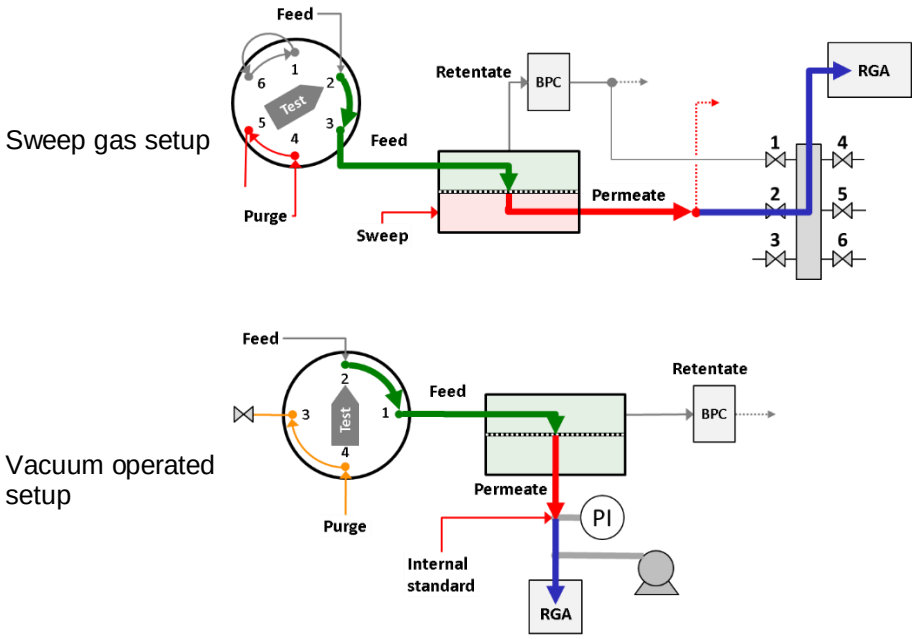

Figure 2.5. Scheme showing for both setups the contributions of the flowing gas to the total time lag of the system just after switching from purge to test mode. The feed flow (thick green arrows), permeate/sweep flow (thick red arrows) and flow through the injection port into the analyser (thick blue arrows) each contribute to the instrumental time lag given by Eq (2.9). Note the fundamental difference between the sweep gas setup with minimum volume lines in the permeate and analysis section and the vacuum operated setup with voluminous vacuum connections but with low pressure.

The instrumental time lag is the sum of the contributions of the feed flow reaching the membrane surface, downstream flow (permeate plus sweep, if used) reaching the inlet of the mass spectrometer, and sampled gas flow reaching the analyser across the capillary or restriction:

$$\Theta_0 = \frac{V_{Feed}}{\phi_{Feed}} + \frac{V_{Downstream}}{\phi_{Downstream}} + \frac{V_{Inlet}}{\phi_{Inlet}} \qquad (2.11)$$

Where V_{Feed}, $V_{Downstream}$, and V_{Inlet} are the volume of the feed side, the volume of the permeate side until the sampling point, and the volume of the injection line, respectively. Note that these volumes are obviously constant, and the term '*variable volume method*', used for this system, refers to the fact that the permeate gas flows away from the system. The terms ϕ_{Feed}, $\phi_{Downstream}$, and ϕ_{Inlet} indicate the respective total volumetric flow rates in that part of the setup at given temperature and pressure:

$$\phi = Q \cdot \frac{p_0}{p} \cdot \frac{T}{T_0} \qquad (2.12)$$

For the downstream side in the sweeping gas setup:

$$\phi_{Downstream} = \phi_{Perm} + \phi_{Sweep} \quad (2.13)$$

where ϕ_{Perm} and ϕ_{Sweep} are the flow rates of the permeating gas and of the sweeping gas, respectively. For the vacuum setup:

$$\phi_{Downstream} = \phi_{Perm} + \phi_{Int.std.} \quad (2.14)$$

where $\phi_{Int.std.}$ is the flow rate of the internal standard. For a membrane with a given thickness, the time lag becomes:

$$\Theta_i = \Theta_0 + \Theta_{Mem,i} = \frac{V_{Feed}}{\phi_{Feed}} + \frac{V_{Downstream}}{\phi_{Downstream}} + \frac{V_{Inlet}}{\phi_{Inlet}} + \frac{l^2}{6D_i} \quad (2.15)$$

In the case of a barrier film with pinhole defect, the membrane time lag becomes negligible and $\Theta = \Theta_0$. Thus, eq. offers two independent ways to determine the instrumental time lag, directly for porous membranes without time lag, or via extrapolation of a set of membranes with different thicknesses via:

$$\Theta_0 = \lim_{l \to 0}(\Theta_i) \quad (2.16)$$

In the sweeping gas system, the value of V_{Inlet} is fixed for the instrument and that of ϕ_{Inlet} is dictated by the capillary used, the type of gas, and the pressure at the permeate side (atmospheric pressure in the current setup). If $\phi_{Perm} = \phi_{Sweep}$, then the gas flowing at the downstream side is nearly pure Argon and ϕ_{Inlet} becomes independent of the permeating gas. Theoretically, ϕ_{Inlet} depends also on the atmospheric pressure, which defines the pressure drop over the capillary, but since atmospheric pressure is constant within a few percent, this is believed to cause negligible variation in the overall time lag. The values of V_{Feed} and $V_{Downstream}$ depend on the membrane size, valves and various connections in the experimental setup. If the stage cut is negligible, then for a series of experiments with different ϕ_{Feed} and ϕ_{Sweep}, V_{Feed} can be determined experimentally from the slope of the curve of Θ_i vs. $1/\phi_{Feed}$, and if $\phi_{Perm} = \phi_{Sweep}$, then $V_{Downstream}$ can be calculated from the slope of the curve of Θ_i vs. $1/\phi_{Sweep}$. Alternatively, the different parameters can be solved simultaneously by a least squares fitting procedure (section 2.5.3.3).

In the vacuum system, $V_{Downstream}$ is fixed and should be determined measuring the volume of the tubings. On the other hand, $\phi_{Downstream}$ depends on the permeate pressure and on the pumping

speed of the vacuum pump, as well as the flow rate of the internal standard, which must all be kept as constant as possible.

2.4.2 Gas permeation on the fixed volume time lag system for pure gases

For a fixed-volume pressure increase setup, the permeability is determined from the steady state permeate pressure increase rate, as described in detail in Annex A1. The permeability is calculated directly from the slope of *dp/dt* in the pseudo steady state regime of the pressure increase curve:

$$P = \frac{V_P \cdot V_m \cdot l}{R \cdot T \cdot A \cdot p_f} \cdot \frac{dp}{dt} \qquad (2.17)$$

In which R is the universal gas constant [$8.314 \cdot 10^{-5}$ m^3 bar mol^{-1} K^{-1}], T is the absolute temperature [K], A is the exposed membrane area [m^2], V_P is the permeate volume [m^3], V_m is the molar volume of a gas at standard temperature and pressure [$22.41 \cdot 10^{-3}$ m^3_{STP} mol^{-1} at 0 °C and 1 atm], p_f is the feed pressure [bar] and S is the gas solubility [m^3_{STP} m^{-3} bar^{-1}]. P is given in [m^3_{STP} m^{-2} h^{-1} bar^{-1}]

After calculation of the diffusion coefficient from the time lag in eq. (2.7) and assuming the validity of the solution-diffusion model, the solubility can be determined indirectly from the permeability and the diffusion coefficient by the simple relation:

$$S = \frac{P}{D} \qquad (2.18)$$

2.4.3 Gas permeation on the variable volume system for pure and mixed gases

Pure and mixed gas permeation experiments were carried out on the variable volume instrument using Argon as a sweeping gas and/or as an internal standard. When using sweeping gas conditions, the permeation rate of each species follows directly from the known sweep flow rate, Q_{Ar}, and the ratio of partial pressures of the gas of interest (eq.(2.3)) and of argon, p_{Ar}:

$$Q_{P,i} = Q_{Ar} \cdot \frac{p_{P,i}}{p_{Ar}} \qquad (2.19)$$

This yields the permeability coefficient, P_i, and permeance, Πl, for each component:

$$P_i = \frac{Q_{P,i} \cdot l}{\left(p_{F,i} - p_{P,i}\right) A} \tag{2.20}$$

$$\Pi_i = \frac{Q_{P,i}}{\left(p_{F,i} - p_{P,i}\right) A} \tag{2.21}$$

Where l is the membrane thickness, A is the membrane area and $p_{P,I}$ is the partial pressure of gas i in the feed:

$$p_{F,i} = x_i \cdot p_F \tag{2.22}$$

Where x_i is the mole fraction of gas I in the feed and p_F is the feed pressure. The mixed gas selectivity is calculated as the ratio of the permeability coefficients or permeances:

$$\alpha_{i/j} = \frac{P_i}{P_j} = \frac{\Pi_i}{\Pi_j} \tag{2.23}$$

An important parameter is the stage cut, defined as the fraction of each component in the feed gas which permeates the membrane, and it is given by:

$$Stage\ cut_i = \frac{Q_{P,i}}{Q_{F,i}} \times 100\% = \frac{Q_{P,i}}{x_i \cdot Q_F} \times 100\% \tag{2.24}$$

Where x_i is the molar fraction of gas I in the feed and Q_F is the total feed flow rate. This value should be low to guarantee that no significant polarization phenomena occur.

A similar data evaluation is used when using the gas permeation under vacuum conditions. In this case, the volumetric flows of the gas(es) under study and the argon in the downstream circuit of the permeation cell, respectively Q_i and Q_{Ar} ($cm^3_{STP}\ min^{-1}$) and the partial pressure of each gas, p_i and p_{Ar} (mbar), are related to each other according to equation:

$$\frac{Q_i}{Q_{Ar}} = \frac{p_i}{p_{Ar}} \tag{2.25}$$

The flux of the gas in the permeate, J_i, ($cm^3_{STP}\ cm^{-2}\ min^{-1}$) is the ratio of the flow rate of the gas through the membrane and the membrane area (cm^2), and can be written as:

$$J_i = \frac{Q_{Ar}}{A} \times \frac{p_i}{p_{Ar}} \tag{2.26}$$

The permeability coefficient and selectivity are the same as in equations (2.20) and (2.23).

2.5 Results and discussion

2.5.1 Membrane preparation

The thicknesses of the membranes prepared in this work are listed in Table 2.1. Both for the Pebax® and for the Hyflon® membranes, there is a slight variation in the properties depending on the casting procedure and the membrane thickness. Pebax® is a semi-crystalline rubbery polymer with microphase separation of the polyether and polyamide domains, and the evaporation rate affects to some degree the microdomain size and the crystallinity. On the other hand, Hyflon® is known to retain residual solvent upon evaporation,[75,76] and since the evaporation speed is thickness dependent, this will influence gas transport properties. Both effects may thus lead to variation of the transport properties and therefore more samples were prepared, and only the ones with the most constant properties were selected for further evaluation. The PIM-EA-TB sample was solvent-cast and then methanol treated to reset the thermomechanical history, and subsequently aged for a sufficiently long time to return close to the properties of the as cast film.

Table 2.1:Average thickness (μm) of the membranes prepared and used in this work

Pebax® 2533		Hyflon® AD60X		PIM-EA-TB	
N1	91	N1	34.6	N1	150.8
N2	103.2	N2	78.4		
N3	157.2	N3	126.0		
N4	192.3	N4	172.9		
N5	225.7				

2.5.2 Pure gas permeation in the fixed volume time lag system

For all measurements, the results of the fixed volume time lag setup were used as a reference. For this purpose, two well-defined and reproducible samples were tested, namely the rubbery Pebax® 2533 and the glassy Hyflon® AD60X. Figure 2.6A and Figure 2.6C show the permeability and ideal selectivity for several gas pairs in four Pebax® 2533 samples with different thicknesses and, Figure 2.6B and D show the same data for four samples of Hyflon® AD60X. Beyond some random scatter in the data due to experimental error, there is no significant impact of the thickness on the permeability and selectivity. Figure 2.6E and Figure 2.6F show the dependence of the time lag on the square of the thickness for both polymers, confirming that for all tested gases the time lag follows eq. (2.9) very well, with only few seconds of experimental error (See Annex A3). This means that also the diffusion coefficient is essentially thickness-independent. For a microphase separated semi-crystalline block copolymers such as Pebax® 2533 this is not obvious because the microdomain formation, and indirectly the transport properties, may depend on the evaporation rate and thus on the thickness of the cast film. In any case, the present tests confirm that these four samples are suitable standards for the evaluation of the mixed gas transport

properties. The same is valid for the Hyflon® samples, although these samples show slightly more scattering in both the permeability and the time lag values, probably because their transport properties are known to be dependent on traces of trapped residual solvent in the polymer [75,76]. For this reason, the data for Hyflon® are suitable for validation of the method, but they are not accurate enough to be used as a reference material for determination of the instrumental time lag (section 2.5.3.2). Due to their glassy nature, the Hyflon® samples show a much stronger size selectivity than Pebax®, resulting in a higher helium permeability than the CO_2 permeability and in a much longer time lag for the relatively bulky CH_4 than for the smaller molecules.

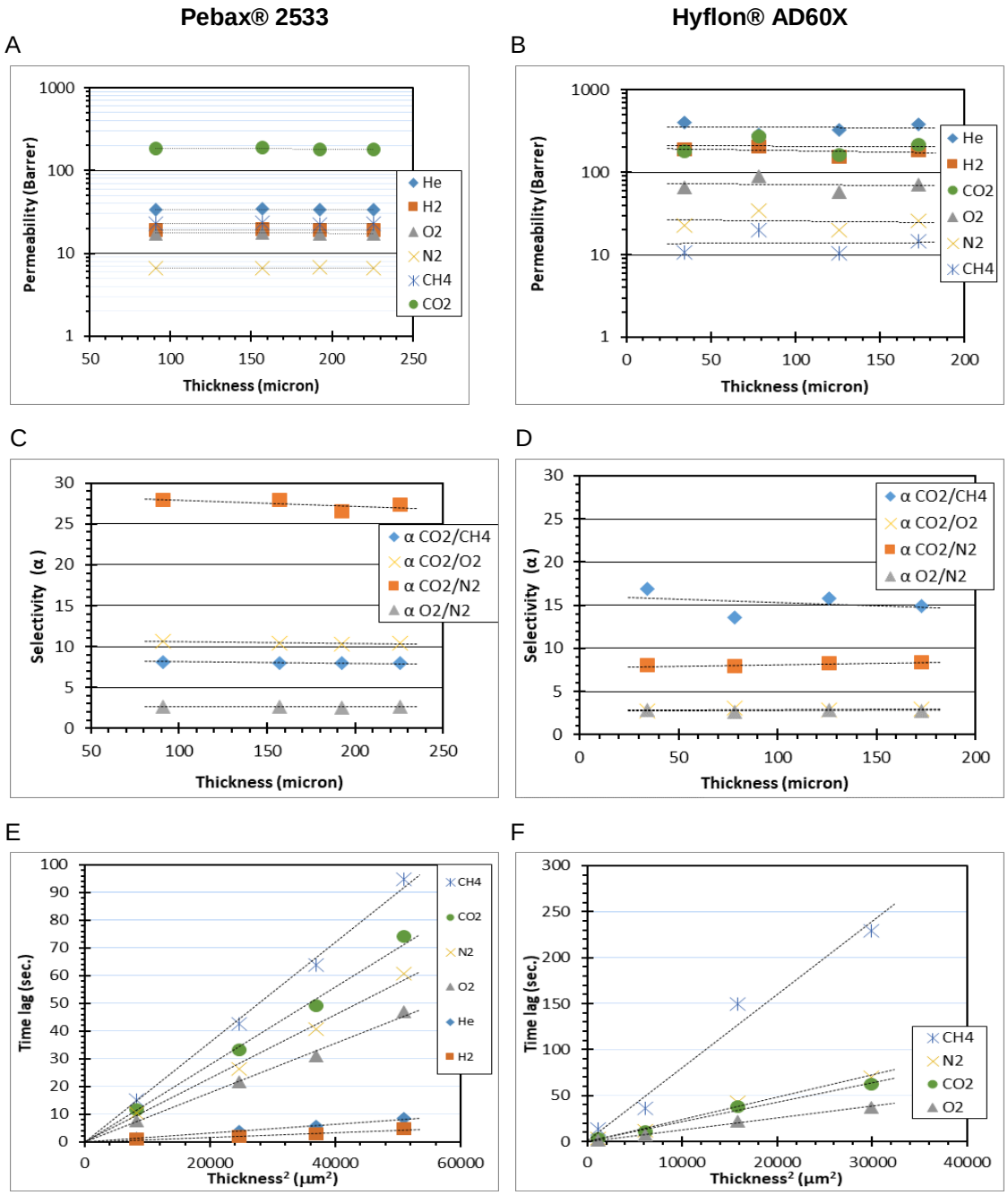

Figure 2.6. Thickness dependence of permeability (A,B) for Pebax® 2533 (left) and Hyflon® AD60X (right) with their ideal selectivity (C,D) for selected gas pairs. Determination of the diffusion coefficient for membranes with different thicknesses according to eq.(2.7) , $D=l^2/6\Theta$ (E,F)

For comparison, Figure 2.7 shows the response of the instrument for a sample of aluminium foil with a single tiny pinhole made with a needle. In spite of the very tiny hole, the pressure increase rate of this film is extremely fast, because pore flow is orders of magnitude faster than diffusion through dense films. All six tested gases show a very short delay of less than 0.1 seconds (inset) in the pressure increase curve, and the pressure of the first point is insignificant compared to the increase rate during the experiment. Thus, the instrumental time lag for this machine is negligible compared to the time lags observed in the Pebax® and Hyflon®samples in Figure 2.6E and Figure 2.6F. The pressure increase rate and thus the apparent permeance of the pinhole show the typical Knudsen behaviour, for which the permeability is inversely proportional to the square root of the molar mass, M_i, of the permeating species and the linear regression curve passes through the origin:

$$P_i \propto \frac{1}{\sqrt{M_i}} \tag{2.27}$$

Since Knudsen diffusion is several orders of magnitude faster than the diffusion in dense polymer membranes, a measurable value of time lag should indeed not be expected.

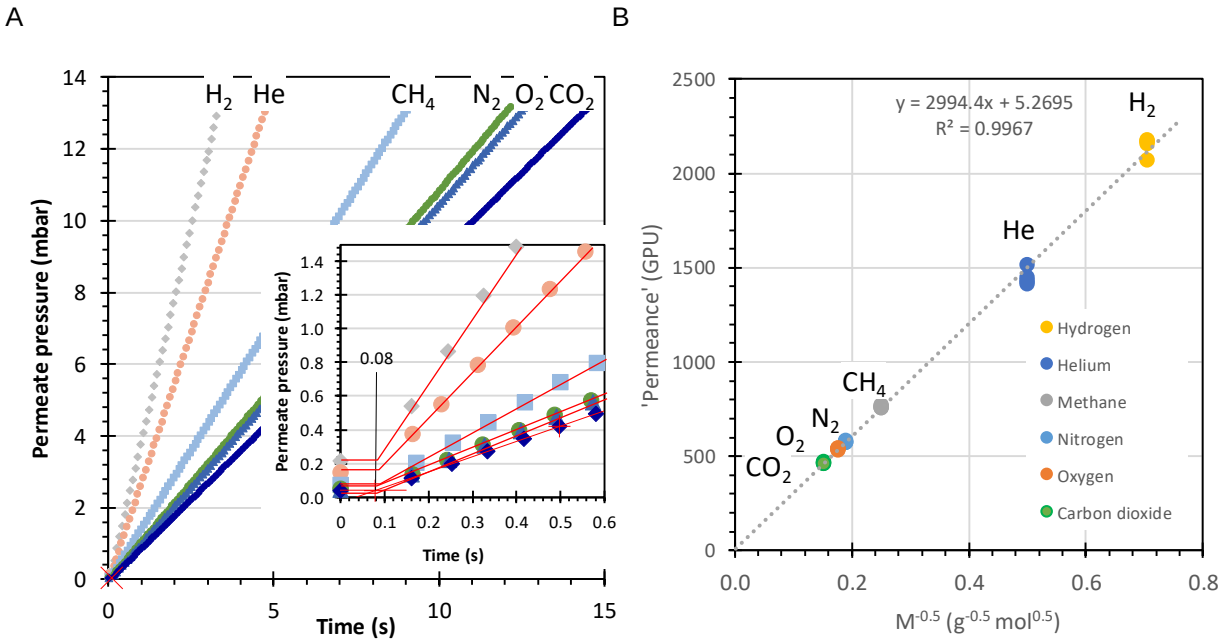

Figure 2.7. (A) Determination of the instrumental time lag by an aluminium foil sample with a pinhole defect. (B) Evidence of Knudsen flux in a plot of apparent permeance versus $M_i^{-0.5}$ at different pressures according to Eq. Error! Reference source not found.. The apparent permeance of different gases calculated on the basis on a hypothetical active area of 2.14 cm^2.

2.5.3 Pure and mixed gas permeation in the variable volume system using mass spectrometry

2.5.3.1 Sensitivity factor calibration

Both MS setups have their advantages and disadvantages. Watson and Baron argue that the low-pressure vacuum measurement device is preferable because it avoids interference of the sweeping gas with the permeation process.[19] On the other hand, operation at room temperature with an excess of sweeping gas allows a more stable analysis because the virtually constant composition (>99% argon) guarantees a constant gas sampling rate through the heated capillary.

The relative sensitivities of the different gases specified by the instrument supplier or tabulated in the literature are not universal enough to be used as a standard for high precision analysis [79] and therefore both mass spectrometric instruments were calibrated for the relevant gases periodically. In the present work, full calibration was performed by mixing each gas of interest with argon in the same concentration range expected during the permeability measurements[80]. The relative sensitivity was then determined at different gas ratios to check that it is independent of the composition of the mixture, as it should ideally be. Therefore, the gas mixture was fed into the MS and the relative sensitivity was determined from the ratio of the background-corrected signals and the ratio of the gas flow rate, and the argon flow rate, Q_{Ar} eq. (2.28):

$$RS = \frac{I_{Ar}}{I_i} \cdot \frac{Q_i}{Q_{Ar}} \qquad (2.28)$$

This procedure was repeated for each gas or gas mixture of interest, using the membrane cell with a perforated aluminium disc as a mixing element. It gives a better quantitative calibration of the partial pressures then the variable leak method used by Tremblay *et al.*[31] for a single gas, followed by correction of the ionization for different gases.

The instrument with sweeping gas was calibrated against the concentration of 36Ar, which is with ca. 0.3% natural abundance small enough to be then in the same range as the permeating gases. The instrument operating under vacuum was calibrated against the ^{40}Ar signal, because operating at much lower pressure this signal remains small enough to use the SEM ion detector for all gases. The relative sensitivity factor of each gas against argon is determined to convert the characteristic intensity of each gas present at the permeate compartment ($^{44}CO_2$, $^{15}CH_4$, ^{4}He, ^{40}Ar) in its corresponding concentration (%vol) or partial pressure (mbar). A method of calibration was set using the software Quadera to obtain the calibration factor of each gas in relation to the Argon internal standard. To perform this calibration, the permeate side is evacuated for 3 hours to ensure that it is clean and free from traces of gases. After this time, the permeate compartment is fed using the mass flow controllers with the internal standard gas (Argon) at 1 $cm^3\ min^{-3}$ and the gas to be studied with a flow rate of 50 $cm^3\ min^{-1}$, which allows to calculate of the volume

concentration of each gas. Having the volume concentration of each gas, Quadera software generates the corresponding sensitivity calibration factor of the gas under study in relation to the internal standard gas.

The resulting values of the relative sensitivities in relation to Argon for both methods are listed in Table 2.2. The values of ionization factor correction given by the supplier or given in the literature are typically represented in relation to nitrogen [31]. Recalculated values are given in Table 2.2 as well. Although, the ionisation of different gases under specific experimental conditions (ionization current and ionization energy) should in principle be very reproducible, and although the relative sensitivities are tabulated by the various producers, the different instruments and operation conditions introduce too large deviations to use these values for the calculation of the gas concentrations in the permeation experiments. Lieszkovszki *et al.* found that in different partial pressure analysers PPAs the response of a trace gas in argon and that of an argon trace in that same gas may depend differently on the partial pressures of each gas.[79] This confirms that calibration must necessarily be performed for each experiment in a specific way that most closely resembles the analysis conditions, and that calculations cannot rely on tabulated data available from other sources.

Table 2.2. Typical relative sensitivity factors for different gases and their selected fragments obtained experimentally in this work and calibrated in relation to Argon.

		Relative sensitivity			
Gas	**Signal**	**Sweeping gas setup** [a)]	**Vacuum setup** [a)]	**Reference values** [b)]	**Reference values** [c)]
Ar	^{40}Ar	n.d.	**1.00**	1.2	n.d.
	^{36}Ar	**1.00**	n.d.	n.a.	**1.00**
CO_2	$^{44}CO_2$	266.2	0.59	1.4	197.6
	^{28}CO	n.d.	0.01	122.8	22.5
O_2	$^{32}O_2$	202.8	n.d.	0.86	320.9
N_2	$^{28}N_2$	n.d.	n.d.	**1.00**	276.7
	^{14}N	29.7	n.d.	13.9	19.9
CH_4	$^{15}CH_3$	254.2	1.02	1.88	172.9
He	^{4}He	n.d.	0.87	0.14	1976

[a)] Experimentally determined under normal operating conditions. Values need frequent calibration.

[b)] From MaSsoft 7 library and Application note 282: Relative Sensitivity Measurements of Gases, Hiden Analytical.

[c)] From MaSsoft 7 library and Application note 282: Relative Sensitivity Measurements of Gases, Hiden Analytical. Values normalized for ^{36}Ar.

2.5.3.2 *Instrumental and membrane time lag determination.*

In contrast to the fixed volume setup, where the pressure in the permeate volume represents the total amount of permeated gas, the standard signal of the Mass Spectrometer is the concentration of the gases in the permeate, which is converted into the gas flow rate for each component, according to eq.(2.19). A typical curve is displayed in Figure 2.8A. Integration of this signal yields the cumulative permeated gas volume. In the present case, the total permeate volume, $V_{P,I}$, is obtained by integration of the flow rate [81]:

$$V_{P,i} = \int_{t=0}^{t} Q_{P,i}\,dt \qquad (2.29)$$

or for discrete measurement intervals:

$$V_{P,i} = \sum_{t=0}^{t} \left(\frac{Q_{P,i,t} + Q_{P,i,t+\Delta t}}{2} \right) \cdot \Delta t \qquad (2.30)$$

The unique feature of this procedure is that the online analysis of the gas composition by the MS signal is fast enough to allow simultaneous analysis of all components as a function of time, in contrast to analysis by gas chromatography, which may take up to several minutes for each single point. The procedure for the determination of the overall time lag is then fully equivalent to that described for the pure gases [81] and an example is given in Figure 2.8B).

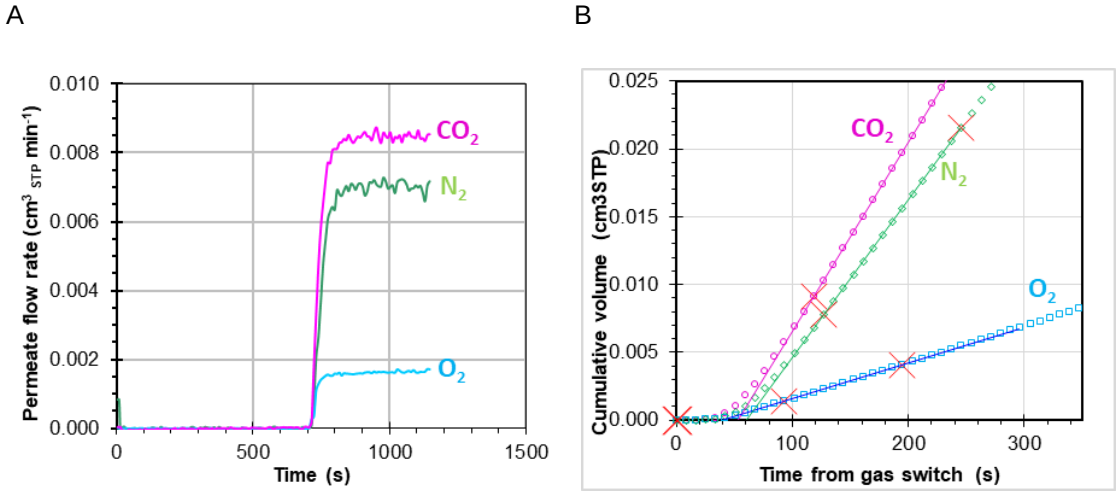

Figure 2.8. A) Example of the N_2, $CO_2$and O_2 permeate flow rates as calculated by eq.(2.19) from the start of the experiment, including 10 minutes for determination of the baseline. B) Corresponding cumulative permeate volumes after switching from purge mode to test mode, as determined by eq. (2.30), allowing for the simultaneous determination of all components in the gas mixture. Gas mixture: $N_2/CO_2/O_2$ 80/10/10 vol%, Membrane: 126 μm Hyflon®AD60X dense film. Red crosses indicate the fitting interval of the tangent.

Flaconnèche *et al.* who anticipated this method [81], apparently overlook the necessity to correct for the instrumental time lag due to the average residence time of the gases in the pipes, as discussed in section 2.4.1.1. The instrumental time lag and the diffusion coefficients were thus

determined as by measuring the time lag for a number of Pebax® 2533 and Hyflon®AD60X membranes with different thicknesses. Fitting of the experimental data with eq.(2.9) in a plot of the time lag as a function l^2 yields Θ_0 as the intercept with the vertical axis, and $1/6D_i$ as the slope of the curve (Figure 2.9). The time lag curve of an aluminium foil with a pinhole is shown for comparison. Watson and Baron use a slightly different setup, and determine the instrumental response from the pressure increase in the permeate chamber when a bypass valve to the pump is suddenly closed.[19]

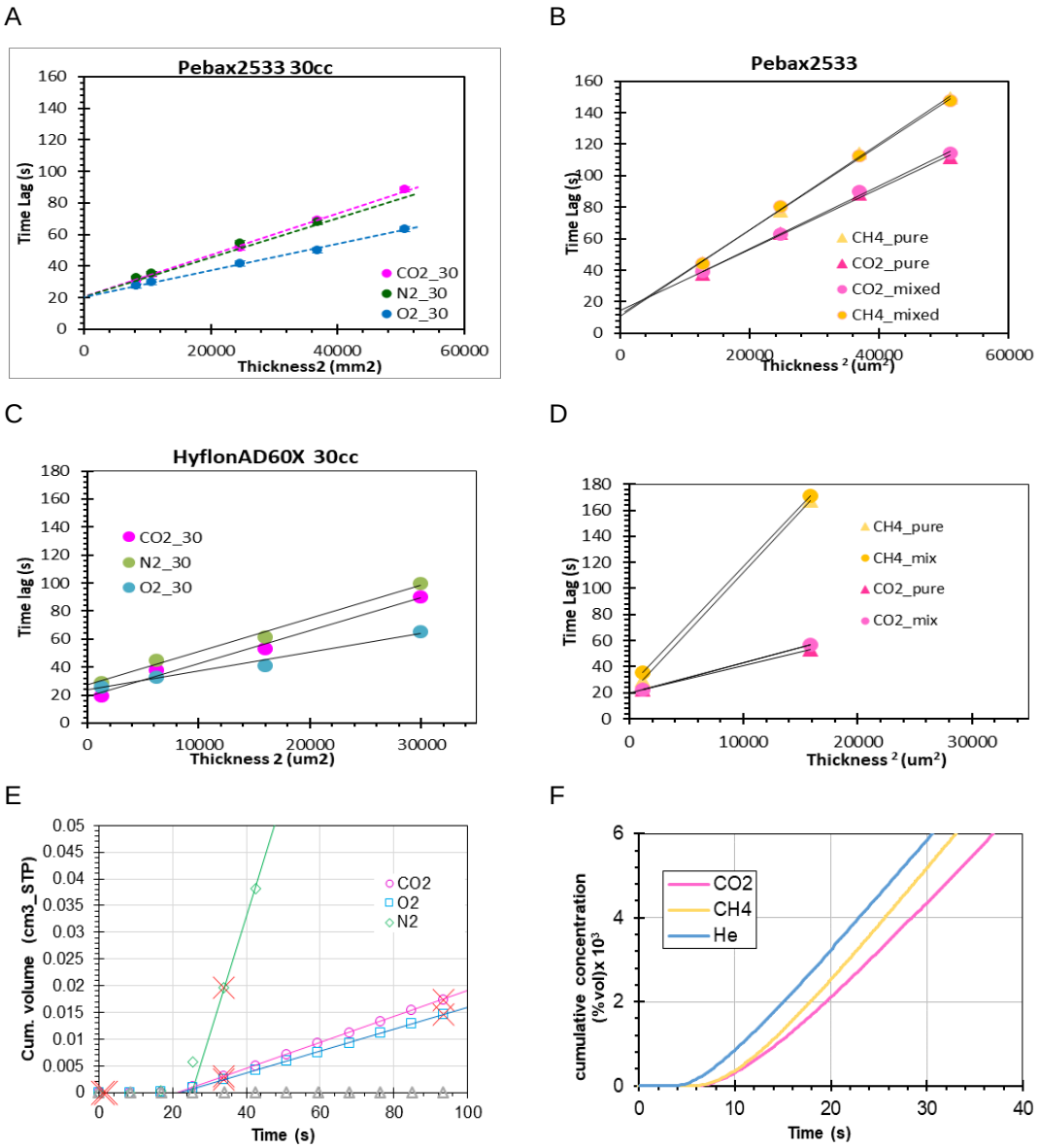

Figure 2.9. Determination of the instrumental time lag for membranes with different thicknesses according to the equation $\Theta_i = \Theta_0 + l^2/6D_i$ for Pebax® 2533 (A) and Hyflon® AD60X (C) in the sweeping gas setup at a sweep flow rate of 30 cm^3 min^{-1} and with gas mixture $N_2/O_2/CO_2$ 80/10/10 vol.%. Analogous results in the vacuum permeate setup (B, D) with pure CO_2 and CH_4 and in the mixture CH_4/CO_2 50/50 vol.%. Comparison with the instrumental time lag determined by an aluminium foil sample with a pinhole defect in the sweeping gas setup (E) and the vacuum setup (F), respectively. {Error bars in A an B are smaller than the symbol}

The Pebax® data extrapolate to an instrumental time lag of 21.5±3.7s in the sweeping gas unit for mixed gas, and to a value of 12.7±1.6s in the vacuum gas unit, for both pure and mixed gas (50% vol CO_2 in CH_4). For the given set of data, the scatter is somewhat large for the Hyflon® sample set, and the instrumental time lag as the intercept with the vertical axis yields too large differences with the different gases to be sufficiently reliable. Nevertheless, even for the Hyflon® samples, the diffusion coefficient of the different gases can still be determined with reasonable accuracy from the slope of the curves by eq.(2.9). The slope of the curves is significantly higher for the vacuum operated system than for the sweeping gas system, indicating a lower diffusion coefficient in the first, but this is mainly a result of the lower measurement temperature (see Table 2.3).

2.5.3.3 Calculation of diffusivities via simultaneous fitting procedure of all parameters

The extrapolation procedures shown in Figure 2.9 are somewhat sensitive to scatter in the individual data series. Therefore, slightly different values of the instrumental time lag may be found for different gases and for different sets of polymers, in particular for the Hyflon® AD60X samples. At constant temperature and pressure, the instrument-related parameters V_{Feed}, $V_{Downstream}$ and V_{Inlet} in eq.(2.15) must be independent of the experimental conditions and the gas species. For very low permeation rates and high sweep flow rate, the sweep stream is essentially pure argon and thus also ϕ_{Inlet} and V_{Inlet}/ϕ_{Inlet} are constants. Thus, a calculation procedure was designed to fit all experimental data simultaneously with eq (2.15) against the independent variables ϕ_{Feed}, ϕ_{Sweep} and l^2, yielding the values of the instrumental parameters V_{Feed}, $V_{Downstrea\imath}$, V_{Inlet}/ϕ_{Inlet} and the diffusion coefficients D_i for each gas. Details of the procedure are given in Annex A3 The corresponding values of the instrumental time lag, Θ_0, and the standard deviation of the individual time lags 21.0 ± 1.7s for Pebax® 2533 and 23.8 ± 3.1s for Hyflon® AD60X. The value of Pebax® 2533 is low enough for accurate determination of the instrumental time lag and, subsequently, of the diffusion coefficient in new membranes. On the other hand, the slight scatter in the Hyflon® AD60X data results in a relatively large error in the instrumental time lag. In this case, the variations in the Hyflon® AD60X results are most likely due to differences in the properties of the membranes due to residual solvent and the casting history. The variation in the results is an effective difference in the properties and not an experimental error in the determination of the time lag. Therefore, the method is reliable for any sample, but for further evaluation of unknown samples, it is best to rely on the instrumental time lag determined with Pebax® 2533 or with an aluminium film with pinhole defect.

2.5.4 Comparison of the diffusion coefficients calculated from the different experimental set-ups used in this work

The calculated diffusion coefficients are listed in Table 2.3 and the values determined by the sweeping gas setup deviate less than 10% from the values determined by the fixed volume setup. The diffusion coefficients obtained for CO_2 and CH_4 in Pebax® 2533 by the vacuum setup deviate around 23% from the values determined by the classical single gas time lag method. This difference is most probably explained by the fact that these experiments were carried out at 17±1 °C instead of 23 °C. In fact, correcting the temperature from 17±1 °C to 23 °C, as explained below using the equation (eq. (2.31)), an error less than 5% is obtained for pure and mixed gases from the values determined by the classical single gas time lag method.

The similarities of the diffusion coefficients calculated by the sweeping gas setup, the vacuum setup and the classical single gas time lag method indicates in the first place the good accuracy of the methods. Additionally it confirms that for these two polymers no anomalous behaviour or significant coupling effect occurs at the given conditions, so that the pure and mixed gas diffusion coefficients are essentially the same.

Table 2.3. Gas diffusion coefficients in Pebax® 2533 and in Hyflon® AD60X determined by different methods.

		Diffusion Coefficient (10^{-12} m^2 s^{-1})			
		Fixed volume setup [a] (25 ± 1 °C)	**Mixed gas variable volume setup**		
			sweep mode [b] (23 ± 2 °C)	**vacuum mode [c] (17 ±1 °C)**	
Polymer	**Gas**	**Pure gases**	**(N_2/CO_2/O_2 80/10/10 Vol%) Mixed gases**	**Pure gases**	**(50%vol CO_2 in CH_4) Mixed gases**
Pebax® 2533	N_2	145 ± 3.9	138.0 ± 4.6	n.d.	n.d.
	O_2	188 ± 4.5	196.8 ± 15.6	n.d.	n.d.
	CO_2	119 ± 3.0	121.8 ± 6.4	85.8±3.5(115.6)[d]	83±2.4 (112.4)[d]
	CH_4	92.5 ± 2.0	n.d.	60.6±1.3 (98.6)[d]	62±1.4 (100.3)[d]
Hyflon® AD60X	N_2	69.0 ± 2.8	68.2 ± 6.2	n.d.	n.d.
	O_2	131 ± 3.7	129.2 ± 10.7	n.d.	n.d.

CO_2	78.1 ± 3.0	64.4 ± 1.7	70.8	79.0
CH_4	20.9 ± 1.2	n.d.	17.8	18.6

[a] Data obtained from the slope of the curves in Figure 2.6E and Figure 2.6F with Eq.(2.10) ($D=l^2/6\Theta$). The indicated error is the standard deviation from the individually calculated diffusion coefficients for each thickness.
[b] Data obtained from the fitting procedure described in section 2.5.3.3 and Annex A3.
[c] Data obtained from the slope of the curves in Figure 2.6B and Figure 2.6D. [d] Values between parentheses are recalculated for 25°C by the Arrhenius equation, using E_{d,CO_2} = 27.2 kJ mol^{-1} reported for Pebax [82] and estimating E_{d,CH_4} = 43.17 kJ mol^{-1}, reported for ABS,[83] along with E_{d,CO_2} = 26.6 kJ mol^{-1}.[83]

The differences between the diffusion coefficients obtained in the mixed gas setup operated under vacuum mode, and on the other two setups, is mostly due to the lower temperature in the former instrument, operated at 17ºC. The values of Pebax were recalculated using the van't Hoff – Arrhenius equation, using the activation energy of diffusion:

$$D = D_0 \times e^{-\frac{E_d}{RT}} \qquad (2.31)$$

After temperature correction, there is much better agreement of the values on vacuum-operated mixed gas setup with those of the other setups. The activation energy for CH_4 was not available but was estimated by that of acrylonitrile–butadiene–styrene copolymer ABS. This choice seems justified, given the very close resemblance of the activation energy reported for CO_2 in Pebax and in ABS (Table 2.3).

2.5.5 Validation experiments - Effect of the CO2 concentration on the CO2/CH4 mixed gas transport in PIM-EA(Me)-TB

The method is validated for the permeation of CO_2/CH_4 gas mixtures in the polymer of intrinsic microporosity PIM-EA-TB [72,74] in order to verify the principle also for materials with nonlinear sorption behaviour. There is only a weak negative effect of the CO_2 concentration on the overall permeability coefficient of both gases (Figure 2.10A&B). On the other hand, typical permeation curves of CO_2 in the CO_2/CH_4 mixture on the vacuum setup show considerably faster permeation kinetics and thus a higher diffusion coefficient with increasing CO_2 concentration in the mixture (see Annex A4, Figure A4. 1). The nearly pressure-independent permeability suggests that the increase in diffusivity is accompanied by decrease in the solubility. This is indeed confirmed if we use the method for the quantitative analysis of the diffusion coefficient (Figure 2.10C), and for the indirect calculation of the solubility coefficient (Figure 2.10D). This is common for membranes with dual mode sorption behaviour. In the sweeping gas setup, the dual mode sorption behaviour affects CO_2 more than CH_4, causing a slight decrease in permselectivity with increasing pressure

(Figure 2.10A). In addition, this experiment shows weak hysteresis between the run with increasing CO_2 partial pressure (closed symbols) and subsequently decreasing CO_2 pressure (open symbols). This is due to CO_2 induced swelling of the aged matrix, leading to a slightly higher permeability and lower selectivity, and highlights the capacity of the in-line method to detect anomalies in the transport properties.

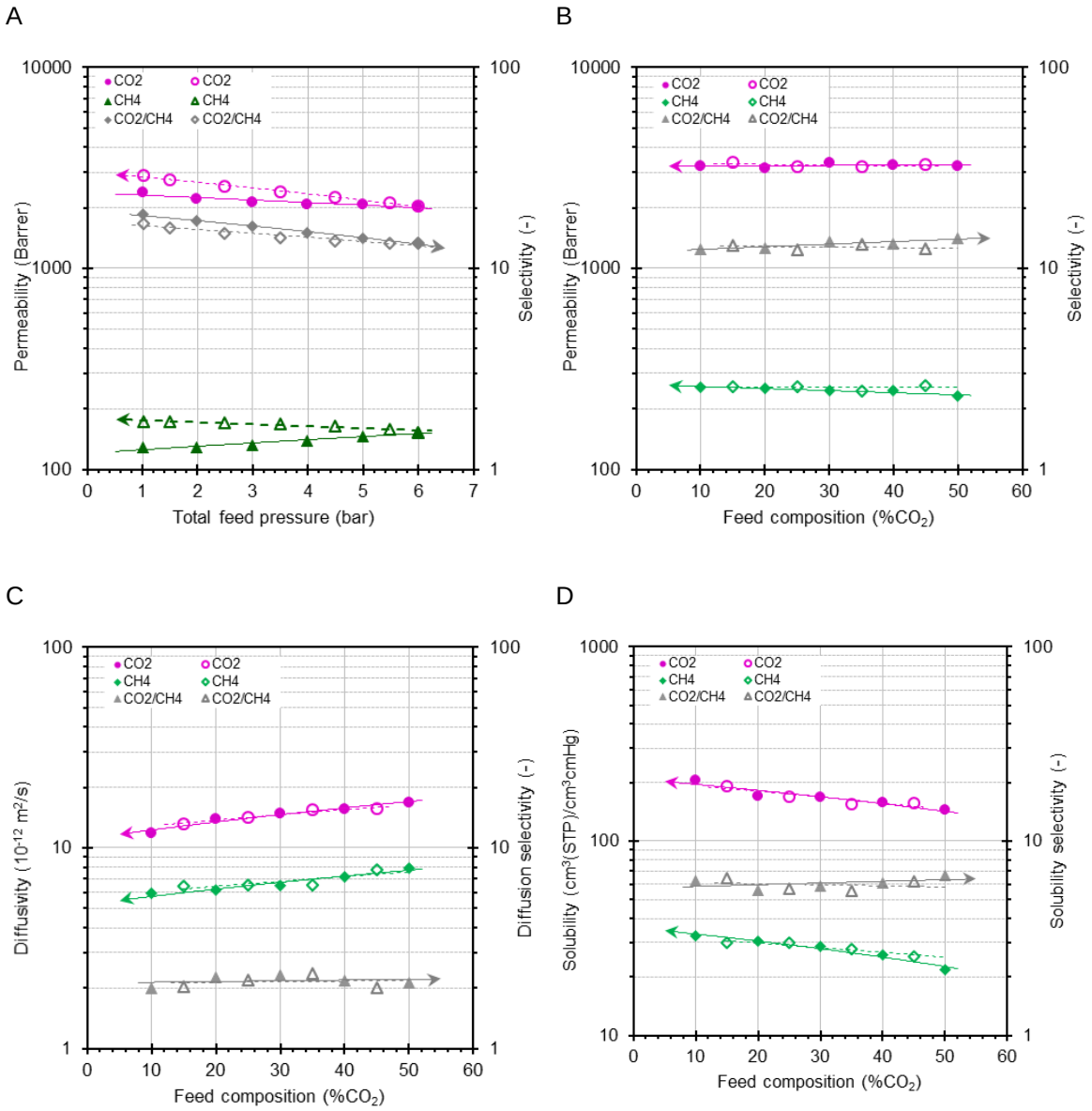

Figure 2.10. Dependence of the mixed gas CO_2 and CH_4 permeability and selectivity of sample PIM-EA-TB as a function of the total pressure in the sweeping gas setup (A) and as a function of the mixture composition in the vacuum setup (B) of sample PIM-EA-TB as a function of the gas mixture composition in the vacuum system. Sweeping gas system operating with mixture of 51/49 vol% CO_2/CH_4 in the pressure range from 1-6 bar(a) and vacuum system operating at a total feed pressure of 1.05 bar(a) and a composition in the range of 10-50 vol% CO_2. Concentration-dependence of CO_2 and CH_4 diffusivity and related selectivity (C) and indirectly calculated solubility (D). Filled symbols represent the runs with increasing pressure (A) or increasing CO_2 concentration (B-D) and open symbols represent the subsequently decreasing pressure or CO_2 concentration.

2.6 Conclusions

A novel method to determine the diffusion coefficient of individual components of gas mixtures in polymeric membranes was developed. The method, based on online analysis of the permeate composition during the transient stage of permeation, is much more powerful than the traditional time lag method in a fixed volume setup because of its unique capacity to detect different gases simultaneously. Rapid sampling by online mass spectrometry of the permeate composition allows accurate determination of the transient behaviour.

The samples used for the method development were first fully characterized on the classical fixed volume time lag instrument. Calibration of the response of this instrument by two independent methods confirms its virtually negligible instrumental time lag of ca. 0.08 s, independent of the gas type. The first method measures the time lag directly from the permeation transient of different gases through an aluminium film with pinhole, and the second method extrapolates the time lag of polymer films with different thicknesses to zero thickness. This method also confirmed the thickness-independent properties of the Pebax test samples. In contrast, the same approach yields a finite instrumental time lag for the mixed gas permeation setup, which represents the average residence time of the gases in the setup between gas exposure of the membrane and detection of the gases by the mass spectrometer. Rubbery Pebax®2533 was found to be more suitable than glassy Hyflon®AD for the method development and calibration of the instrumental parameters, requiring time- and history-independent membrane properties. In the sweeping gas setup, boundary conditions for accurate and reproducible determination of the mixed gas diffusion coefficients require that the time lag is independent of the permeation rate, and thus the latter must be negligible compared to the sweep flow rate. A low stage cut, by setting the feed flow rate much higher than the permeation rate, then guarantees that the measured transport properties only depend on the gas composition and pressure and not on other operation conditions.

The instrumental time lag is approximately 20 seconds in the sweeping gas setup and approximately 10 seconds in the vacuum operated setup. After correction for the instrumental time lag, the novel method can determine the mixed gas diffusion coefficients with reasonably low error for any gas mixture and any polymeric membrane with an intrinsic time lag of some ten seconds and higher.

The first validation experiments on the polymer of intrinsic microporosity, PIM-EA-TB, not only demonstrated the success of the method, but showed also the ability to detect the concentration and pressure dependency of the transport parameters, and other anomalous phenomena related to CO_2-induced dilation.

3 EVALUATION OF HYBRID POLYSACCHARIDE MEMBRANES FOR GAS DEHYDRATION USING ON-LINE MASS SPECTROMETRY

Submitted to Journal of Membrane Science as: Inês T. Meireles, Sofia C. Fraga, Rosa M. Huertas, Carla Brazinha, João G. Crespo, Isabel M. Coelhoso

The author was involved in planning all the experiments related with the gas permeation experiments coupled to the Mass Spectrometry, as well as on the data elaboration..

3.1 Summary

The removal of water from gas streams, in particular flue gas and biogas, is an important industrial operation. To mimic these industrial dehydration processes, permeation of water vapour, pure gases (CO_2, CH_4 and N_2) and gas mixtures containing 20 vol.% CO_2 + 80 vol.% N_2 and 70 vol.% CH_4 + 30 vol.% CO_2, at different conditions of relative humidity, was monitored by mass spectrometry. The potential of using hybrid polysaccharide membranes obtained from a low cost carbon source (glycerol) and crosslinked using (3-Glycidyloxypropyl) trimethoxysilane (GPTMS) as silica precursor by a sol-gel method was evaluated. The hybrid membranes developed showed barrier properties to all gases studied, with a gas permeability below 1 barrer, while exhibiting high water permeabilities and selectivities. When process in a biogas mixture, the water permeability was found to be three times higher than water permeability in a flue gas mixture, leading to a H_2O/CH_4 selectivity much higher than H_2O/N_2 selectivity. These membranes showed, under close-to-real conditions, that they have the ability to dehydrate mixtures, with the advantage of not losing CO_2 or CH_4, due to the low permeability values of these gases.

3.2 Introduction

Gas dehydration has a high industrial interest, since it can be used for the dehydration of natural gas, drying of compressed air, drying of gases for packaging purposes, roofing covers, humidity control in closed spaces, such as air conditioning in buildings, aviation and space flight, as well as water recovery from waste steam [84,85]. In particular, dehydration of flue gas, originated in the production of electricity by coal-fired power plants, has a great interest due to the energy saving in power plants and reduction of diffusion of pollutants through water that can cause “gypsum rain” [86,87]. Other potential application is biogas dehydration which, after purification, can be used as an alternative to natural gas and be distributed as power supply in rural and urban areas [88,89].

When compared to other dehydration methods (e.g. adsorption using desiccants and condensation), membrane-based dehydration (or drying) of gaseous streams has numerous benefits [90]. Membrane technology may involve a lower energy consumption (since the only energy consumed is the one required to maintain a partial pressure difference across the membrane [90]) and smaller footprint. Additionally, this technology is usually rather flexible and involves a compact modular design, easy to maintain and control [91,92].

In gas dehydration, hydrophilic polymers, such as ethyl cellulose, cellulose acetate, polyacrylonitrile, sulfonated polyetheretherketone (SPEEK) and poly(vinyl alcohol) are usually used [85]. The –OH groups present in these type of polymers are able to interact with water molecules, which are incorporated and diffuse through the polymers [84,93,94]. In the present work, the potential of using hybrid polysaccharide membranes for gas dehydration is investigated. Hybrid polysaccharide membranes were prepared using a microbial exopolysaccharide rich in fucose (FucoPol) obtained from a low-cost, abundant carbon source: glycerol, produced as a by-product by the biodiesel industry. This biopolymer was purified using a solvent free method (dia-ultrafiltration), similarly to[95] in order to reduce the environmental impact and increase the membrane process sustainability. The hybrid membranes were prepared, as described in our previous work [96], by incorporation of a SiO_2 network homogeneously dispersed by a sol-gel method using (3-Glycidyloxypropyl) trimethoxysilane (GPTMS) as a crosslinker silica precursor, combining the best properties of the inorganic network with the selectivity of the microbial polysaccharides. Preliminary results [96] demonstrated that these membranes are able to selectively transport water vapour, are stable and have reproducible performance for nitrogen dehydration during extensive operation.

Understanding the water vapour interaction with the membrane is extremely important, since water has a high affinity to the polymer inducing swelling or plasticization effects in the membrane structure [97,98]. The rearrangements caused by water vapour in the membrane structure impact on the membrane transport properties, namely in its flux and selectivity. On-line monitoring mass spectrometry (MS) has proved to be an efficient tool allowing to obtain the composition of the permeate stream at one data point each second (or less, if required), making possible to perform real-time monitoring during the whole permeation process. It has been used to characterize gas transport through dense membranes [31,39,97–99] as well as solute transport in pervaporation processes [39,40,70,100]. Moreover, mass spectrometry monitoring has the advantage of speed, smaller volume of samples, fewer losses of analytes and higher detection range, when compared to other techniques of detection, such as gas chromatography [40,101].

In this work, on-line mass spectrometry is used to monitor the permeation of water vapour and pure gases (CO_2, CH_4 and N_2) across the membranes developed, under different conditions of relative humidity. Gas mixtures containing 20 vol.% CO_2 + 80 vol.% N_2 and 70 vol.% CH_4 + 30 vol.% CO_2 have also been studied to mimic industrial applications, namely flue gas and biogas dehydration [8,88]. Experimental

3.2.1 Materials

(3-Glycidyloxypropyl) trimethoxysilane (GPTMS) purchased from Sigma-Aldrich (USA) and acetic acid glacial (99-100%) purchased from J.T. Baker (USA), were used as precursor and acid catalyst, respectively, in the sol-gel process. Calcium chloride (CaCl2) (>93.0 %) used as crosslinking agent was obtained from Fluka Analytical (USA); Magnesium nitrate hexahydrate (98.0 %) and magnesium chloride (99.0 %) were supplied by Alfa Aesar (UK), while sodium chloride (99.5 %) was purchased from Panreac Applichem (Spain). All these compounds were used to prepare the salt saturated solutions to adjust the water activity / relative humidity of the gases used in this work. Nitrogen (99.99 %), helium (99.99 %), carbon dioxide (99.99 %) and methane (99.99 %) used in the gas dehydration experiments were obtained from Irmasolda (Portugal).

3.2.2 Membrane preparation

The hybrid membranes were prepared as described in the previous work of Meireles *et al.* (2018) [96]. The pure dried biopolymer (1.5 %w/v) was diluted in distilled water during 8 h, at room temperature (20.0 ± 2.0 ºC). Then, 0.04 %v/v of acetic acid glacial was added as acid catalyst, and 7.0 w/w% of GPTMS precursor containing silica, was also added dropwise under vigorous magnetically stirring to the aqueous solution. The film forming solution for production of the hybrid polysaccharide membranes was maintained under stirring overnight at room temperature (around 22 ºC). After this, the aqueous solution was sonicated during 25 min, for degasification, before casting the membranes in Teflon petri dishes and drying at 30.0 ºC in an oven during 72h. When the membranes were dried, a crosslinking reaction was accomplished by immersion of the membranes in a solution of calcium chloride (2 g/100 ml) during 5 min. The liquid in excess was removed using a tissue paper and the membranes were dried at an ambient temperature and relative humidity of 20.0 ± 2.0 ºC and 40.0 ± 3.0 %, respectively.

3.2.3 Single and mixed gas permeation experiments under dry and humidified conditions

The permeability of three different pure gases - CO_2, N_2 and CH_4 - was evaluated analysing the permeate composition by on-line mass spectrometry (MS) under vacuum conditions. The experimental set-up is represented in Figure 3.1.

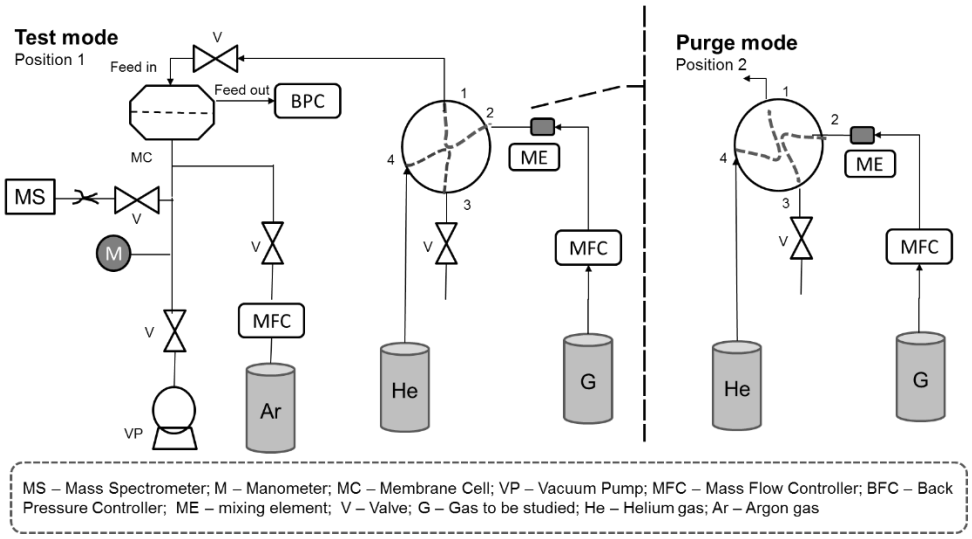

Figure 3.1: Experimental set-up for pure dry gas permeation

The experimental set-up consists in a membrane cell containing the membrane under study, mass flow controllers for each gas to be studied (EL-FLOW electronic, Bronkhorst, The Netherlands) and a back pressure controller (EL-PRESS electronic), in order to control the pressure of inlet and outlet streams of the membrane cell. A mass spectrometer (Prisma Plus QMG 220 M2, Pfeiffer Vacuum, Germany) with an axial beam ion source with an emission current of 1.0 mA and electron energy of 70.0 eV, single quadrupole and secondary electron multiplier SEM detection was used. The permeate side was maintained at low pressures through a dry, oil free diaphragm vacuum pump (Pfeiffer vacuum, MVP 015, Germany) and using a constant argon flux of 1.0 ml/min as an internal standard control fed directly to the permeate. The following operating parameters were controlled in all permeation experiments: feed pressure of gas at 1.05 bar, total flow rate of the inlet feed stream (pure gas) at 50.0 ml/min and argon flow rate of 1.0 ml/min. The temperature of the system was kept at 22.0 ± 2.0 ºC, to avoid variations in the signal of the MS during different permeation experiments. In order to clean the system and membrane, before and after each experiment, the feed side of the membrane cell is purged with helium. A four-way valve (as can be seen in Figure 3.1) is used to switch from the purge mode (position 2) to the test mode (position 1) in a fast way, without changing the inflow feed rate to the membrane cell. When the concentration of all gases under study in the permeate are at their lowest values (indicating that the system is completely clean), the gas stream under study is connected to the feed circuit using the four-way valve (test mode, position 1). After that, the permeate is monitored on-line with the MS for the composition of each gas (CO_2, N_2 and CH_4). The MS electrical signal is acquired and converted to volume fraction and partial pressure through the calibration method described in 2.5. In this study, the following m/z signals were selected to detect the respective gases or vapours: m/z=4 for helium, m/z=18 for water vapour and m/z=40 for argon. For CO_2 we choose m/z=44 and 28, for N_2 m/z= 28 and 14 and for CH_4 m/z= 15 and 14, in order to increase the signal of these gases, taking into account that the experiments were performed under vacuum and the flux of gases through the membrane was low. In addition, it is necessary to assure which signals

correspond to each gas when they are mixed, since some gases have overlapping signals (such as m/z=28, which corresponds to CO_2 and N_2).

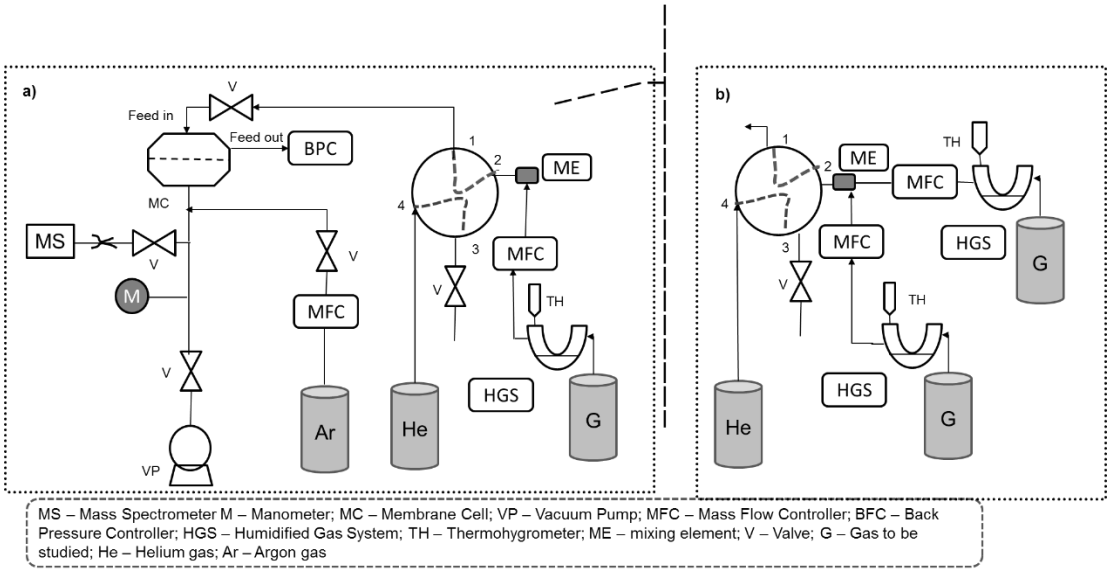

Figure 3.2: Experimental set-up for permeation in test mode (position 1) of: a) humidified single gas and b) humidified mixture of gases

When testing the permeation of humidified gases (see Figure *3.2* a) and b)), each gas under study circulates through a trap that contains a saturated salt solution, with a defined water activity (referred in Figure 3.1 as HGS – Humidified Gas System). Three different salt solutions were used, corresponding to different water activities (a_w) for the system water-air: magnesium chloride (a_w=0.324), magnesium nitrate (a_w=0.520) and sodium chloride (a_w=0.769). The water activity was calculated through eq. (3.1)

$$a_w = \frac{p_w}{p_w^*} \qquad (3.1)$$

where p_w corresponds to the partial pressure of water in the feed and p_w* is the vapour saturation pressure of water calculated with the Antoine equation.

The temperature (ºC) and % gas humidity content, expressed as the percentage of the mass of water and the mass of dry gas/mixture of gas, were measured with a thermohygrometer (Vaisala HMI41 indicator and HMP42 probe, Finland). This humidity sensor uses as operating principle the changes on the capacitance of the sensor (thin polymer film) by absorbing water molecules [102]. The experiments were performed at least two times.

The experimental set-up shown in Figure 3.2 b) was used to study the dehydration of flue gas and biogas. Before mixing, each gas circulates separately through the magnesium nitrate saturated solution (a_w=0.52) and through the mass flow controller to assure a defined flow of each humidified gas and, consequently, a given mixture. After this, and before starting permeation, the humidified gas mixture is circulated through the mixing element, in order to ensure a good mixing.

The experimental procedure is the same as described above for single gases under humidified conditions. The mixture used in order to mimic the biogas is composed by 70.0 v/v% of CH_4 and 30.0 v/v% of CO_2, while to mimic the flue gas composition, a mixture of 80.0 v/v% of N_2 and 20.0 v/v% of CO_2 was used. Each experiment was repeated at least twice.

3.2.4 Calibration method

The MS calibration is based on the work of Fraga *et al.* (2017) [99]. A mass spectrometer (Prisma Plus QMG 220 M2, Pfeiffer Vacuum, Germany) was used with an axial beam ion source, emission current 1 mA, electron energy 70eV, single quadrupole, secondary electron multiplier SEM detection. Mass spectrometry identifies and quantifies the target compounds, according to their specific mass to charge ratio (m/z) and intensity of electric signal, providing a characteristic mass spectrum for each specific compound. The calibration was performed using the software Quadera (v4.61) (Pfeiffer Vacuum, Germany), which converts the characteristic intensity (m/z) of each gas (m/z_{N2}=28 and 14, m/z_{CO2}=44 and 28, m/z_{CH4}=15, m/z_{Ar}=40, m/z_{He}=4 and m/z_{H2O}=18), present in the permeate compartment, into volumetric concentration (vol%) or partial pressure.

3.2.5 Calculation methods

The permeation flux of each gas, J_i, based on the flow-rate and molar fraction of standard gas argon, can be calculated, according to Hasegawa *et al.* (2008) [103], as:

$$J_i = \frac{Q_{Ar}}{A} \times \frac{y_i}{y_{Ar}} \qquad \left(\frac{m^3[STP]}{m^2 \cdot s}\right) \tag{3.2}$$

where Q_{Ar} is the volumetric flowrate of standard gas argon, A is the effective membrane area of permeation (4 cm^2), y_i and y_{Ar} denotes the mole fraction of gas i in the permeate side and the molar fraction of the argon, respectively.

Taking into account that gas permeation is described based on the solution-diffusion model, the permeation flux of gas i is described also as follows [28]:

$$J_i = \frac{P_i}{l}(p_{i0-}p_{il}) \tag{3.3}$$

where l is the membrane thickness, P_i is the gas permeability, p_{io} and p_{il} are the partial pressures of gas i in the feed and the permeate side, respectively.

3.3 Results and discussion

3.3.1 Permeability for pure gases under dry conditions

From the MS results the volumetric concentration of each compound is obtained along time. Using Equations (3.2) and (3.3), respectively, the flux and permeability of each compound can be calculated. The permeation data for CO_2, is given as an example in Figure 3.3

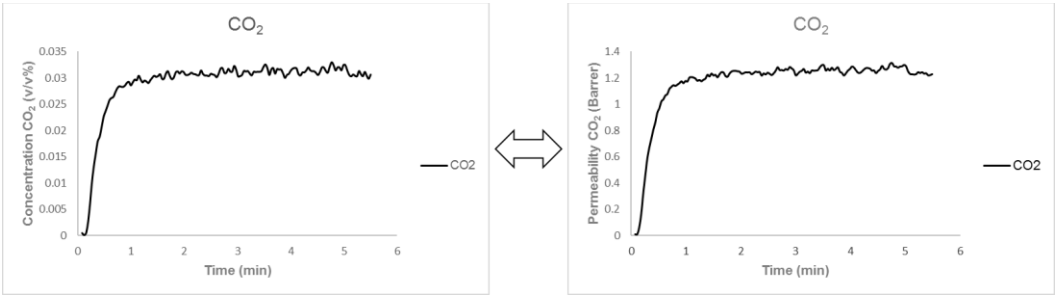

Figure 3.3: Permeation experiment with dry CO2: concentration of CO2 in the permeate when using the FucoPol+GPTMS+CaCl2 membrane, and corresponding permeability, represented against time (T=21 ºC and pperm=70 mbar)

The results of permeability for the various pure dry gases studied are presented in Table 3.1.

Table 3.1: Permeability of dry gases.

Gas	P (barrer)
CO_2	1.33 ± 0.13
N_2	0.17 ± 0.01
CH_4	0.02 ± 0.01

Regarding the results obtained, CO_2 has the highest permeability, 1.33 ± 0.13 barrer, followed by N_2 with a permeability of 0.17 ± 0.01 barrer and CH_4, with a permeability value of 0.02 ± 0.01 barrer. These very low values of permeabilities, in the range of membranes with excellent barrier properties, were possible to be accurately and reproducibly obtained by Mass Spectrometry. According to the literature, the low values of gas permeability are characteristic of polysaccharides [104,105] and, in addition, the higher values of carbon dioxide permeability compared with the other gases are characteristic of membranes that present hydrophilic groups [106]. These membranes follow the general behaviour of glassy polymers, where the permeability is controlled by diffusion instead of solubility, which means that the permeability decreases with the increase of the kinetic diameters (3.30 Å for CO_2; 3.64 Å for N_2 and 3.80 Å for CH_4 [107]) of the penetrants (permeability of CO_2>N_2>CH_4) [108].

3.3.2 Permeability of humidified gases – effect of water vapour on the permeability of pure gases

Figure 3.4 shows the permeability of each gas (CO_2, N_2 and CH_4) against different percentage of the gas humidity content (% of $g_{H2O}/g_{dry\ gas}$). The different salts used in the trap (see Figure 3.2a))) led to different humidified conditions at the feed compartment measured by the thermohygrometer, in terms of the percentage of the gas humidity content.

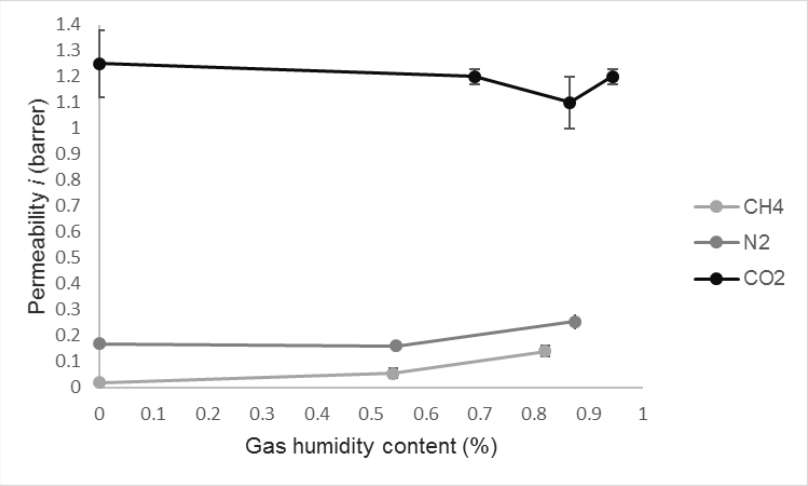

Figure 3.4: Results for pure gas permeation with different gas humidity content

From the results obtained (Figure 3.4) it is possible to infer that the CO_2 permeability was found to be almost constant, throughout the whole gas humidity content studied. The N_2 permeability was constant till a gas humidity content of 0.55 %, while the CH_4 permeability slightly increased with the increase of water vapour content, in the same conditions. At higher water mass fractions, the N_2 and CH_4 permeabilities increase dramatically, due to plasticization effects that occur in the membrane, leading to a most significant increase of gas diffusivity [109]. In the case of CH_4, the permeability value could not be measured for the highest humidity content (1.20 %) because a sharp increase of permeate pressure was observed and, hence, permeability (much high than 3.2 barrer), strongly suggesting a membrane leak. This behaviour may be due to the extremely high extent of membrane swelling. Similar results were reported by Chen *et al.* (2015) [109] for the permeation of humidified CO_2 and CH_4 through cellulose acetate membranes which, at a water vapour activity of 0.45, suffer from a high swelling effect leading to an exponential increase of CO_2 and CH_4 permeability.

Taking into account the results obtained, it may be concluded that the hybrid polysaccharide membrane is affected by swelling and plasticization with increasing of gas humidity content to the values above (0.94 % of gas humidity content)). Nevertheless, it is also noticed that water vapour affects more the permeability of gases controlled by diffusion (CH_4 and N_2) than the permeability of CO_2, which permeability is mostly controlled by solubility [110]. In the work of Neves *et al.*

(2010) [110], it was found a similar behaviour for ionic liquid membranes. The higher permeability of CO_2 when compared to N_2 and CH_4 may be explained by the high solubility of this gas in water, when compared with other gases – 34.0, 1.3 and 1.0 mmol/l_{water} at 25.0 ºC, respectively, for CO_2, CH_4 and N_2 [111,112].

The water permeability at different gas humidity content is presented in Figure 3.5

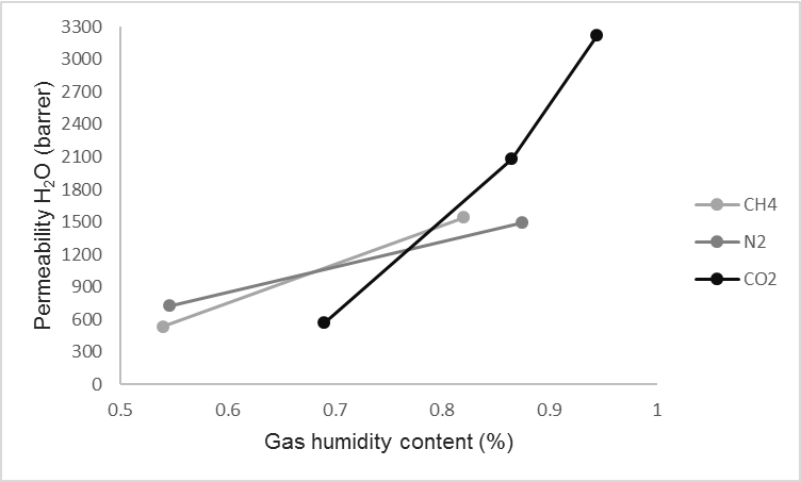

Figure 3.5: Water permeability of the humidified gases (CO2, N2 and CH4) for the hybrid polysaccharide membrane at 22.0 ºC.(The errors are so low that not appear in the graph)

Comparing the water vapour permeability values (Figure 3.5) with the gases' permeability (Figure 3.4), it can be concluded that this hybrid polysaccharide membrane presents much higher water vapour permeability values, for all gases studied. These results suggest that this membrane can be considered for gas dehydration due to the high water vapour/gas selectivities.

Analysing the water vapour permeability from humidified gases under study, it is observed an increase of water vapour permeability with the increase of gas humidity content. This may be related to plasticization of the biopolymer and, simultaneously, which promotes the increase of solubility of water vapour in the membrane [90] and also the diffusivity. Many studies reported [7,8,86,109,113] the same membrane behaviour with the increase of water content.

The selectivity results of H_2O/gas (CO_2, N_2 and CH_4) in different gas humidity content are represented in Figure 3.6.

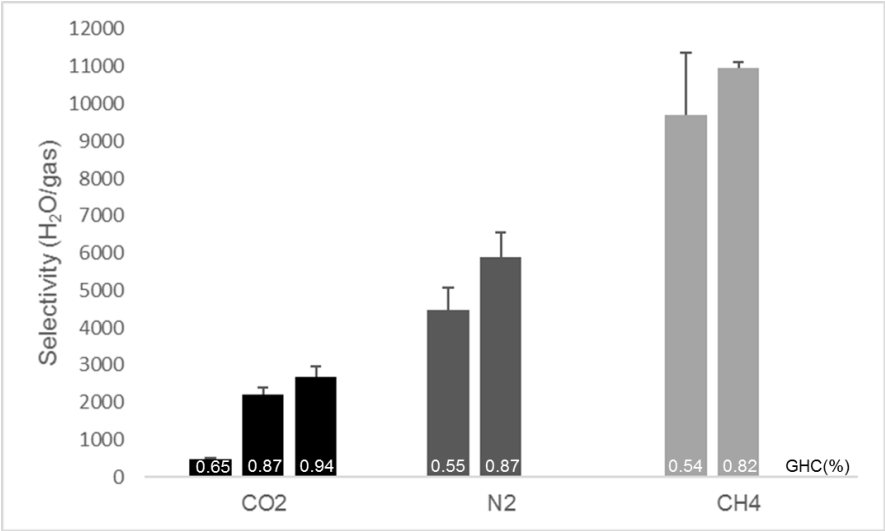

Figure 3.6:H2O/gas (CO2, N2 and CH4) selectivity for the dehydration process with the membrane FucoPol+GPTMS 7+CaCl2 at 22.0 ºC. (GHC corresponds to gas humidity content)

Comparing the selectivity of water vapour to all gases studied, the selectivity follows the sequence H_2O/CH_4 > H_2O/N_2 > H_2O/CO_2 (Figure 3.6). This occurs due to the very low values of CH_4 permeability compared with N_2 and CO_2 which, despite increasing with the water content, is always lower than 0.2 barrer (until 0.82 % of gas humidity content). As a consequence, a H_2O/CH_4 selectivity of, approximately, 11000 was achieved.

The FucoPol+GPTMS+$CaCl_2$ membrane showed high water vapour selectivity values for all gases studied, until 0.9 % of gas humidity content. For this reason, the gas humidity content chosen to infer about the potential of the hybrid polysaccharide membranes in industrial applications was around this value. In fact, the industrial biogas has a water vapour content, at this temperature, around 1.2 vol.% [114] which is quite similar to gas humidity content under study (0.8 % of gas humidity in ternary mixture corresponds to 1.0 vol.% of water vapour).

3.3.2.1 Comparison with literature

Most published studies report membrane separation performance for dry and pure gases. However, from a practical point of view, permeation data for gases and water vapour in binary mixtures is required, in order to understand the real interaction between the mixture and the membrane.

A comparison of water vapour permeability and selectivity values for dehydration of various gases in different membranes is given in Table 3.2.

Table 3.2: Comparison of transport performance of different membranes referred in the literature

Gas	Membrane	Operating Conditions	GHC (wt. %)	a_w	P_{gas} (barrer)	P_{H2O} (barrer)	α (H_2O / gas)	Reference
CO_2	TR HAB-6FDA PBO[1]	35 ºC and 4 bar (feed) and 1 bar (perm)	0.35	0.6	358.4	40500	~113	[115]
	PEO-ran-PPO[2]	50 ºC and 2.5 bar (feed) and 1 bar (perm)	1.35	0.65	598.8	100000	~167	[113]
	FucoPol+GP TMS+$CaCl_2$	22 ºC and 1.05 bar (feed),~70 mbar (perm)	0.69	0.8	0.9	2080	2205	This work
CH_4	TR HAB-6FDA PBO[1]	35 ºC and 4 bar (feed) and 1 bar (perm)	1.28	0.6	18.0	41000	~2278	[115]
	CDA[3]	35 ºC and 7.5 bar (feed) and 1 bar (perm)	0.68	0.8	0.2	~22500	~102273	[109]
	FucoPol+GP TMS+$CaCl_2$	22 ºC and 1.05 bar (feed) and ~70 mbar (perm)	0.82	0.31	0.1(4)	1543	10958	This work
N_2	PEBAX® 1074	30 ºC and 2.5 bar (feed) and 1 bar (perm)	0.89	>0.8	1.6	50000	~32000	[8]
	PSf/Si-TFN membrane[4]	30 ºC and 1 bar (feed) and 0.2 bar (perm)	2.13	~0.75	1.8	880	501	[116]
	FucoPol+GP TMS+$CaCl_2$	22 ºC and 1.05 bar (feed) and ~70 mbar (perm)	0.87	0.51	0.3	1494	5891	This work

[1]Polyimide blend films; [2]poly(ethylene oxide) based block copolymers; [3]cellulose diacetate; [4]nanocomposite polysulfone hollow fiber membrane with a thin film with nano-Silicon particles incorporated.

Comparing the transport performance of the hybrid polysaccharide membrane with other membranes reported in the literature (Table 3.2), it is possible to note that the membrane developed in this work is an excellent barrier membrane for all gases studied, presenting gas permeabilities below 1 barrer. Moreover, it is also important to note that this membrane presents, in most cases, a higher selectivity for water. The selectivities obtained for the hybrid

polysaccharide membrane are higher or similar to the others referred (with exception of the work of Chen *et al.* (2015) [109] for CH_4 and Potreck *et al.* (2009) [8] for N_2), due to the low values of gas permeability, characteristic of polysaccharides.

According to Baker & Lokhandwala, 2008 [117], for specific applications such as natural gas dehydration, a membrane process cannot lose more than 1% of methane to be economically competitive, when compared with dehydration with glycol. Under these conditions, the use of membranes with very low methane permeabilities, as the hybrid polysaccharide membrane developed in this work, and with a water vapour/methane selectivity ≥ 500 could be an interesting industrial alternative.

3.3.3 Permeability of gas mixtures – Flue gas and biogas dehydration

In order to simulate a real industrial application a N_2/CO_2 mixed gas with a proportion of 80/20 v/v%, and CH_4/CO_2 with a proportion of 70/30 v/v%, were prepared to mimic dehydration of flue gas and biogas, respectively. The experiments were carried out under controlled relative humidity conditions, by promoting the contact of these gas streams with a saturated solution of known water activity, a_w=0.52 (air/water system). These results presented in Table 3.3 were obtained by on-line mass spectrometry as previously described.

The simultaneous determination of the gas(es) permeabilities, as well as water vapour permeability, is very relevant to mimic a real industrial application. Still, similar procedures are rarely described in the literature. In addition, it is important to note that membrane transport performance is related to the difference in gas permeability for the components of the feed mixture, which also depends on many factors, such as kinetic diameter and condensability of penetrant, the free volume of the membrane matrix and gas-polymer interactions [108]. The presence of more than one gas species may affect the individual gas solubility, especially for the most condensable gases, due to the competitive sorption and plasticization effects, causing a reduction of the membrane transport performance [7,118].

Table 3.3: Transport performance of hybrid polysaccharide membranes for synthetic flue gas and biogas dehydration

Mixtures	Gas humidity content (wt. %)	P_{gas} (barrer)*	P_{CO2} (barrer)	P_{H2O} (barrer)	α (H_2O/CO_2)	α (H_2O/gas*)
Flue gas (N_2/CO_2)	0.0	1.6 ± 0.1	0.9 ± 0.0(5)	-	-	
	0.7	1.9 ± 0.0(3)	2.6 ± 0.1	565.0 ± 23.0	218.3 ± 11.6	294.4 ± 12.7
Biogas (CH_4/CO_2)	0.0	0.6 ± 0.0(3)	1.3 ± 0.1	-	-	
	0.8	0.4 ± 0.0(4)	2.0 ± 0.2	1766.3 ± 43.6	888.4 ± 76.9	4041.9 ± 344.0

*gas represents N_2 or CH_4, respectively for flue gas or biogas mixtures

From Table 3.3, it is important to note that the hybrid polysaccharide membrane showed to be effective in flue gas and biogas dehydration (ternary mixtures). Moreover, this membrane presented high water selectivities for the two mixtures analysed, and gas permeabilities were always below 3.0 barrer.

Taking into account the results obtained for the two dry gas mixtures studied, it is possible to see that both mixtures showed similar values for CO_2 permeability relative to pure CO_2 permeability (0.9 barrer and 1.3 barrer, respectively for flue gas and biogas mixture compared to 1.3 in pure CO_2 permeation – see Table 3.1). In contrast, N_2 and CH_4 permeability increased to 1.6 barrer (compared with 0.17 barrer in pure N_2 permeation - Table 3.1) and 0.6 barrer (compared with 0.02 barrer in single gas permeation - Table 3.1).

Due to the plasticization effect of water, when the mixture of gases is humidified all permeability values increased with exception of CH_4, which permeability suffered a decrease (0.6 to 0.4 barrer). This slight decrease of the absolute value of the CH_4 permeability, in contrast with the high increase of CO_2 permeability in both mixtures (in the presence of water), can be related with the blocking of diffusional pathways by water, which has a higher impact on CH_4 transport than CO_2 due to the larger volume of the CH_4 molecule [7]. This is consistent with the results of other researchers for polyimide membranes [7,119].

Analysing the water permeability, it was found that in the biogas mixture the water permeability is three times higher than the water permeability in the flue gas mixture (see Table 3.3). This result, together with the CH_4 permeability decrease, leads to a H_2O/CH_4 selectivity much higher than the H_2O/N_2 selectivity (4042 and 294, respectively).

The hybrid polysaccharide membranes showed that, in real situations, they have the capacity to dehydrate mixtures, due to the low gas permeability characteristic of polysaccharides [104] and also the introduction of inorganic particles in the polymer matrix by the sol-gel technique used, which increases the gas barrier properties of the polymer [120]. In addition, for other relevant industrial dehydrations, such as natural gas (which presents 600-1200 ppm of water vapour [121]), the hybrid polysaccharide membranes may have a high potential, with the advantage of not losing CH_4, due to the low permeability values of these gases.

3.3.4 Membrane Stability

The membrane properties that are important to assure are the permeability of the target solute (water vapour) and of the gas components of the mixture, the selectivity towards the target solute and the membrane stability under operating conditions [108]. To analyse the stability of the membrane, the same membrane was operated during 20 consecutive experiments (during approximately 7 h each experiment, taking into account the purge and testing time-length), with pure and humidified gases. Afterwards, the pure gas permeation experiments of new membranes are compared with “used membranes” in consecutive experiments, in the presence of water vapour.

According to Tsvigu *et al.* (2015) [108], glassy polymers, as this membrane, can be influenced by the polymer free volume (that strongly affects the diffusion of small molecules), which is also regulated by the material history (membrane preparation), the exposure to swelling agents or different thermal treatments. Moreover, when plasticizer gas molecules or vapours, such as CO_2 and water, are diffusing through the membrane, the interaction between the penetrants can swell the polymer matrix, increasing the free volume, and, simultaneously, the diffusivity for all gaseous species increase.

For CO_2 permeation there was no significant increase in the permeability value. In contrast, the N_2 and CH_4 transport behaviour was slightly different when using a fresh or a repeated used membrane after a total of 7 h of operation in 20 consecutive experiments. Still, it is worth mentioning that, despite increasing, the permeability values for these gases are always lower than 3.0 barrer. This means that the membrane maintains its gas barrier characteristics after long-term exposure to water vapour.

When comparing the water vapour permeation for the fresh and the used membranes, it could be concluded that permeation is rather constant, irrespectively from the gas stream studied. These results are extremely positive and show that the membrane developed keeps its ability for gas dehydration, even after repeated use.

3.4 Conclusions

Hybrid polysaccharide membranes, prepared from a low-cost substrate and developed by a sol-gel method, were evaluated for their potential use in gas dehydration. Two relevant industrial dehydration processes were selected: flue gas and biogas dehydration. In order to mimic real conditions, permeation of pure gases (CO_2, N_2 and CH_4), binary mixtures (CO_2/H_2O, N_2/H_2O and CH_4/H_2O) and ternary mixtures ($80\%N_2/20\%CO_2/H_2O$ and $70\%CH_4/30\%CO_2/H_2O$) was analysed at different relative humidity conditions by on-line mass spectrometry. This technique proved to be a fast, useful and effective tool for gases and water vapour monitoring, even in complex mixtures. The FucoPol+GPTMS+$CaCl_2$ membranes developed revealed to be an excellent gas barrier to all gases studied with permeability values below 1.0 barrer, and presented high selectivity for water vapour transport.

In close-to-real conditions, the hybrid polysaccharide membranes showed the ability to dehydrate gas mixtures (binary mixtures and ternary mixtures), with the advantage of not losing gases to the permeate stream, due to their low permeability for the gases studied (CO_2, CH_4 and N_2). This characteristic makes these membranes potential alternatives for other relevant dehydration processes in industry, such as natural gas and air dehydration.

4 STEADY-STATE AND TRANSIENT TRANSPORT STUDIES OF GAS PERMEATION THROUGH DENSE MEMBRANES USING ON-LINE MASS SPECTROMETRY

Published as: Sofia C. Fraga, Maria A. Azevedo, Isabel M. Coelhoso, Carla Brazinha, João G. Crespo, "Steady-state and Transient Transport Studies of Gas Permeation Through Dense Membranes Using On-line Mass Spectrometry" Separation and Purification Technology (2017)

The author was directly involved in planning and execution of all the experiments, as well as on the discussion, interpretation and preparation of the manuscript.

4.1 Summary

Polydimethylsiloxane PDMS, polyethylene PE (the most used polymer in food packaging) and pectin (biopolymer potentially used as wound dressing material and in food packaging) were characterised in terms of their gas transport properties. This characterisation was performed by on-line mass-spectrometry, MS, with the upstream and downstream compartments of the membrane unit at atmospheric pressure, in order to mimic the operating conditions of the applications addressed. A simple, direct restriction was used for allowing the downstream gas mixture to reach the mass spectrometer detector. Monitoring of gas permeation by on-line mass spectrometry proved to be a highly precise and reproducible technique, which makes possible the study of multicomponent gas mixtures in dry and humidified gas conditions, without requiring sampling and additional off-line procedures and analysis. Data acquisition, with time intervals as short as one second, makes possible the comparative study of permeation processes of each gas present in different feed streams (pure gases, gas mixtures under dry and humidified conditions) during the initial transient period, allowing for inferring about solute-membrane interactions. Information about steady-state transport may also be acquired, and are in agreement with values reported in literature.

4.2 Introduction

The design and fabrication of new materials is in continuous development for a large variety of applications: membrane separation processes for liquid and gaseous mixtures, biomedical applications, catalysis, etc [26]. A significant advancement on the design of membrane materials has been achieved. Nevertheless, adequate transport characterisation tools are required for improving strategies of membrane design through the understanding of the properties of the

materials developed and their transport performance in terms of the most relevant functional properties: permeability and selectivity.

Most literature describes methods and tools for characterisation of membrane behaviour under steady-state operation (or quasi steady-state operation). However, as shown previously [12,39,70,100], characterisation of membrane behaviour under transient conditions may provide extremely useful information, which is essential for understanding the interaction of permeants with the membrane material and their transport mechanism. From permeation transient data it is possible to estimate the diffusion coefficient [122], in particular during the beginning of the permeation process.

Gas chromatography (GC) is the most commonly used method for qualitative and quantitative analysis in mixed gas permeation systems and, more recently, GC has been proposed using the method of continuous flow permeation measurement [122][13][37][31]. However, on-line, real-time monitoring of permeation with GC requires gas sampling, which represents a discontinuous analysis with a loss of information about the transient state.

On-line mass spectrometry, MS, is a technique that allows to on-line monitor the mass transport through a membrane to the permeate side, allowing to obtain one data point each second (or less if required) in real-time. MS proved to be a suitable tool for membrane characterisation, of pure gas transport processes through dense materials [31] and of pervaporation processes [70,100]. By using on-line mass spectrometry it is possible to measure and acquire data in the transient state of multicomponent mixtures, allowing to follow the membrane transport behaviour when exposed to different penetrating solvents and solutes [100].

In this work, three different materials were selected for study with permeabilities from 7 up to more than 3000 Barrer for O_2 and CO_2. The rationale was supported on the selection of membranes covering a large range of permeabilities for O_2 and CO_2 and with fields of application also rather different. Polydimethylsiloxane (PDMS) is a rubbery material with high permeability to gases. This polymer is widely used in several applications, namely in bioreactors where gaseous pollutants and oxygen are transferred through a membrane to the liquid phase, along with the degradation of pollutants by micro-organisms [123]. Polyethylene (PE) is one of the most used polymers in food packaging [5,124] due to its barrier properties. Finally, pectin is a biopolymer with potential use as a wound dressing material[125][126] or in food packaging applications [127], due to its antimicrobial properties.

While the PDMS and the PE membranes characterised in this work are commercial membranes, the pectin membrane was prepared specifically for this work. The pectin membrane was characterised in more detail: the transport of O_2 from air (80% N_2 and 20% O_2) was measured on-line by MS, and compared with the transport of pure O_2. Also, the transport of O_2 and the transport of CO_2 was measured by on-line MS both in dry conditions and in a humidified gas streams (relative humidity of 32%). This work demonstrates the ability of on-line mass spectrometry to

monitor the process of gas permeation in pure systems, gas mixtures and humidified gas streams. Moreover, it is shown how steady-state and transient state conditions can be characterised and, from the data gathered, infer about the impact of the penetrating solutes on the behaviour of the membranes.

4.3 Materials and Methods

4.3.1 Materials

The polydimethylsiloxane (PDMS) membrane was obtained from Shielding Solutions Limited, UK and the polyethylene (PE) membrane was purchased from the Auchan group. The PE material used in this work is a commercial coextruded film with 3 layers LDPE/HDPE/LDPE, with a density between 0.89-0.96 g/cm^3 [128]. These membranes have thicknesses of 754 ± 5.0 μm and 28.7 ± 2.1 μm, respectively. The thicknesses of the membranes were measured by an average of multi-point analysis and the associative error was considered to be the standard deviation of the measurements. Pectin from citrus fruit with 74% of galacturonic acid was purchased from Sigma–Aldrich Chemical Co. Ltd. (St. Louis, MO, USA). The non-condensable gases used in this work were: Nitrogen (99.999 % Praxair), oxygen (99.999%, Praxair), carbon dioxide (SFE 99.998 %, Praxair) an air mixture containing 80% of nitrogen and 20 % of oxygen (99.999 %, Praxair) and and a gas mixture containing 30% of carbon dioxide and 70 % of oxygen (99.999 %, Praxair).

4.3.2 Experimental procedure

4.3.2.1 Preparation of pectin films

Pectin was dissolved in distilled water with a concentration of 0.02 g/ml (0.035 g of pectin) under stirring conditions (300 rpm) at 50 °C. When pectin was dissolved, the heating was turned off and 0.01 g/ml of glycerol (0.035 g of glycerol) was added to the pectin solution. Then, the solution was filtrated to remove impurities and placed on a Teflon plate during 24 h at 30 °C. A membrane with 110.2 ± 8.2 μm thickness was obtained.

4.3.2.2 Gas analyser calibration and monitoring

A mass spectrometer (Prisma Plus QMG 220 M2, Pfeiffer Vacuum, Germany) was used with an axial beam ion source, emission current 1mA, electron energy 70eV, single quadrupole, secondary electron multiplier SEM detection. Mass spectrometry identifies and quantifies the target compounds, according to their specific mass to charge ratio (m/z) and intensity of electric signal, providing a characteristic mass spectrum for each specific compound. Prior to the permeation experiments, a method of calibration was set using the software Quadera (v4.61) supplied by Pfeiffer Vacuum. N_2 was selected to be the sweep gas as N_2 is the most abundant

gas in air and this work intended to mimic the operating conditions of the applications described in the Introduction section. Moreover, N_2 does not have high permeabilities in the polymers studied: pectin, PDMS and PE [11]. Jimenez et al. published a review comparing the permeability of CO_2, O_2 and N_2 in starch films (polysaccharide films as pectin). N_2 permeability is, in fact, the lowest (11 x 10^{-12} cm^2 m^{-1} s^{-1} Pa^{-1}), followed by O_2 (350 x 10^{-12} cm^2 m^{-1} s^{-1} Pa^{-1}) and finally CO_2, with the higher permeability (1400 x 10^{-12} cm^2 m^{-1} s^{-1} Pa^{-1}) [129]. Regarding the low values of N_2 permeability comparing with other gases, back diffusion of N_2 is not expected. The mass spectrometer was calibrated, converting the characteristic intensity of each gas present in the permeate compartment (m/z_{CO2} = 44, m/z_{O2} = 32, m/z_{N2} = 28, with m/z as the ratio of mass to charge of each gas) to its corresponding concentration (% v/v) or partial pressure. The subsequent steps were followed:

- The background signals, related to the residual gases present in the permeate compartment, were subtracted;
- The permeate compartment was fed using a mixture of gas streams with a known concentration in a way that simulates the real application. In particular, the calibration procedure was performed by mixing each gas of interest with N_2 (the sweeping gas) in the same concentration range expected during the permeability measurements, as in [80]. For validating the calibration factors, bottles of gas mixtures (with known composition) containing the gases under study (CO_2 and O_2) were also used. The bottles of gas mixtures used were an air mixture containing 80% of nitrogen and 20% of oxygen and a gas mixture containing 30% of carbon dioxide and 70% of oxygen. The volumetric concentration (% v/v) is determined by using two mass flow controllers with defined flow-rate of gas stream sent to the permeate compartment.
- When a stable value of intensity of each gas is achieved, the Quadera software is used to calculate the calibration factor of the gas under study in relation to the internal standard gas (N_2). The calibration values obtained are shown in Table 4.1

Table 4.1: Calibration fact ors obtained for CO_2 and O_2 in relation to N_2

Gas	Calibration Factor
N_2.	1.00
CO_2	0.689
O_2	0.732

In order to assess the effect of the presence of water vapour on the gas calibration [78], calibrations were also performed with humidified gases at a relative humidity of 32.4% (same water concentration as during the permeation experiments) at 1 cm3/ min and at constant addition of N_2 at 6 cm3/ min to the permeate compartment. The calibration factors for CO_2 and O_2 under humified conditions were the same as the calibration factors under dry conditions

The calibration factor (*CF*), obtained with the Quadera software, were calculated based on the characteristic intensity of each gas *I* (A) and its corresponding concentration (% v/v) as described in eq (4.1):

$$\frac{[N_2]}{[gas_i]} = CF \times \frac{I_{N_2}}{I_{gas_i}} \quad (4.1)$$

4.3.2.3 Gas permeation experiments

The permeation apparatus used in this work is represented in Figure 4.1.The unit was set to be compact, with a total permeate volume of 3.4 cm^3, and it comprises a membrane cell with the membrane, mass flow controllers, EL-FLOW electronic Mass Flow Controllers (Bronkhorst) for each gas, and an EL-PRESS electronic back pressure controller (Bronkhorst), to control the gas volumetric flow-rate and pressure of inlet and outlet streams of the membrane cell. The permeate compartment is connected to the Mass Spectrometer (*Prisma Plus QMG 220 M2*, Pfeiffer Vacuum, Germany) by a heated restriction at 80 ºC which allows to work at atmospheric pressure in the permeate compartment without overloading the mass spectrometer compartment. In each permeation experiment with a defined feed gas, the following operating parameters were controlled and measured: the feed and permeate pressure of gas were maintained at 1.05 bar (absolute pressure); the flow rate of the inlet feed stream was 10 cm^3/min of the gas; the flow rate of the sweep gas N_2 in the inlet permeate stream was 6 cm^3/min; the flow rate of the outlet permeate stream was 1 cm^3/min of N_2 and of the gas that permeated through the membrane. N_2 was selected to be the sweep gas, as explained in sub-section 4.3.2.2.

The experiments were performed in a closed room with air conditioned maintained at 30ºC. The temperature was controlled regularly with the thermo-hygrometer. When the humidified gas system was used, the restriction between the MS and the atmospheric pressure was heated at 95ºC in order to avoid water condensation. The humidified gas system comprises a trap with a saturated saline solution of Mg_2Cl, corresponding to a relative humidity of 32.4% in the feed stream. The gas to be study is bubbled into the saline solution and the relative humidity is measured at the end of the gas-liquid contactor with a digital thermo-hygrometer, which confirmed that the feed water concentration was constant during the experiments.

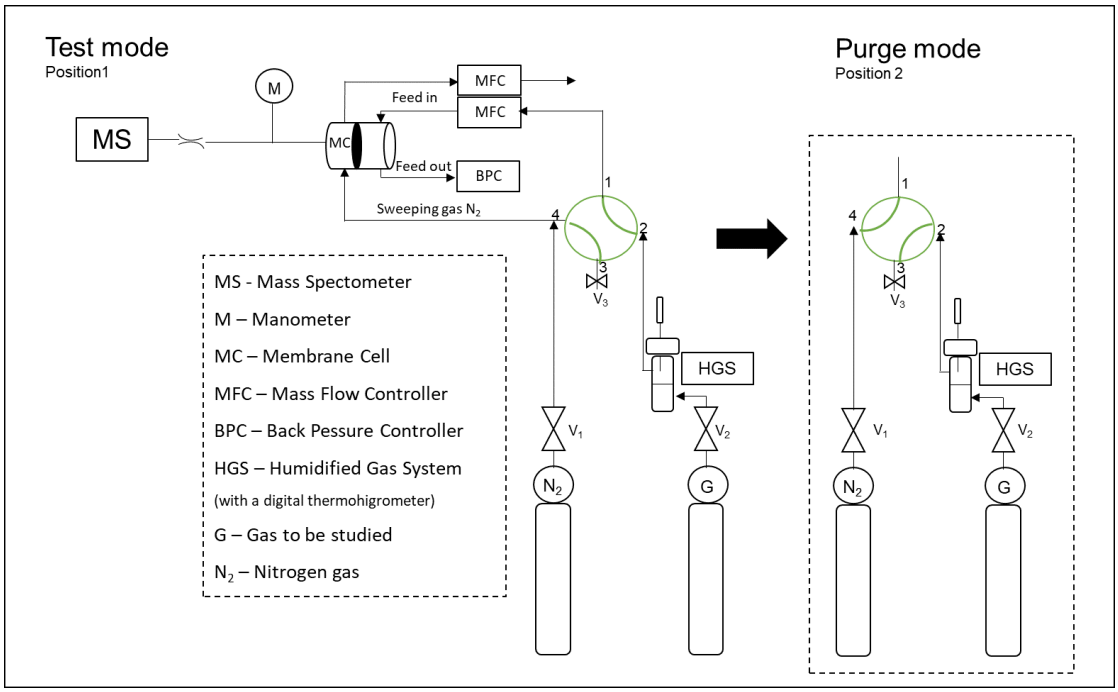

Figure 4.1: Schematic representation of gas permeation apparatus performed at 30 ºC. The Humidified Gas system, HGS, was used to assure the desirable humidity in the air stream, during the studies with the pectin membrane

Before each analysis, the membrane was flushed for at least 1 hour at both sides with two independent N_2 streams until the MS signal was stable, purge mode (see Figure 4.1). Thus, the membrane is solute-free and accommodated to the solvent compound. Subsequently, the N_2 flux in the feed side is replaced by the pure gas or gas mixture at atmospheric pressure (absolute pressure 1.05 bar) via the 4-way valve, test mode (see Figure 4.1), and the gas concentrations (% v/v) in the permeate were measured along time.

In order to calculate gas fluxes, a partial mass balance of each gas *i* of interest (O_2 and CO_2) was performed to the permeate compartment in each permeation experiment. Particularly, the molar flow rate of gas *i* which enters the permeate compartment through the membrane, $Q_{molar.i.inlet}$ (mol/s), is equal to the molar flow rate of gas *i* in the outlet sweep gas stream that leaves the permeate compartment, $Q_{molar.i.outlet}$ (mol/s), expressed by

$$Q_{molar.i.outlet} = Q_{molar.outlet} \cdot \frac{p_{perm.i}}{p_{perm}} \qquad (4.2)$$

where $Q_{molar.outlet}$ (mol/s) is the total molar flow rate of the outlet sweep gas stream. The flux of gas *i* is expressed by

$$J_{.i} = \frac{Q_{molar.outlet}}{A_{membrane}} \cdot \frac{p_{perm.i}}{p_{perm}} \qquad (4.3)$$

where $A_{membrane}$ (m^2) is the membrane area. The gas permeabilities, P_i (mol/(m.s.Pa)) were calculated using the equation of transport through dense films considering the partial pressure difference between compartments as the driving force:

$$P_i = \frac{J_i \cdot \delta}{p_{feed.i} - p_{perm.i}} \tag{4.4}$$

where J_i (mol/m^2.s) is the molar flux through the film gas *i*, δ (m) is the thickness of the membrane and $p_{feed.i}$ (Pa) is the feed partial pressure of gas *i*.

The permeability is given by:

$$P_i = S_i \times D_i \tag{4.5}$$

where S_i (mol/ m^3 Pa) is the sorption coefficient and D_i (m^2/s) is the diffusion coefficient of the gas *i* through the membrane.

The sorption coefficient may be expressed in (cm^3(STP)/cm^3.nar), as mostly presented in the literature, by calculating the volume of gas *i* corresponding to the moles of gas *i* in the membrane at STP conditions (1.01 bar, 273.15K). The permeability may be expressed in Barrer (1barrer = $10^{-10}$$cm^3$gas(STP).cm/$cm^2$.cmHg.s).

4.3.2.4 Sorption experiments

The scheme used to determine the sorption coefficient in the different materials is represented in Figure 4.2.

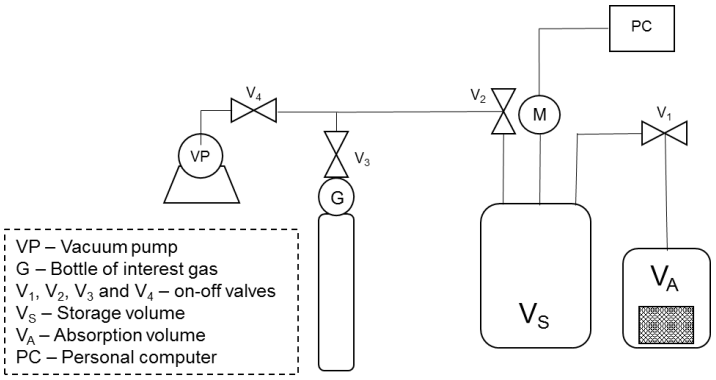

Figure 4.2: Experimental apparatus for sorption experiments of the gas in the membrane material, performed at 30ºC

In the beginning of the experiment about 4 g of membrane material is placed in the absorption chamber, with volume, V_A, (46 cm^3). With valves V_1, V_2 and V_4 opened, vacuum is applied with a

rotary pump (Duo 2.5, Pfeiffer Vacuum, Germany) and the pressure is monitored with a highly accurate manometer (WIKA P-30, Megacontrol) which has an error of 5 x 10^{-5} bar; this membrane desorption step finishes after 1 hour at constant pressure (10^{-2} mbar), experimentally measured. After this time, V_1 and V_4 are closed and the selected gas is introduced in the storage chamber, with volume, V_S (90 cm^3) until a pressure of 1.6 bar is reached and V_2 and V_3 are closed. After reaching a stable pressure, in a few minutes, V_1 is opened and the gas is expanded. The gas is then absorbed by the membrane material causing a decrease in the pressure which is monitored until reaching a plateau, $p_{equilibrium}$.

Using the pressure decay, the amount of gas *i* absorbed in the material, n_i (mol) can be calculated using the following expression:

$$n_i(t) = \frac{p_0 V_S - p(t)(V_S + V_A - V_{memb})}{RT} \quad (4.6)$$

where p_0 (mbar) is the pressure used to fill the storage volume, V_S, p is the monitored pressure (mbar), V_{memb} is the membrane volume (dm^3), R the ideal gas constant (dm^3.mbar.$K^{-1}mol^{-1}$) and T the temperature (K).

The sorption coefficient, S_i, is calculated using eq (4.7):

$$S_i = \frac{V_{i,membrane}(STP)}{V_{membrane} \times p_{equilibrium}} \quad (4.7)$$

expressed in (cm^3(STP)/cm^3.bar), where $V_{i,membrane}$ (cm^3) is the volume of gas *i* corresponding to $n_{i,membrane}$ at STP conditions (1 bar, 273.15K), and $p_{equilibrium}$ (bar) is the pressure at equilibrium conditions.

4.4 Results and Discussion

4.4.1 Sorption coefficients of pure O_2 and pure CO_2 in dense polymers

The sorption coefficient is essential to calculate the diffusion coefficient as described in eq. (4.5). The pressure decay method explained in section 4.3.2.4 was used to experimentally determine the sorption coefficients of pure O_2 and pure CO_2 in the three different types of polymers studied, using equations (4.6) and (4.7).

Table 4.2: Sorption coefficients of pure O2 and CO2 in the polymers PDMS, PE and pectin with 50% glycerol, obtained in this work at 30 ºC

Membrane	Permeating gas	Sorption coefficients (cm^3 (STP)/cm^3 atm)
PDMS	CO_2	4.76±0.006
	O_2	0.59±0.005
PE	CO_2	2.30±0.006
	O_2	1.23±0.007
Pectin + 50% glycerol	CO_2	3.36±0.009
	O_2	0.20±0.008

The results, in Table 4.2, shows that for all polymers, the sorption coefficient is higher for CO_2 than for O_2 indicating that CO_2 has a higher affinity for these materials. This result could be expected due to higher polarizability of CO_2, which may lead to higher molecular interactions with the hosting polymer. Moreover, the sorption coefficient of CO_2 in PDMS is higher than in PE and pectin, due to the elastomeric character of this polymer. The results obtained in Table 4.2, shows an agreement between the experimental data and the values reported in literature.

4.4.2 Steady state transport of pure O_2 and pure CO_2 through dense polymers

CO_2 and O_2 permeation at 30 ºC in PDMS, PE and pectin were monitored by MS during the whole transient period, as well as, in the steady-state period. MS clearly identifies the steady state in each permeation process (corresponding to a plateau in each graph of permeability against time). The steady-state permeabilities of the different polymers under study for pure O_2 and pure CO_2 were calculated by eq.(4.4) and were compared to values reported in the literature (see Table 4.3).

Table 4.3: Comparison of permeability and diffusion coefficient values of O_2 and CO_2 for the polymers PDMS, PE and Pectin with 50% glycerol under steady state, obtained in this work (at 30ºC and 1.05 bar. absolute pressure) and reported in the literature

Membrane	Permeating gas	Permeability (Barrer)	Diffusion coefficient (cm^2/s) x 10^6	Operating conditions	source
PDMS	CO_2	3182±4.12	6.7±0.012	1.05 bar,30ºC	This work
		2700			Supplier
		3800	22	p_{feed}:0-16 bar, 35ºC	[130]
		3200	-	-	[131]
	O_2	433±0.60	7.3±0.07	1.05 bar,30ºC	This work
		500	-	-	Supplier
		592	14.6	p_{feed}: 2 bar, 25ºC	[132]
PE	CO_2	12.7	$0.05±2.2x10^{-4}$	1.05 bar,30ºC	This work
		13±0.04	0.25	p_{feed}: 4 bar 25ºC	[5]
	O_2	7.4±0.03	$0.06±3.9x10^{-4}$	1.05 bar,30ºC	This work
		2.9	0.021	p_{feed}: 4 bar 25ºC	[5]
Pectin with 50% glycerol	CO_2	1460±1.46	4.3±0.06	1.05 bar,30ºC	This work
	O_2	47.6±0.10	2.2±0.08	1.05 bar,30ºC	This work
	Air (80%N_2+20%O_2)	38.7±0.13	-	1.05 bar,30ºC	This work

CO_2 and O_2 permeabilities of PDMS are slightly different from the ones obtained from the supplier, probably due to different conditions of pressure and temperature (not reported) used by the supplier during the permeation experiments. Nevertheless, in general, experimental permeability values of CO_2 and O_2 in PDMS and PE, under comparable operating conditions, were similar to those obtained in the literature.

Based on equation (4.5), the steady state diffusion coefficients were calculated at 30 ºC, using the sorption coefficients presented in Table 4.3. The diffusion coefficient decreases with increasing critical volume, V_c (cm^3/mol) [5,11,130,131]. Since O_2 has a smaller critical volume (V_c= 73.4 cm^3/mol) than CO_2 (V_c = 93.9 cm^3/mol) and with a lower affinity to the materials under study, it is expected that its diffusion through these polymers is faster. Actually, the diffusion

coefficients of O_2 were found to be slightly higher than the diffusion coefficients of CO_2 n the PDMS and PE membranes, but an inverse situation was observed for diffusion through the pectin membrane. Indeed, CO_2 has an extremely high solubility in glycerol (17.2 g/l in glycerol at 25°C [111]) and, when permeating the pectin+glycerol membrane, may induce a plasticisation of the polymer with a consequent increase of the CO_2 diffusion coefficient which becomes higher than the O_2 diffusion coefficient. This in line with the fact that the sorption selectivity of CO_2 in relation to O_2 was 16 for pectin+glycerol membrane and was only 8 and 2 for PDMS and pectin respectively. Furthermore, for each gas (CO_2 and O_2), the diffusion coefficient in PDMS was found to be higher than in the PE and pectin membranes.

4.4.3 Transient transport of pure O_2 and pure CO_2 through dense polymers

The transient transport studies were performed aiming at obtaining information about the transport behaviour from the initial instants of permeation process until steady-state. The way permeation evolves during these initial instances reveals relevant information about membrane-solute interactions and how the membrane polymer rearranges to accommodate the penetrating solute molecules. In fact, in the beginning of the permeation process the membrane is solute-free and accommodates only nitrogen (N_2) used as sweeping gas, which is introduced in the feed and in the permeate circuits to clean the membrane from other gases. In instant t_0, the gas to be studied is introduced in the feed compartment (after the feed valve) and permeation through the membrane is followed every second by on-line mass spectrometry. The membrane polymer readjustment to accommodate the solute can be evaluated using the information obtained from MS data during the transient state [100].

On-line MS monitoring of gas permeation experiments comprises the experimental measurement, each second, of the volumetric concentration (% v/v) of the gases under study in the permeate side, and further conversion to the corresponding gas partial permeate pressures and permeability using equations (4.2) – (4.4). Regarding Figure 4.3, CO_2 permeability is higher than O_2 permeability for the three membranes tested, as expected, due to different affinity and diffusivity in the materials under study. Regarding the membranes tested, the permeabilities for O_2 and for CO_2 in PDMS are higher than in PE. The pectin membrane shows the lowest values of permeability, similarly to what happens with the sorption coefficients for CO_2. On-line mass spectrometry proved to be an excellent tool for monitoring gas permeation, even when the flux through the membrane is extremely small as in the case of the oxygen through the PE membrane, capable of following permeabilities ranging from 7 to more than 3000 Barrer. In Figure 4.3 and other Figures below, long transient periods of time were observed. This behaviour is explained by the experimental set-up used in this work, which mimics the conditions occurring in the applications described in the Introduction section. In fact, the transport of each species is assured by a small driving force, which is the partial pressure difference of each gas species between the upstream and downstream compartments, but at constant total pressure. Consequently, the

fluxes obtained are small and steady-state is only reached after several hours (in Figure 4.3, the transient time for the different permeating gas species varied between 3 to 10 hours).

Figure 4.3 represents the permeability and the normalised diffusion coefficient, calculated respectively by eq(s) (4.4) and (4.5). The data shown are not fitting or smoothing lines, these are experimental data points acquired every second. This time span could even be reduced if required. Due to the very low fluxes in the beginning of the permeation process, the values of diffusion coefficient near t=0 are extremely low. Although not null, these values can be 2 or 3 orders of magnitude lower.

This data allows for determining steady-state conditions very precisely, measure a wide range of permeabilities (and normalised diffusion coefficients) and compare the behaviour of the membrane materials when exposed to penetrating solutes. The solute-membrane interactions may promote a rearrangement of the membrane polymer during the initial stage of permeation. It is interesting to notice that the time required to reach a plateau for the permeability (and also normalised diffusion coefficient), which corresponds to steady-state conditions, is shorter for O_2 than for CO_2 in the PDMS and the PE membrane. This behaviour shows that O_2 induces smaller and faster membrane rearrangement effects, which agrees with the fact that this solute presents a lower sorption to these materials and exerts a lower plasticisation effect in these polymers. This result is in agreement with Mulder [11] where O_2 is considered to be a non-interacting gas in contrast with CO_2 considered to be an interacting gas.

Although similar in qualitative terms - a higher affinity of CO_2 to the pectin+glycerol membrane corresponds to a slower process of membrane rearrangement and time required to reach steady-state – this material is interesting to analyse in detail. Actually, as mentioned above, CO_2 has an extremely high solubility in glycerol while O_2 has a rather low solubility in glycerol (lower than in water at the same temperature). This fact explains the extremely high permeability of CO_2 in the pectin+glycerol membrane and the relatively low permeability of O_2. The time for CO_2 to reach steady-state is therefore longer.

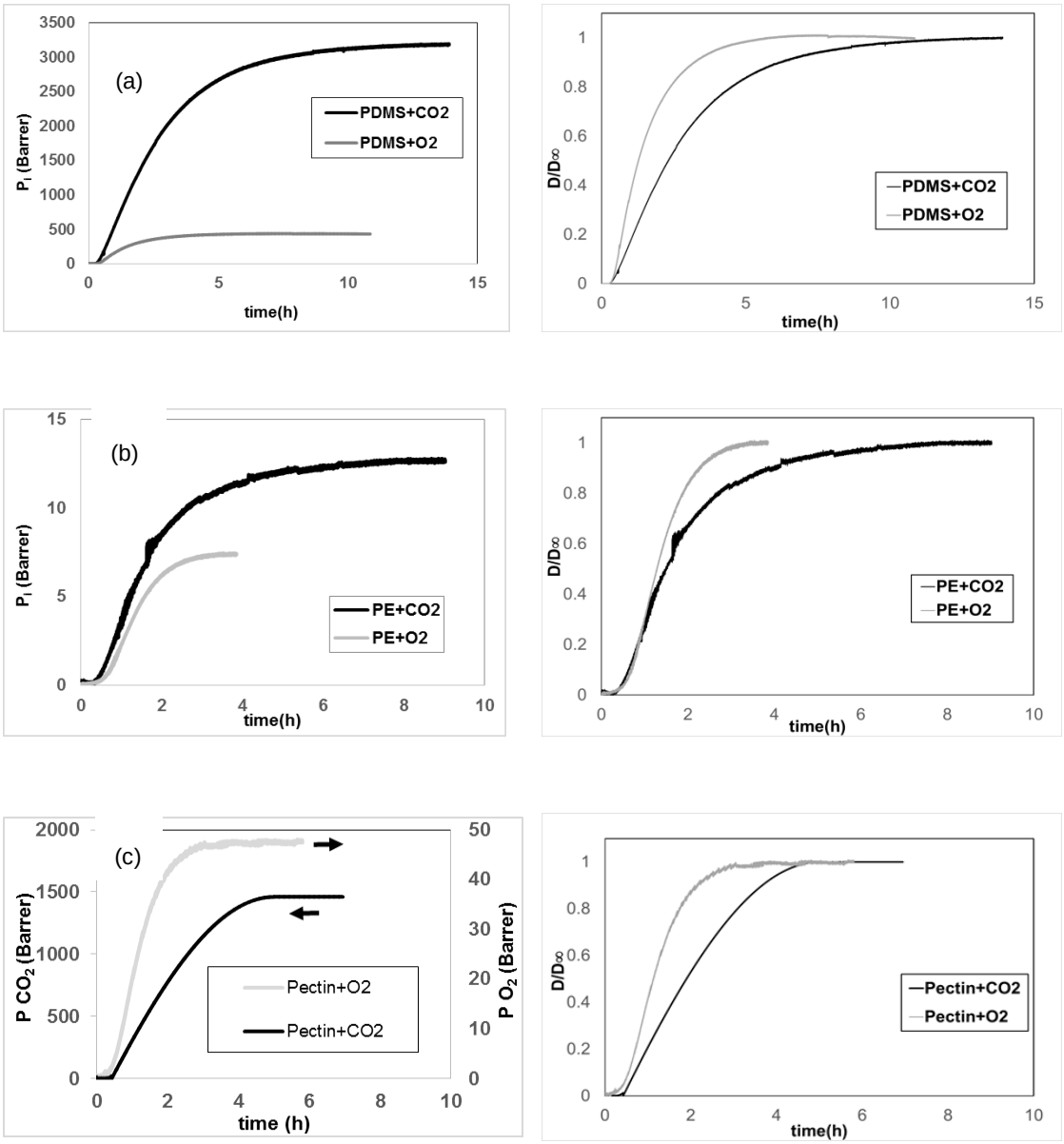

Figure 4.3: MS on-line monitoring of CO_2 and O_2 permeation at 30ºC and at 1.05 bar (absolute pressure) in terms of permeability (Barrer) and normalised diffusion coefficient (cm^2/s) versus time through different membranes: (a) PDMS, (b) PE and (c) Pectin + 50% glycerol

The membrane more selective (ideally) for CO_2 is pectin membrane, with a CO_2/O_2 ideal selectivity of 30.7, followed by the PDMS membrane with an ideal selectivity of 7.3 and finally PE with the lower CO_2/O_2 ideal selectivity of 1.7.

4.4.4 Effect of N_2 on the O_2 permeation through the pectin membrane

In order of simulate a real situation for the specific application of the pectin membrane, a feed mixture containing 80% of nitrogen and 20% of oxygen (air model mixture) was used and the permeation of oxygen was monitored for pure gas and the gas mixture. The effect of one component (N_2) on the permeation performance of the other component (O_2) was studied by

measuring the flux and the permeability of O_2: the results obtained by on-line mass spectrometry monitoring are represented in Figure 4.4.

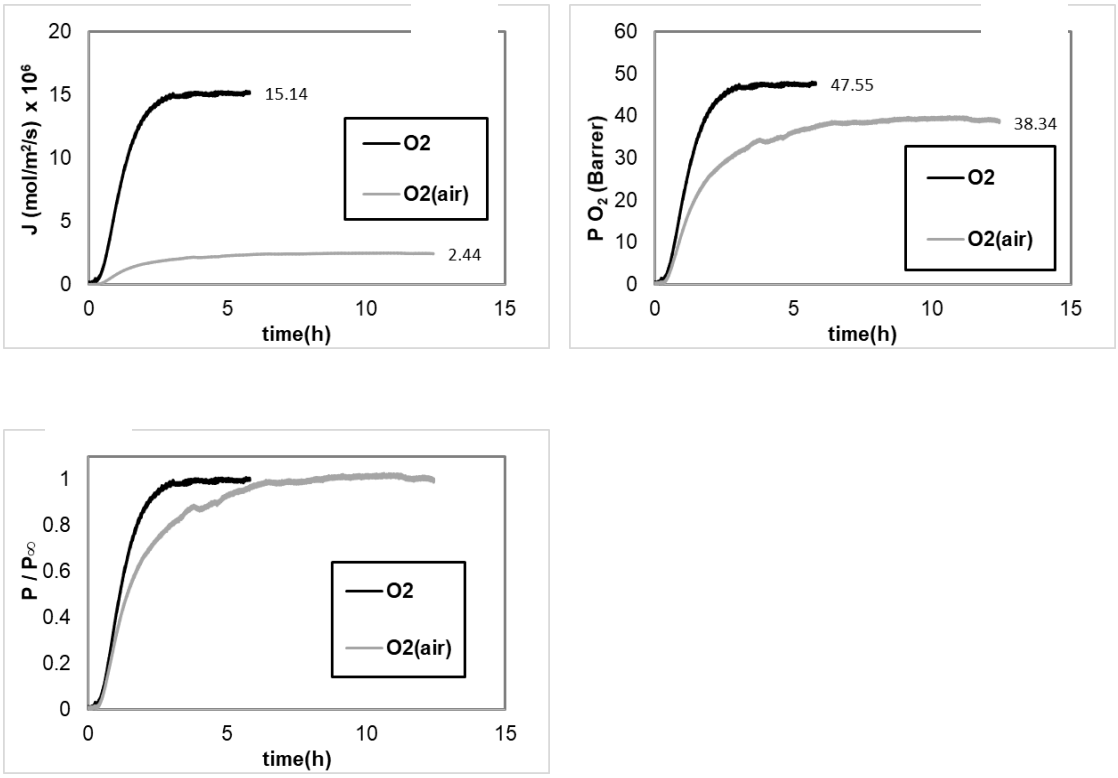

Figure 4.4: Evolvement of (a) the flux (mol/(m^2.s)), (b) the permeability (Barrer), and (c) normalised permeability (-) of pure O_2 and of O_2 in a model air mixture (20% O_2 and 80% N_2)

Figure 4.4 (a) shows that the flux of pure oxygen and in the presence of 80% of nitrogen decreased from 15.10 x 10^{-6} to 2.41 x 10^{-6} mol/(m^2.s). The observed flux decay was partially expected since the O_2 concentration in the binary mixture is 5 times lower (20% v/v of the overall gas) the concentration in the pure gas. However, the flux of oxygen observed in the mixture permeation experiment is 16% of what was obtained for the pure gas. This value, is not within the error margin of these experiments because the on-line mass spectrometry technique used in this work allows for determining permeabilities with a high precision (with an error below of 0.5%). The permeability measured at steady-state for pure oxygen is 47.55 Barrer while, when oxygen is mixed with N_2, it decreases to 38.34 Barrer. This decrease in permeability should not happen in an ideal situation, considering that permeability should be independent of the composition and driving force applied in the feed. These results suggest that the presence of nitrogen in the mixture hinders the permeation of oxygen through the membrane, which is reflected on the absolute value of permeability and the time to reach steady-state (Figure 4.4(c)). This phenomena may be related to a coupling effect, where the presence of a second gas in the feed affects the interaction between the gas molecules of the two components and the membrane [133,134], resulting on changes in the permeability and, consequently in the selectivity, deviating from an ideal behaviour. Yeom et al [38] studied the coupling effect which occurs during the permeation of

mixtures of CO_2/N_2 in PDMS films. A depression in permeability was also observed for the binary mixture when compared with pure gases, attributed to a negative sorption coupling effect related to the competition of two gases in the polymer. Reijerkerk et al. [134] studied the coupling effect in PEBAX 1657/PDMS-PEG membranes for CO_2/CH_4 and CO_2/H_2 and a similar result was obtained.

The relevant aspect in this study is the fact that on-line mass spectrometry offers the possibility to accomplish binary gas mixtures studies (or higher complex gas mixtures), with a very high quality data acquisition, making possible to clearly quantify these type of effects.

4.4.5 Effect of water vapour on gas permeation through the pectin membrane

Plasticisers are used to modify the mechanical properties of the membrane, since they decrease the intermolecular forces between the chains causing changes in the transport properties. In this work glycerol was incorporated to the polymeric matrix to increase the membrane flexibility. However, as known, many plasticisers are hygroscopic and solubilise water molecules, with a consequent impact on the permeation of different gases through the membrane [127].

The transport of O_2 in air and of pure CO_2 were followed during the permeation process, for dry (0% humidity) and wet (32% relative humidity) gas streams (see Figure 4.5).

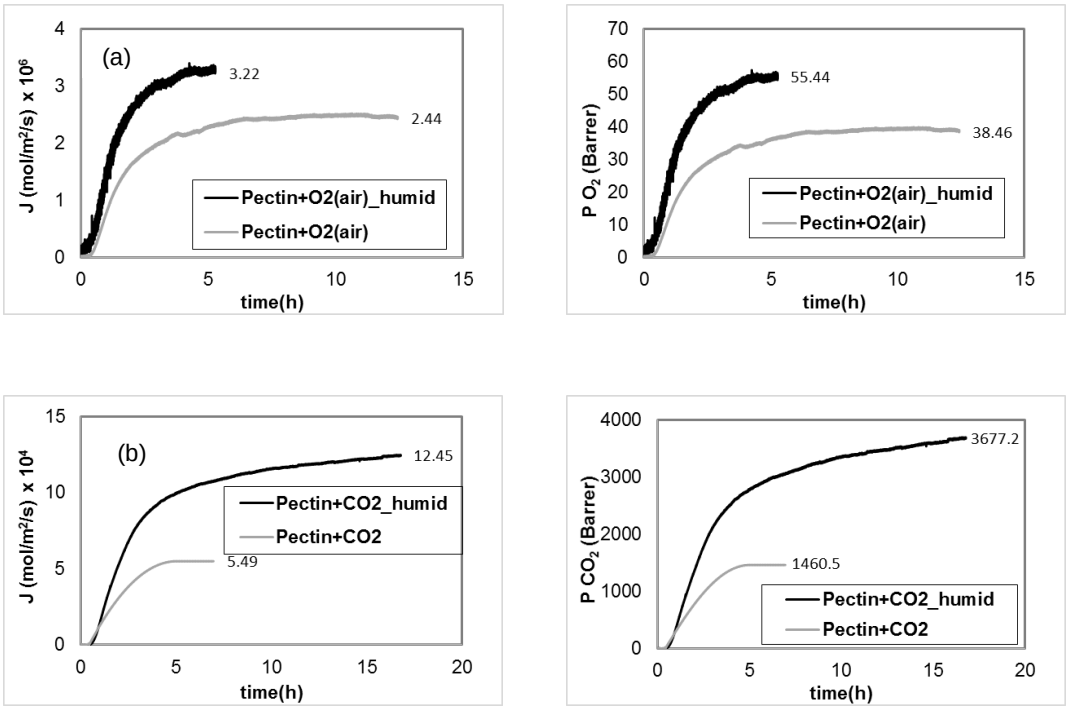

Figure 4.5: Evolvement of flux (mol/(m^2.s)) and permeability (Barrer) along time of: (a) O_2 (in an air mixture) in dry and humid conditions (32% relative humidity) and (b) pure CO_2, in dry and humid conditions (32% relative humidity)

The flux and permeability of O_2 and of CO_2 increased when present in humidified streams. This result may be expected due to possible plasticization of the pectin membrane due to the hydrophilic nature of the polymer and the high solubility of water in glycerol [135]. Nevertheless, even if the permeabilities are higher in the presence of water, when normalising the permeability (the permeability divided by the permeability in the steady state, see Figure 4.6) different behaviours are also observed for both gases.

The normalised permeabilities of the pectin membrane for O_2 (in an air mixture) and for pure CO_2 are represented in Figure 4.6. The behaviour of the normalised permeability of O_2 in an air mixture under dry and in humidified conditions were quite similar (see Figure 4.6 (a)), meaning that the presence of water makes the membrane structure slightly more flexible (Figure 4.6 (a)) but does not influence significantly the transient permeation and consequently the interaction oxygen-membrane. Contrarily to what happens with oxygen, the behaviour of the normalised permeability of CO_2 in humidified conditions is different to that obtained when using dry conditions (see Figure 4.6 (b)). Particularly, the permeation of humidified CO_2 through the pectin membrane takes much longer to achieve steady-state. This behaviour may be associated with the fact that the molecule of CO_2 has a large affinity to H_2O (high water solubility) which consequently results in a higher interaction of this gas with the membrane, which is modified in the presence of water.

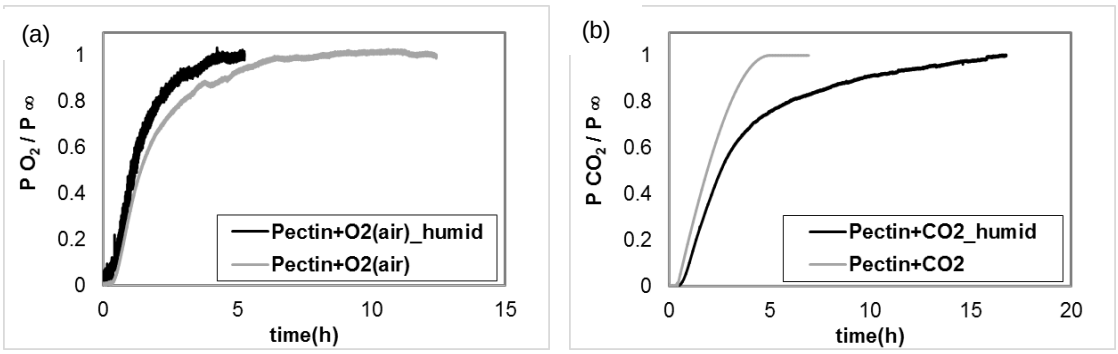

Figure 4.6: Normalised permeabilities through the pectin membrane for (a) O_2 in an air mixture, in dry and humid conditions (32% relative humidity) and (b) pure CO_2, in dry and humid conditions (32% relative humidity).

The ideal selectivity of CO_2 in relation to O_2 (Table 4.4) increased from 37.7 to 65.7 in the presence of water vapour in the feed stream with a relative humidity of 32% turning the permeation much more selective for CO_2 under a humidified atmosphere. This will be extremely important for the applications envisaged for this membrane, food packaging of fresh products and as wound dressing material.

Moreover, it is important to stress the potential of on-line mass spectrometry technique, which allows to acquire permeation data, even for complex systems, as is the case of oxygen permeation in humidified air (three components).

Table 4.4: Permeability and ideal selectivity of CO_2 against O_2 in an air mixture, at a relative humidity of 0% and of 32%. A pectin membrane was used at 30ºC.

Membrane	Permeating gas	Permeability (Barrer)	$\alpha_{CO2/O2}$
Pectin with 50% glycerol	CO_2 (RH=0%)	1460	30.7
	CO_2 (RH=32%)	3680	46.0
	O_2 in air (RH=0%) (80%N_2+20%O_2)	38.7	37.7
	O_2 in air (RH=32%) (80%N_2+20%O_2)	56	65.7

4.5 Conclusions

This work describes, tests and validates an on-line mass spectrometry method for monitoring gas permeation processes through different dense membranes (PDMS, PE and pectin), within a large range of gas permeabilities. This technique proved to be extremely robust and reproducible, making possible to acquire experimental data points with time intervals of one second (and even lower if required). This feature makes this technique particular attractive for the study of transient transport processes, and learn about solute-membrane interactions, which can be inferred from the evolvement of gas permeation during its initial stage.

The method was firstly validated for the permeation of pure O_2 and CO_2 through PDMS and PE membranes, with a general agreement with values reported in the literature. It was also applied to monitor O_2 and CO_2 transport through a biopolymer membrane of pectin. This technique allowed also to monitor changes in gas permeation, in a binary gas mixture, potentially due to a coupling effect. Finally on-line mass spectrometry was used to monitor the impact of water vapour on the permeation of O_2 and CO_2, suggesting that membrane plasticisation may occur.

It is worth noting that on-line mass spectrometry is a suitable tool to be used for monitoring gas permeation with an extremely high precision in multicomponent mixtures (in this study a maximum of three components - O_2, N_2 and water vapour – was used), without the need for sampling and off-line analysis. Particularly, mass spectrometry is appropriate for monitoring the CO_2 capture by membrane processing from flue gas [6] and the gas dehumidification [93].

5 TRANSPORT OF DILUTE ORGANICS THROUGH DENSE MEMBRANES: ASSESSING IMPACT ON MEMBRANE-SOLUTE INTERACTIONS

Published as: Sofia C. Fraga, Anna Kujawska, Wojciech Kujawski, Carla Brazinha, João G. Crespo, "Transport of dilute organics through dense membranes: Assessing impact on membrane-solute interactions" Journal of Membrane Science 523 (2017) 346–354.

The author was directly involved in planning and execution of all the experiments, as well as on the data elaboration, discussion, interpretation and preparation of the manuscript.

5.1 Summary

Polydimethylsiloxane (PDMS) membranes were synthesised by varying the degree of crosslinking and were characterised in a pervaporation system coupled to a mass spectrometry (MS) for on-line monitoring and collecting data points with an interval of 2 seconds. This monitoring approach allows obtaining very precise information about the impact of solutes' solubilisation within the membrane and their influence on solvent permeation. Using dilute aqueous solutions of ethyl acetate and hexyl acetate, it is shown how solutes with diverse nature and diverse partitioning into the membrane, determine the transport of solvent and solute by progressively modifying the membrane transport properties. From the evolvement of the time-dependent diffusion coefficients of the selected solutes during transient transport, it is possible to infer about solute-membrane molecular interactions and their impact in terms of membrane rearrangement and fluidification.

5.2 Introduction

The degree of crosslinking of a polymeric membrane may determine its physicochemical properties: a higher degree of crosslinking leads to a more rigid polymer and, contrarily, a lower degree of crosslinking leads to a more flexible polymer network [136]. Polydimethylsiloxane, PDMS, is a silicone-based polymer widely used in different areas of separation processes [137], e.g. gas separation and hydrophobic pervaporation for the selective transport of organics from water [138–141]. The permeation of a solute through PDMS is commonly described by the solution-diffusion model, which is based on solute-polymer interactions [10]. These interactions may be important in pervaporation processes, especially when the permeating species have high affinity to the membrane causing alterations in its structure, which impact the properties of solute transport in a structure-transport relationship [142]. These modifications in the membrane

structure and, consequently in the membrane properties, may be particularly noticeable during the transient state of the permeation process. Indeed, the membrane is dry in the first instants of permeation and then it shows a progressive solubilisation of solute within its structure with time. This increase of local solute concentration inside the membrane may lead to a rearrangement of the membrane polymeric matrix. Namely, a fluidification of the membrane may occur, leading to a faster transport of solutes, which may be quantified by an increase of the concentration-dependent diffusion coefficients of solutes as in [12] or, as in our previous work [70], by an increase of the time-dependent diffusion coefficient of solutes. Therefore, the study and estimation of the transport properties and, in particular, the time-dependent diffusion coefficients of solutes, in the whole transient period, is a key factor for a better understanding of the membrane internal structure rearrangement when solutes permeate through [70].

Previous works [39,40,70,103] proved that Mass Spectrometry (MS) is a suitable tool for monitoring of pervaporation systems with binary or multicomponent solutions in the feed stream. MS is able to follow the transport of each species present in the feed solution to the permeate side, following and characterising the permeation of the whole operation period (transient and steady-state regimes) of mixtures of compounds through dense films. Therefore, permeate partial pressures and composition, fluxes, and solutes' selectivities and diffusivities may be measured on-line with a time interval of two seconds or less if intended (depending on the number of compounds followed) [70]. Design and fabrication of new materials can directly benefit from this study. Applying this methodology of characterisation of mass transport through dense membranes [70], solutes with different molecular mass and affinity to the membranes' may be selected, in order to understand their impact on the membrane structure and transport behaviour.

The separation of organic compounds from aqueous media by hydrophobic pervaporation is commonly subject to mass transfer limitations in the liquid boundary layer adjacent to the membrane, leading to concentration polarisation effects. Schäfer et al. [143]determined the degree of concentration polarisation of aroma compounds in pervaporation experiments as a function of the cross-flow velocity over a membrane with a hydrophobic top-layer relatively thin. The author concluded that compounds with a high sorption coefficient into the membrane polymer, such as hexyl acetate, were strongly affected by concentration polarisation compared to those with low sorption coefficient. Baker et al. [144] demonstrated that this phenomenon can be overcome using thick silicone rubber membranes (more than 20 μm). In this case, the permeation of organic compounds is controlled by the transport across the membrane, which dominates over the transport across the stagnant boundary layer. Similarly, thick PDMS membranes were prepared in this work (much thicker than 20 μm) and used in order to prevent concentration polarisation effects, allowing for a more detailed interpretation of the mass transport mechanisms of the solute transport across the membranes under study.

In this work the impact of various operating conditions, involved in the permeation of dilute organic solutes, on potential rearrangements of the polymeric membrane, was assessed. The effect of

these operating conditions was evaluated by measuring the solvent (water) flux (expected to be constant when the structure of the membrane remains constant), and by measuring the solutes' transport properties at steady state (diffusion coefficients and selectivities) and during the transient regime (time-dependent diffusivities), using on-line MS as a monitoring tool. Time-dependent diffusion coefficients, D(t), were calculated, from the initial transient period until steady state was reached. Based on these values it is possible to conclude about the relevance of solute–membrane interactions and rearrangement of the membrane structure due to the presence of permeant solutes.

5.3 Theorical concepts

5.3.1 Mass transport in the feed boundary layer

In pervaporation, the feed-side concentration polarisation phenomena may be severe especially in the presence of solutes, such as hexyl acetate, with high affinity to the PDMS membrane material. This phenomenon represents a mass resistance to the solute transport, due to the fact that the transport of the solute in the feed boundary layer towards the membrane is not fast enough to compensate the sorption of the solute occurring at the upstream surface of the membrane [143,144]. Consequently, the solute concentration in the boundary layer decreases and, thus, its driving force and flux decrease as well. The model most commonly used to describe this phenomenon is the thin film model where it is assumed a stagnant boundary layer adjacent to the membrane [143,144], as shown in Figure 5.1, in which the solute transport is diffusive rather than convective.

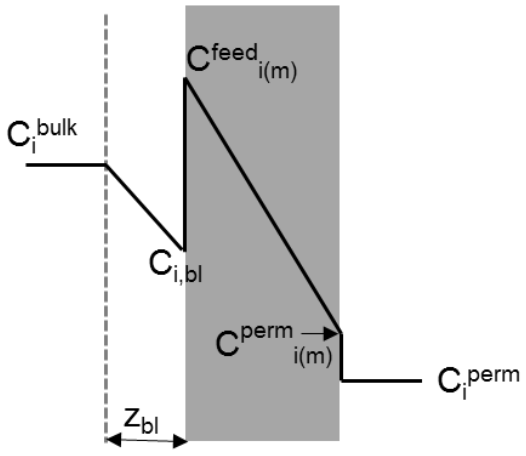

Figure 5.1: Representation of solute concentration profile in a pervaporation process, adapted from [25]

At steady state, assuming Fickian diffusion across both boundary layer and membrane, the flux across the boundary layer, $J_{i,bl}$, and across the membrane, $J_{i,m}$, are equal yielding a defined overall flux, $J_{i,ov}$, such that $J_{i,bl} = J_{i,m}$, = $J_{i,ov}$ ($m^3\ m^{-2}\ s^{-1}$) [143].

$$J_{i,bl} = k_{i,bl}\left[c_{i,bulk} - c_{i,bl}\right] \quad (5.1)$$

$$J_{i,m} = k_{i,m}S_i^L\left[c_{i,bl} - c_{i(m)}^{perm}\right] \quad (5.2)$$

$$J_{i,ov} = k_{i,ov}\left[c_{i,bulk} - c_i^{perm}\right] \quad (5.3)$$

where $k_{i,bl}$ (m s^{-1}) is the boundary layer mass transfer coefficient; $k_{i,m}$ (m/s) the membrane mass transfer coefficient; $k_{i,ov}$ (m/s) the overall mass transfer coefficient and $c_{i,bulk}$, $c_{i,bl}$, c_i^{perm} (-) are the concentrations of the solute *i* in the bulk, in the liquid boundary layer and in the permeate respectively. S_i^L(-) is the liquid-phase sorption coefficient of the solute i and z_{bl} (m) is the boundary layer thickness. The "resistance in series model" is obtained in eq.(5.4), combining eqs. (5.1) – (5.3) and assuming vacuum conditions in the downstream side of the membrane, which allows to consider the solute concentration in permeate negligible:

$$\frac{1}{k_{i,ov}} = \frac{1}{k_{i,bl}} + \frac{1}{k_{i,m}S_i} \quad (5.4)$$

The concentration polarisation phenomena in an aqueous phase, in a cell with radial flow was determined by Urtiaga et al. [145]. Particularly, a correlation was developed to calculate the boundary layer mass transfer coefficient [146] in a cell similar to the one used in this work:

$$k_{bl} = 131.2{Re_R}^{0.5}Sc^{0.33}D \quad (5.5)$$

where D_{ij} (m^2 s^{-1}) is the diffusion coefficient of the solute *i* in the solvent *j* calculated using the Wilke-Chang equation [147]. The feed boundary layer thickness z_{bl} (m) was calculated as the ratio of the boundary layer mass transfer coefficient $k_{i,bl}$ (m/s) and D_{i-j} (m^2 s^{-1}) given by

$$k_{bl} = \frac{D_{ij}}{z_{bl}} \quad (5.6)$$

Re_R is the Reynolds number at the feed side of the cell given by

$$Re_R = \frac{F\rho}{\pi\mu R} \quad (5.7)$$

where *F* ($m^3.s^{-1}$) is the volumetric flow rate of the feed, ρ ($kg.m^{-3}$) the density, μ ($kg.m^{-1}.s^{-1}$) the viscosity and *R* (m) the radius of the cell. Combining, eq. (5.4) and eq (5.5):

$$\frac{1}{k_{i,ov}} = \frac{1}{131.2xRe_R^{0.5}Sc^{0.33}D_{i-j}} + \frac{1}{k_{i,m}S_i} \quad (5.8)$$

Eq. (5.8) may assess whether concentration polarisation phenomenon is relevant in a particular overall transport of solute. In this case, the term related to the mass resistance of the transport of solute across the liquid boundary layer, $\frac{1}{131.2xRe_R^{0.5}Sc^{0.33}D_{i-j}}$, is comparable or higher than the term related to the mass resistance of the transport of solute across the membrane, $\frac{1}{k_{i,m}S_i}$.

5.3.2 Steady-state transport

The flux of a solute *i* at steady state, assuming a Fickian diffusion (1st Fick's law), is expressed as:

$$J_i = \frac{D_i}{L} \times \left(c_{i(m)}^{feed} - c_{i(m)}^{perm} \right) \quad (5.9)$$

The permeability of a solute *i* at steady state may be calculated, from a modification of eq. (5.2), as reported by Baker et al [10]:

$$J_i = \frac{P_i}{L} \times \left(c_i^{feed} - c_i^{perm} \right) \quad (5.2')$$

where P_i (m^2/s) is the (liquid-phase) permeability of solute *i* and *L* (m) is the thickness of the membrane. The diffusion coefficient D_i (m^2/s) under steady state is calculated by the sorption-diffusion model, and using the sorption coefficient of compound *i* experimentally obtained, as follows:

$$P_i = S_i \times D_i \quad (5.10)$$

At the liquid solution / membrane feed interface, considering equal chemical potentials on either side (interfacial equilibrium), the concentration is given by:

$$c_{i(m)}^{feed} = \frac{\gamma_i^{feed} c_i^{feed}}{\gamma_{i(m)}^{feed}} = S_i^L \times c_i^{feed} \quad (5.11)$$

where S_i^L (-) is the liquid-phase sorption coefficient. The equivalent expression for the permeate side is given by:

$$c_{i(m)}^{perm} = \frac{\gamma_i^{perm}}{\gamma_{i(m)}^{perm}} \times \frac{p_i^{perm}}{p_i^{sat}} = S_i^G \times p_i^{perm} \quad (5.12)$$

where S_i^G (Pa^{-1}) is the gas-phase sorption coefficient. The feed and permeate concentrations in the membrane, respectively $c_{i(m)}^{feed}$ and $c_{i(m)}^{perm}$, can be substituted in the Fick's law eq.(5.2') respectively as a function of p_i^{feed} and p_i^{perm}. However, the feed sorption coefficient is a liquid-phase sorption coefficient, S_i^L(-), and the permeate sorption coefficient is a gas-phase sorption coefficient, S_i^G (Pa^{-1}). These two factors can be combined considering a hypothetical vapour in the equilibrium with the liquid, what can be written as follows:

$$c_i^{feed} = \frac{\gamma_i^{feed,G}}{\gamma_i^{feed,L} p_i^{sat}} p_i^{feed} = \frac{S_i^L}{H_i} p_i^{feed} \quad (5.13)$$

where p_i^{feed} is the partial pressure of compound *i* in the feed liquid and the term $\gamma_i^{feed,L}.p_i^{sat}/\gamma_i^{feed,G}$ is the Henry's law coefficient, H_i (Pa^{-1}). The liquid-phase and gas-phase sorption coefficients, respectively S_i^L and S_i^G relates as

$$S_i^L = S_i^G H_i \quad (5.14)$$

Therefore, the feed concentrations in the membrane, $c_{i(m)}^{feed}$, may be calculated combining equations (5.11) and (5.13):

$$c_{i(m)}^{feed} = \frac{S_i^L}{H_i} \times p_i^{feed} = S_i^G \times p_i^{feed} \quad (5.15)$$

From equation (5.2') and using equation (5.13) and the definition of the Henry's law coefficient we obtain:

$$J_i = \frac{P_i^G}{L} \times \left(p_i^{feed} - p_i^{perm}\right) \quad (5.16)$$

$$J_i = \frac{P_i^G}{L} \times \left(\frac{c_i^{feed} \gamma_i^{feed,L} p_i^{sat}}{\gamma_i^{feed,G}} - p_i^{perm}\right) \quad (5.17)$$

$$J_i = \frac{P_i^G}{L} \times \left(c_i^{feed} H_i - p_i^{perm}\right) \quad (5.18)$$

where P_i^G ($m^2\ s^{-1}\ Pa^{-1}$) is the gas-phase permeability of compound *i*, which is the product of gas-phase sorption coefficient S_i^G and the diffusion coefficient D_i.

Therefore, permeability of solute *i,* P_i (m^2/s), is calculated for systems at steady-state, using the sorption coefficient of compound *i* experimentally obtained, as in

$$J_i = \frac{P_i}{L} \times \left(c_i^{feed} - \frac{c_i^{perm}}{H_i}\right) \quad (5.19)$$

The selectivity of the solute *i* (ethyl acetate or hexyl acetate) in relation to the solvent *j* (water), α_{i-j} (-), corresponds to the ratio of the solute and the solvent permeabilities, $P_{solute}/P_{solvent}$, and the enrichment factor of the pervaporation process of solute *i*, EF (-) [28], is the ratio between the permeate weight fraction, $w_i^{permeate}$ and the feed weigh fraction, w_i^{feed}, $w_i^{permeate}/w_i^{feed}$.

5.3.3 Transient transport

The transient transport of solute *i* (ethyl acetate and hexyl acetate) through PDMS membrane was monitored by online mass spectrometry and characterised in terms of its flux using eqs (5.20) – (5.22). The partial flux of the compound *i* under steady-state, J_i (t = ∞) (m s^{-1}) is calculated multiplying the total flux, J_T (m s^{-1}), obtained through the condensed vapours in the trap, by the solute concentration, $[i]_{perm,(t=\infty)}$, (-) in the permeate in the steady state given by the MS. The solute concentration is calculated as the ratio between the solute partial pressure and the total pressure under steady-state, as described elsewhere [70].

$$J_i(t = \infty) = J_T \times [i]_{perm\ (t=\infty)} \tag{5.20}$$

Considering the linear relation between the fluxes and the corresponding electrical signal intensities of the characteristic mass peak, the online partial flux is calculated as follows:

$$J_i(t) = J_i(t = \infty) \times \frac{I_i(t)}{I_i(t=\infty)} \tag{5.21}$$

where $I_i(t)/I_i(t = \infty)$is the ratio between the electrical signal intensity of the compound *i* in the instant *t* and at the steady state (t=∞). Time-dependent diffusion coefficients, $D_i(t)$ (m^2/s), are calculated in a simplification of equation (5.18), as the ratio C_i^{perm} / H_i is negligible compared to the feed concentration of solute *i* in the bulk feed side, C_i^{feed} :

$$D_i(t) = \frac{J_i(t)}{S_i^L} \times C_{i,feed} \tag{5.22}$$

Time-dependent diffusivity reflects the evolvement of solute's transport process across the membrane from the first initial instants of permeation, when the membrane contains no permeating species, until the steady state is reached, when the solute-membrane interactions are already well established. Therefore, time-dependent diffusivities may assess potential rearrangements of the membrane structure when permeated by different solutes (especially with affinity to the membrane). Additionally, on-line MS monitoring allows an accurate identification of the commencement of the steady state.

5.4 Experimental

5.4.1 PDMS membranes preparation

EL.LR 7660A (component A) elastomer and EL.LR 7660B (component B) curing agent, kindly provided by Wäcker Chemie GmbH (Germany), were used for the preparation of PDMS membranes. According to the supplier's information, component A was a vinyl-methyl-

polysiloxane (molecular weight of ca. 40,000 g/mol) containing platinum based catalyst, and component B was a hydrogen functional crosslinker. Hexane, of analytical grade, was purchased from Avantor Performance Materials Poland S.A. (Gliwice, Poland).

A solution containing 20 wt.% of component A in n-hexane was prepared and subsequently crosslinking component B was added to the solution to obtain the desired B:A ratio (2:10 or 1:10). The solution was mixed on a magnetic stirrer overnight. Next, a weighted amount of the solution was spread out onto a previously levelled stainless steel mould (round of 125 mm diameter or rectangular of 360 x 65 mm). The mould was left overnight for evaporation of the solvent (hexane). Subsequently the mould with the membrane was placed in an oven at defined temperature for a given period of time to complete membrane crosslinking. Afterwards, the crosslinked membrane was peeled off from the mould. Detailed information of membrane preparation conditions and membranes properties is summarised in Table 5.1.

Table 5.1: Conditions of PDMS membranes preparation and resulting chosen properties.

Membrane	Crosslinking agent/PDMS weight ratio (-)	Crosslinking temperature (^{o}C)	Crosslinking time (h)	Water contact angle (deg)	Membrane thickness (μm)
PDMS 25	1:10	70	2	103±3	269±66
PDMS 50	1:5	70	2	104±1	330±62

The thicknesses of the PDMS membranes obtained were high, in order to avoid the influence of the feed boundary layer, and consequently feed polarisation effects, during the transport of the solutes across these membranes [144]. In that way, a better understanding of the transport mechanisms of a solute across these membranes is simpler to carry out.

5.4.2 Compounds

Feed solutions used in this work were prepared using the following compounds: ethyl acetate - EtAc (99.5%, Merck, USA), hexyl acetate - HxAc (99%, Sigma-Aldrich, USA) and deionised water. Ethanol (99.8%, VWR, Germany) was also used for the homogenisation of the two phases in the permeate before the Gas Chromatography analysis.

5.4.3 Experimental set-up

The pervaporation-condensation system was combined to the on-line mass spectrometry monitoring tool as shown in Figure 5.2

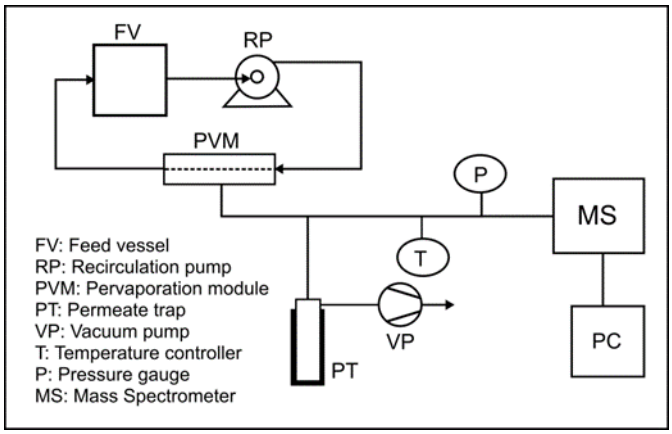

Figure 5.2: Experimental pervaporation setup with online monitoring of the permeate stream through Mass Spectrometry (MS).

The experimental set-up is composed of a flat membrane stainless steel test cell, which provides a radial flow, and a U-shaped glass trap, immersed in liquid nitrogen, to condense all the permeate vapours. The feed solution was placed in a jacketed vessel in which the temperature of water was controlled by a thermostated bath (model CW 05G, JeioTech, Korea). The pervaporation module and the permeate circuit was covered with a heating tape connected to a temperature controller (CB100, from RKC Instruments Inc., Japan) to maintain a temperature of 40ºC. To assure vacuum conditions in the downstream circuit, a rotary vane pump (DUO 2.5, Pfeiffer Vacuum, Germany) was used. The pressure was measured using a pressure gauge consisting of a capacitance manometer, model 600 Barocel, and a transducer power supply model 1575 (BOC Edwards, UK). The pervaporation circuit was connected to the MS by a splitting system consisted of a sapphire needle valve heated at 60ºC to avoid vapour condensation in this line. The mass spectrometer (Prisma Plus QMG 220 M2, Pfeiffer Vacuum, Germany) was used with an axial beam ion source, emission current 1mA, electron energy 70 eV, single quadrupole, secondary electron multiplier SEM detection.

5.4.4 Operating conditions

Various feed solution compositions were used; i.e. 2wt %, 0.5 wt % and 300 ppm of ethyl acetate in deionised water and 300ppm of hexyl acetate in deionised water. An appropriate amount of solvent was added to the feed tank (in the beginning of the experiments) after four hours of membrane conditioning in the contact with pure solvent. This moment was regarded as the beginning of experiments. The volume of the feed tank was equal to 1 and 11 L in the case of ethyl acetate and hexyl acetate, respectively. These volumes were kept constant in a closed vessel using a reduced headspace. The feed Reynolds was maintained constant at 430 [143]. The temperature of the feed vessel and the permeate circuit was kept at 40 ºC.

5.4.5 Sorption experiments

Sorption experiments of aroma compounds in the PDMS membrane material were conducted at 40ºC with various binary mixtures of ethyl acetate (EtAc) and hexyl acetate (HxAc) in water with concentration similar to those in the pervaporation experiments (2wt.% EtAc, 0.5wt.% EtAc and 300 ppm EtAc in water and 300 ppm HxAc in water). Small pieces of PDMS material were placed in contact with the solution in a mass ratio of solution to material of 4:1, in GC vials of 10 mL also used for headspace analysis in order to assure a closed system. The vials were stirred in a mixer under controlled temperature during 48h to ensure a system at equilibrium conditions at the end of each sorption experiment. The concentrations of aroma compounds at the beginning and at the end of each sorption experiment were obtained by Gas Chromatography GC (CP-3800, Varian, USA) connected to an automatic sampler (Combi PAL, CT Analytics, Switzerland). The static headspace sampling technique used is reported in [148]. The GC column and method used are reported in [149].

5.4.6 Mass spectrometry monitoring

A mass spectrometer detects compounds according to their specific mass to charge ratio (m/z) and intensity of electric signal, providing a characteristic mass spectra of a specific compound. To detect all mass fragments (m/z) of a defined compound, the mass spectra are acquired in the scan mode and the characteristic mass peaks are chosen. MS data is shown in a multiple ion detector (MID) mode with the electric signal chosen for each compound as explained in [39]. The selected mass fragments monitored were: m/z 18 for water, m/z 43 for ethyl acetate and m/z 43 also for hexyl acetate (ethyl acetate and hexyl acetate were not present simultaneously in the samples).The calibration procedure used is described in detail elsewhere [40]. Briefly, it converts the MS intensity of each individual utilised compound into its corresponding pressure assuring that each compound under study is the only specie in the circuit. The temperature is maintained constant as in the pervaporation experiments and measured and controlled with a temperature controller (CB100, from RKC Instruments Inc., Japan) connected to a heating tape in the circuit. This calibration procedure can be performed within a wide range of partial pressures.

5.5 Results and Discussion

Since this study aims at evidencing and understanding the role of solute-membrane interactions in the transport of solvent and solute through dense membranes during a pervaporation process, it was necessary, as the first step, to assure that the behaviour observed could be associated to the membrane itself and not to the external mass transfer phenomena occurring in the feed phase boundary layer.

5.5.1 Effect of feed boundary layer

Experiments were performed with the membrane with the higher degree of crosslinking, PDMS 50. For the overall transport of 300 ppm of ethyl acetate and 300ppm of hexyl acetate in aqueous solution, and as explain in detail in section 5.3.1, the overall mass transfer resistance $1/k_{i,ov}$ (s/m), the feed boundary layer resistance $1/k_{i,bl}$ (s/m), the membrane mass transfer resistance $1/k_{i,m}S_i^L$ (s/m) and the feed boundary layer thickness z_{bl} (m) were calculated respectively by equations (5.3) – (5.6). The obtained values are listed in Table 5.2.

It was found that the membrane mass transfer resistance is two orders of magnitude higher than the feed boundary layer resistance (Table 6.2). Therefore, it may be concluded that most of the resistance during the overall transport of the solute occurs during transport across the membrane. This result was expected for ethyl acetate since its sorption coefficient is relatively low and the fluid dynamic conditions used in the feed compartment of the pervaporation cell are good enough to minimise concentration polarisation effects [143], but concentration polarisation effects could be expected for hexyl acetate, which exhibits a much higher affinity towards the membrane. In order to avoid this effect we decided to use thick PDMS membranes (approximately 330 µm). As reported in Baker et al [144], the permeation of volatile organic compounds is controlled by the membrane for thick silicone rubber membranes (more than 20 µm) and this phenomenon dominates over the stagnant boundary layer. In this case, the thickness of the membrane PDMS 50 selected in this work was similar to the calculated thicknesses of the feed boundary layer (Table 5.2). For a similar thickness, the diffusion of the solute in the liquid (i.e. in the boundary layer) is faster than its diffusion across the membrane. Therefore, it can be assumed that in all studies accomplished and discussed in this work, the overall mass transfer resistance is controlled by the membrane mass transfer resistance. From Table 5.2 it can be observed that the boundary layer thickness was similar for both solutes, since the fluid dynamics in the pervaporation cell was the same, and this data is in a good agreement with results reported in literature [140].

Table 5.2: Transport parameters determined for 300 ppm ethyl acetate (EtAc) and 300 ppm hexyl acetate (HxAc) during pervaporative separation with PDMS 50 membrane.

PDMS 50 (δ=330 μm)		
	EtAc	HxAc
J_i (10^{-10} m s^{-1})	0.14	0.38
$1/k_{i,ov}$ (10^{-4} m s^{-1})	426.2	98.3
$1/k_{i,bl}$ (10^{-4} m s^{-1})	1.2	1.5
$1/k_{i,m}$ S_i (10^{-4} m s^{-1})	425.0	96.8
z_{bl} (μm)	369.3	327.9
D_{i-j} (10-8 m^2 s^{-1})	3.1	2.1

5.5.2 Determination of sorption experiments

The knowledge of sorption coefficient is essential to calculate the diffusivities of the solutes across the membrane. Therefore, sorption experiments were performed under the same conditions used in pervaporation experiments. Figure 5.3 represents the sorption isotherm of ethyl acetate in contact with the PDMS 50 membrane at 40ºC, with $C^*_{i,m}$ and $C^*_{i,f}$ correspond to equilibrium concentrations (in weight fractions units), respectively in the membrane and in the liquid, obtained by gas chromatography. The sorption coefficient of ethyl acetate in PDMS was calculated using equation(5.23):

$$S_i = \frac{C^*_{i,m}}{C^*_{i,f}} \qquad (5.23)$$

The values of the sorption coefficient of ethyl acetate were found to vary with its concentration and may be easily obtained as the slope of the equilibrium isotherm for each value of liquid composition (Figure 5.3). The concentration of the solute in the boundary layer next to the membrane was considered to be the same as the bulk concentration of the solute, since feed-side concentration polarisation effects were found to be not relevant in the systems under study, as proven in the previous section [144]. As expected, the sorption coefficient of ethyl acetate in PDMS 50 varied with the concentration of the solute in the liquid phase, in particular in the region of higher solute concentration (usually a linear relationship is observed for very diluted systems). Due to the similar characteristics for both membranes (as the transport results shows in the transient transport section), the sorption isotherm of ethyl acetate was considered to be identical for the PDMS 25 membrane.

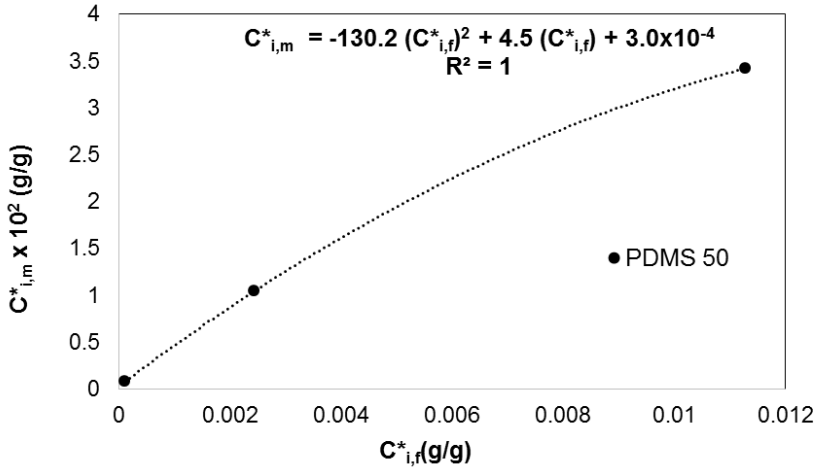

Figure 5.3: Ethyl acetate concentration in the membrane as a function of its concentration in solution, at 40ºC. Symbols correspond to experimental data obtained for PDMS 50.

The sorption coefficient of hexyl acetate (at the concentration of 300 ppm in aqueous solution) in PDMS 50 was calculated directly through equation (5.23). Considering that hexyl acetate was extremely diluted in the aqueous solution (300 ppm in the feed solution), the sorption coefficient of hexyl acetate was assumed to be constant in the range of concentrations between infinite dilution and 300 ppm. Table 5.3 summarises the experimental sorption coefficients of ethyl acetate and hexyl acetate in the PDMS 50 membrane, for different feed concentrations.

Table 5.3: Sorption coefficient S^L_i of ethyl acetate (EtAc) and hexyl acetate (HxAc) in contact with PDMS 50 membrane.

Feed solution	Sorption coefficient S^L_i (-)
20 000 ppm (2.0 wt.%) EtAc	2.0
5 000 ppm (0.5 wt.%) EtAc	3.9
300 ppm EtAc	5.4
300 ppm HxAc	530

The hexyl acetate sorption coefficient in PDMS 50 was found to be two orders of magnitude higher than that for ethyl acetate (Table 5.3), indicating an extremely high affinity of hexyl acetate to the membrane material. A similar behaviour was observed for the sorption coefficients of hexyl acetate and ethyl acetate in poly(octylmethylsiloxane) POMS material [150].

5.5.3 Permeation experiments

5.5.3.1 Steady state transport

The first objective of this study was to assess the impact of solute partitioning and penetration in the membrane material on the transport of solvent. Such impact is expected because, as the solute solubilises within the membrane material, it promotes changes on the internal arrangement of the polymeric chains. This rearrangement, required to accommodate the new entity, may lead to a process of membrane fluidification which impacts the transport of all chemical species present in solution.

Figure 5.4 shows the solvent flux (water) through different membrane materials, when using different concentrations of ethyl acetate in the feed compartment (300 ppm, 0.5wt % and 2wt % of ethyl acetate in water) and different solutes (ethyl and hexyl acetate).

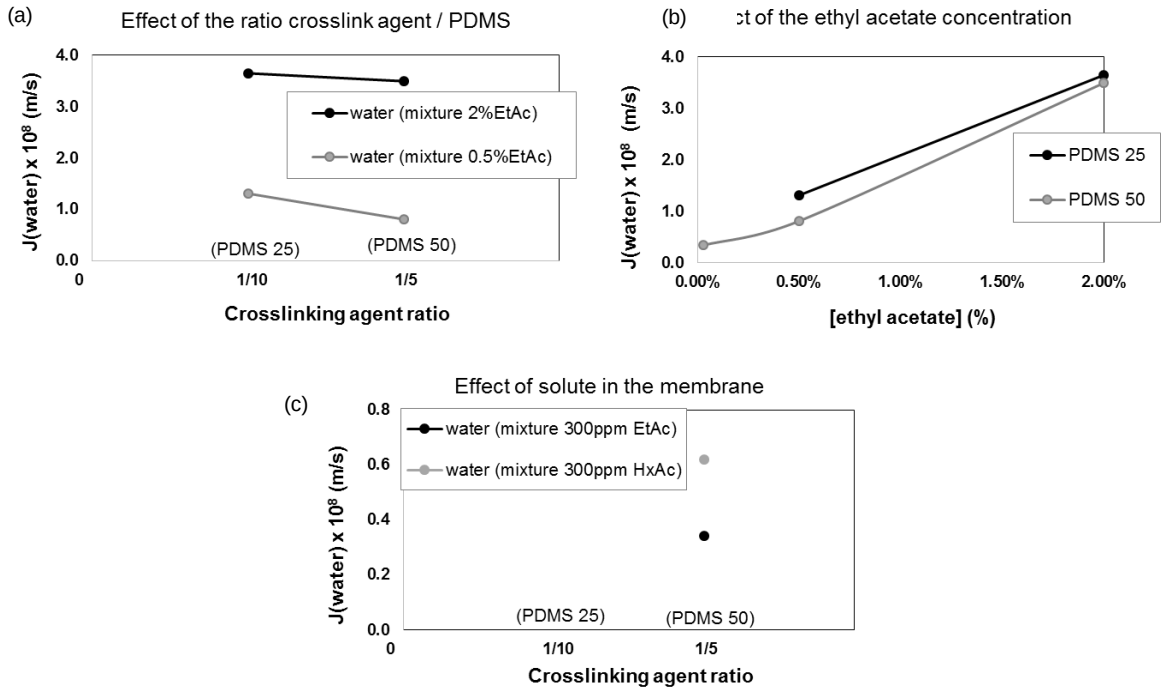

Figure 5.4: Flux of water through PDMS membranes: (a) membranes prepared with different crosslinking degree; (b) effect of solute (ethyl acetate) concentration in the feed solution; (c) effect of solute type (ethyl acetate and hexyl acetate)

Figure 5.4(a) shows, in first place, the extremely high impact of solute (ethyl acetate) concentration on the flux of solvent across PDMS membranes, irrespectively from their degree of crosslinking. This impact is impressive and translates how the penetration of the solute inside the membrane, even for a solute with a relatively modest sorption coefficient for PDMS, promotes an internal rearrangement of the polymeric material that leads to a much faster diffusion of water molecules across the membrane. Also, from Figure 5.4(a) we may conclude that the two membranes prepared do not differ much from each other. Actually, it is possible to observe a

slightly lower water flux through the membrane prepared with a higher degree of crosslinking, PDMS 50, but this effect is not particularly significant.

The minor effect of the degree of crosslinking is also noticeable in Figure 5.4(b) where the flux of water is slightly lower for the PDMS 50 membrane in the whole range of solute concentration. Figure 5.4(b) emphasises again how important is the influence of solute concentration on the flux of solvent. The results obtained represent a 10 fold increase in water flux, if we compare the situation of pure water with the processing of an aqueous solution with 2wt% of ethyl acetate. As discussed above, solute solubilisation in the membrane material involves the need for accommodating its molecules within the polymeric structure, inducing a significant fluidification effect, with impact on the diffusion of labile water molecules.

This effect is even more pronounced when comparing the water flux for two different aqueous solutions, one with ethyl acetate and the other with hexyl acetate, at the same concentration of 300 ppm. Hexyl acetate presence leads to a higher water flux (80% increase), which reflects a higher degree of membrane rearrangement and fluidification, which is naturally explained by the extremely high sorption coefficient of hexyl acetate towards the membrane. This means that the local concentration within the membrane is much higher for hexyl acetate. This feature, together with the fact that hexyl acetate is a more bulky solute, which accommodation induces a higher degree of rearrangement, explains the behaviour observed.

Table 5.4 summarises the impact of solute concentration on its own transport across membranes with a different degree of crosslinking. Solute partial fluxes (calculated from the total fluxes and permeate composition), permeabilities, diffusion coefficients, selectivities and enrichment factors, obtained from the steady state data, are listed in this table for ethyl acetate/water and hexyl acetate/water systems

.

Table 5.4: Impact of solute concentration on its own transport across PDMS membranes, for aqueous solutions with 2% wt, 0.5% wt and 300 ppm of ethyl acetate and 300 ppm of hexyl acetate in water at 40ºC

Membrane	Feed composition	J_i (10^{-11} m s^{-1})	P_i (10^{-10} m^2 s^{-1})	D_i (10^{-12} m^2 s^{-1})	Selectivity α_{i-j} (-)	Enrichment EF (-)
PDMS 25	2.0 wt% EtAc	650.0±7.0	4.3±0.0(2)	220.0±2.1	43.9±0.2	7.8±0.0(4)
	0.5 wt% EtAc	64.0±0.8	1.7±0.0(2)	40.0±0.6	47.3±0.6	9.3±0.0
PDMS 50	2.0 wt% EtAc	603.0±4.0	5.2±0.0(3)	260.0±1.6	43.7±0.3	7.8±0.0
	0.5 wt% EtAc	53.0±0.4	1.8±0.0(1)	50.0±0.3	63.9±0.5	12.3±0.0(8)
	300 ppm EtAc	1.4±0.0(4)	0.8±0.1	10.0±0.3	68.9±1.7	14.0±0.3
	300 ppm HxAc	3.8±0.0(4)	3.5±0.0(1)	0.7±0.0(1)	163.9±2.2	20.3±0.1

The first observation is that there is a minor effect of the degree of crosslinking on the transport of solutes. For the same ethyl acetate concentration in the feed solution, the crosslinking ratio does not seem to affect significantly the membrane transport properties since solute partial flux, permeability and diffusion coefficients are similar. These results are comparable with those obtained by Nguyen et al [151] where the diffusion coefficients found are negligibly affected by different crosslinked PDMS membranes. On the other hand, an increase of solute concentration leads to an increase of solute flux, permeability and diffusivity, evidencing that membrane fluidification induced by the partitioning of solute impacts strongly the transport of solute.

When comparing solutes with different affinity towards the membrane (ethyl acetate and hexyl acetate), a significantly higher solute flux, permeability and selectivity were found for hexyl acetate. This behaviour is explained by the much higher affinity and interaction of hexyl acetate with the membrane material, which induces a stronger rearrangement / fluidification of the membrane.

5.5.3.2 Transient transport studies

Transient transport studies were performed with the objective of obtaining information about transport behaviour in the initial period of operation, when the membrane is adjusting to the solubilisation and interaction of solute within its material.

5.5.3.2.1 Effect of degree of crosslinking

Pervaporation experiments were performed using on-line mass spectrometry monitoring. These experiments were accomplished for the membranes prepared with different crosslinking ratio, as shown in Table 5.1, in order to evaluate the impact of this parameter in the performance of the pervaporation process. From Figure 5.5a and Figure 5.5b, similar behaviours were observed for the diffusion coefficients of ethyl acetate, and their evolvement along the time, for both membranes under study. Diffusion coefficients of ethyl acetate through both membranes, crosslinked at different degrees, are similar suggesting that the membranes' behaviour and their potential rearrangement induced by solute solubilisation is also similar in both cases.

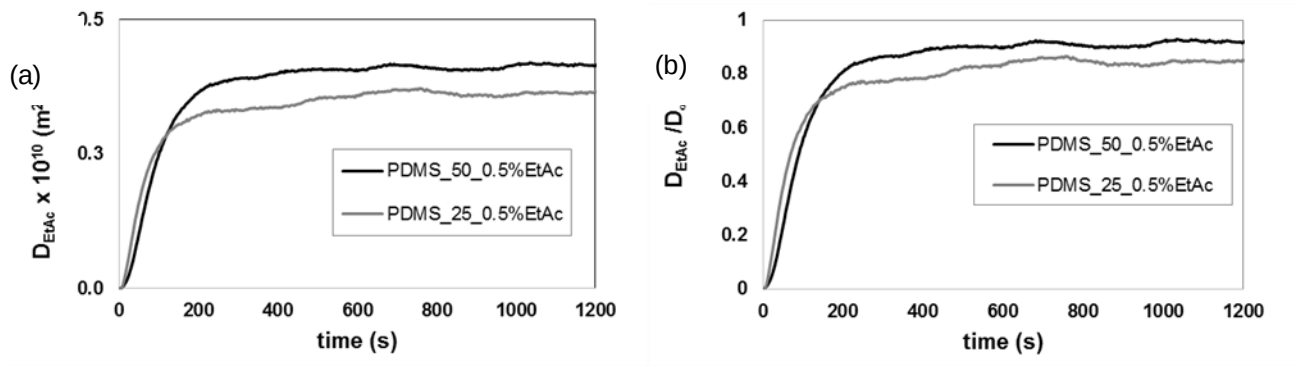

Figure 5.5: (a) Ethyl acetate diffusion coefficient and (b) normalised ethyl acetate diffusion coefficient for PDMS 25 and PDMS 50, using a feed aqueous solution of ethyl acetate with a concentration of 0.5wt.% at 40ºC. Data obtained by on-line mass spectrometry.

5.5.3.2.2 Effect of solute concentration

Different concentrations of the same solute were also tested using the PDMS 50 membrane, in order to evaluate the impact of this parameter on the membrane behaviour and, consequently, on solute transport. As shown in Figure 5.6, higher ethyl acetate concentrations led to higher solute diffusion coefficients in both membranes. This result was expected since higher local solute concentrations within the membrane lead to higher solute-membrane interactions, which determine a deeper degree of membrane fluidification with the corresponding impact in terms of solute diffusion. This is the reason why the solute diffusion coefficient progressively increases along time, translating the progressive modification of the membrane. It is also interesting to notice (Figure 5.6b) that, when the concentration of solute is lower, the process of membrane rearrangement / increase of normalised solute diffusion coefficient ($D(t)/D_{(t=\infty)}$) is slower, taking longer to reach a steady-state condition.

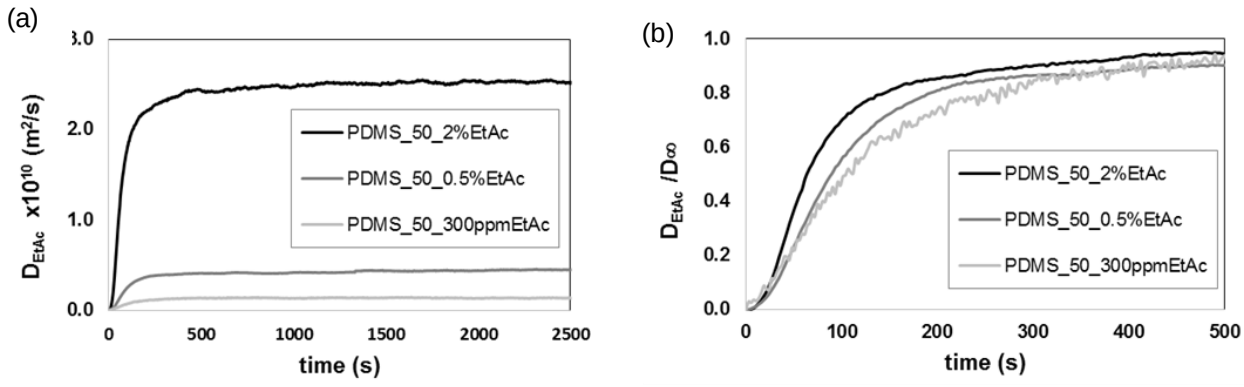

Figure 5.6: Comparison of (a) evolvement of solute diffusion coefficient and (b) evolvement of normalised diffusion coefficient of ethyl acetate in PDMS 50, when using aqueous solutions 2% wt, 0.5% wt and 300ppm of ethyl acetate, at 40ºC.

5.5.3.2.3 Effect of solute nature

Ethyl acetate and hexyl acetate were selected to perform studies aiming to understand the impact of the solute type on the membrane fluidification and, ultimately, solute diffusion. The pervaporation experiments were performed exactly in the same conditions for both solutes.

These two solutes were selected because chemically they are both esters but hexyl acetate has a much higher affinity towards the PDMS membrane than ethyl acetate, quantified by their sorption coefficients in PDMS (two orders of magnitude higher). This higher affinity translates into a much higher local concentration within the membrane, leading to a higher membrane fluidification. Nevertheless, the absolute values of the diffusion coefficient of hexyl acetate were lower than the values for ethyl acetate (Figure 5.7a), because this solute has a significantly higher molecular mass and, being bulkier, its diffusion within the polymeric membrane structure is significantly more hindered.

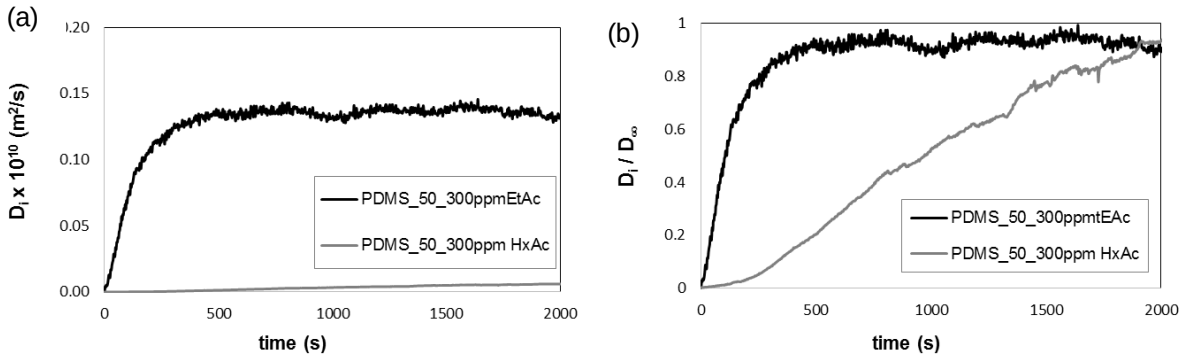

Figure 5.7:Evolvement of (a) the diffusion coefficient for ethyl acetate and hexyl acetate and (b) normalised diffusion coefficient, through a PDMS 50 membrane, for a concentration of solute of 300ppm in water, at 40ºC.

The normalised diffusion coefficients (Figure 5.7b) clearly show a great difference between the permeation of the two solutes. Hexyl acetate permeation reaches steady-state during a much slower process, which is explained by the more extensive rearrangement induced within the membrane structure, as discussed (in the section 5.5.3.1).

5.6 Conclusions

In this work, organophilic sorption and pervaporation studies were carried out in order to assess the impact of selected parameters involved in the permeation of organic compounds from dilute aqueous media under transient and steady states. The thickness of prepared membranes was high, which allowed to neglect the influence of concentration polarisation on the transport

The main results that should be retained are:

- The Mass Spectrometry technique used proves to be a very powerful technique that allows for obtaining high quality data for studying membrane transport phenomena, in particular when information from transient regime is required.
- Solute solubilisation within the membrane polymer matrix induces internal rearrangements that impact not only on the transport of solutes themselves, but also on the transport of solvent. It was found that flux of solvent increases substantially with an increase of solute concentration in feed.
- Solute transport evolves during the transient period during which the impact of solute solubilisation translates into a rearrangement of the membrane polymeric structure. This impact is more relevant for bulky solutes with a high partitioning affinity to induce strong membrane rearrangement;
- The approach discussed in this work is very useful for further research on solute transport (not only in pervaporation studies but also vapor permeation and gas permeation [152], which can be easily monitored by MS) and design of novel membrane materials [32].

As a future work, the rearrangement of the membrane polymeric structure during solute transport might be monitoring by PALS Positron Annihilation Lifetime Spectroscopy, in order to complement the data obtained from the MS.

6 CHARACTERISATION AND MODELLING OF TRANSIENT TRANSPORT THROUGH DENSE MEMBRANES USING ON-LINE MASS SPECTROMETRY

Published as: S.C. Fraga, L. Trabucho, C. Brazinha, J.G. Crespo "Characterisation and modelling of transient transport through dense membranes using on-line mass spectrometry" Journal of Membrane Science 479 (2015) 213–222.

The author was directly involved in planning and execution of all the experiments related with isopropanol dehydration, as well as on the data elaboration, discussion, interpretation and preparation of the manuscript. The mathematical model presented in this work was developed by Professor L. Trabucho.

6.1 Summary

This work presents a methodology for characterising solute transport through pervaporation membranes or, more generally, through dense membranes, in the whole transient regime. A real-time characterisation of transport through dense membrane is obtained by using on-line mass spectrometry (MS) monitoring, which allows to acquire the concentration of solutes in the permeate compartment with time intervals of 2 seconds (and shorter if required). Time-dependent diffusion coefficients, *D(t)*, were calculated for the whole operation period, including the initial transient period. Based on these values it is possible to infer about the relevance of solute-membrane interactions and rearrangement of the membrane structure due to the presence of permeant solutes. Finally, based on the information acquired, a mathematical model was developed in order to obtain solute concentration profiles inside the membrane and their evolvement along time.

6.2 Introduction

Mass transport through dense membranes is most commonly studied under steady-state conditions, when constant permeate flux of solutes and solvent are observed. The study of the transient period of mass transport, although more complex, has attracted the attention of researchers because it may offer a route for a better understanding of the membrane under study and how it interacts with the permeating species. Mass transport in pervaporation but also in organic solvent nanofiltration [153], gas and vapour permeation, is usually described by the solution-diffusion model [4,10,154,155]. Therefore, estimation of diffusion coefficients during the time-course of the transient transport process is critical. This issue is relatively simple when the permeating species do not induce major alterations in the structure of the membrane, as is the

case of most gases when permeating through polymeric membranes, but it becomes rather complex when the permeating species have very high affinity to the membrane, causing swelling and rearrangements in the membrane structure [11], which impact in their flux and selectivity.

The most common technique used to characterise mass transport through dense membranes is the time-lag method, originally conceived by Daynes in 1920 [14], in order to study mass transfer through an elastomeric material. This method was refined and extended by authors as Barrer and Crank, and applied to a large variety of materials. Rutherford and Do published an excellent review of the most significant work developed with this technique up to 1997 [17]. The time-lag permeation method is a flexible and powerful technique that can give both equilibrium (sorption coefficient) and transport properties (diffusivity and permeability) in a single experiment [18]. Nevertheless, the standard mathematical analysis used with this technique assumes that the concentration of the permeating compounds is null inside the membrane at the downstream side and that the diffusion coefficient is constant throughout the transient permeation period. Therefore, the calculated diffusion coefficient does not account for possible material rearrangements that permeating solutes may cause during the initial stage of the transient regime [12,13,34]. Some authors [9,26,27] calculated concentration-dependent diffusion coefficients from transient sorption data. These studies were performed by changing and monitoring solute concentration at the upstream face of the membrane, in order to determine the plasticisation parameters of a penetrant, which diffusivity is assumed to depend exponentially with its concentration. However, the treatment of data is established assuming a Fickian diffusion process with a constant diffusion coefficient.

Most time-lag work has been performed with mono-component gas systems, where data is obtained by an accurate recording of pressure in the receiving compartment but, more recently, several papers have been published using on-line mass spectrometry in order to characterise the simultaneous permeation of multiple species [9,12,27,34,156]. On-line mass spectrometry (MS) is a suitable monitoring tool for characterising the whole transient regime of permeation of mixtures of compounds through dense films, because it allows for determining permeate compositions and partial pressures, fluxes and selectivities in real-time [40]. Bowen et al. [34] measured constant diffusion rates of different compounds in zeolite membranes using the time-lag analysis through transient responses in the permeate, monitored with a quadrupole mass spectrometer. A similar technique was used by Tanaka et al. [12] to measure the diffusion coefficient in polymeric membranes.

The challenge still relies on the development and validation of an on-line mass spectrometry technique able to acquire composition data in the permeate compartment with a minimal time interval. Ideally, one data-point per second would allow studying systems that undergo a fast change during the initial transient stage of species penetration in the membrane [39,40]. Additionally, the transport of vapours through dense membranes introduces a degree of complexity which results from the non-constancy of the diffusion coefficient along the time-course

of permeation during the transient period [17,18], due to the progressive increase of concentration of the permeating species inside the membrane. This increase in concentration may lead to membrane swelling and rearrangement of the polymer material with impact on the permeation process and, ultimately, the diffusion coefficient of these species.

The changes occurring in a membrane during the whole transient regime depend on its internal structure and impact directly on the diffusion of the permeating species through the membrane. Therefore, the study of the whole transient regime may contribute for the fundamental understanding of structure-transport relationships in dense membranes. The design, development and fabrication of new and improved membranes for specific applications will directly benefit from this knowledge.

The goal of this work is to develop an adequate methodology for characterising solute transport through pervaporation membranes or, more generally, through dense membranes, in the whole transient regime. A real-time characterisation of transport through dense membrane is obtained by on-line MS monitoring in terms of the solute partial pressures and fluxes. Diffusion coefficients were calculated from time-dependent partial pressures and fluxes, where each increment of time was as low as 2 seconds. Therefore, diffusion coefficients are indirectly dependent on time. With these experimental parameters, together with the sorption coefficients of the solutes in the membranes under study, a mathematical model is developed in order to estimate the permeating solutes concentration profiles across the membrane, along time. The characterisation of the transient regime was carried out in this work for evaluating the changes that occur in the membrane material when exposed to penetrating solutes. Time-dependent diffusion coefficients, $D(t)$, were calculated, supported on the on-line MS monitoring technique, where each increment of time was as short as 2 seconds.

Two case-studies were selected, corresponding to different systems, using permeating solutes with different affinity towards the membranes under study. The dehydration of solvents, in this case of isopropanol, was selected because it is the most relevant industrial application of pervaporation processes, with important economical savings when compared to conventional distillation processes [148,157,158]. This system was also selected because, due to the character of the membrane (ceramic, hybrid silica-based, HybSi®), minimal changes are expected to occur in the membrane structure during permeation [159,160]. The second case-study selected involves the recovery of aromas from dilute aqueous streams, in this case of dilute ethyl acetate in water. A modified silicon–rubber composite membrane (polyoctylmethylsiloxane-polyetherimide, POMS-PEI) is used in this organophilic pervaporation process and a higher degree of polymer rearrangement is anticipated.

6.3 Experimental

6.3.1 Materials

The components used to prepare the feed solutions were isopropanol (99.8% Merck, Germany), ethyl acetate (99.5%, Merck, USA) and deionised water. Two different types of dense membranes were used, a tubular Hybrid Silica selective ceramic membrane HybSi® (Pervatech, The Netherlands) and a modified silicon–rubbery composite membrane of polyoctylmethylsiloxane supported on a porous structure of polyetherimide POMS-PEI (GKSS, Germany). These membranes were selected to be used, respectively, in the dehydration of solvents [161] and in the recovery of a representative aroma compound from wine-must [39,40,143,148,157–161]. These membranes were used for isopropanol dewatering and for ethyl acetate recovery. The properties of these membranes are in listed in Table 6.1

Table 6.1: Properties of the membranes used in this work.

Active layer	Support	Active Layer Thickness (µm)	Internal diameter (m)	Effective active area (m^2)
HybSi	Alumina	0.15 – 0.20	2×10^{-3}	7.5×10^{-3}
POMS-PEI	PEI	10.0	-	1.0×10^{-2}

6.3.2 Experimental set-up

The pervaporation-condensation system used was coupled on-line to a mass spectrometer using the experimental setup represented in Figure 6.1

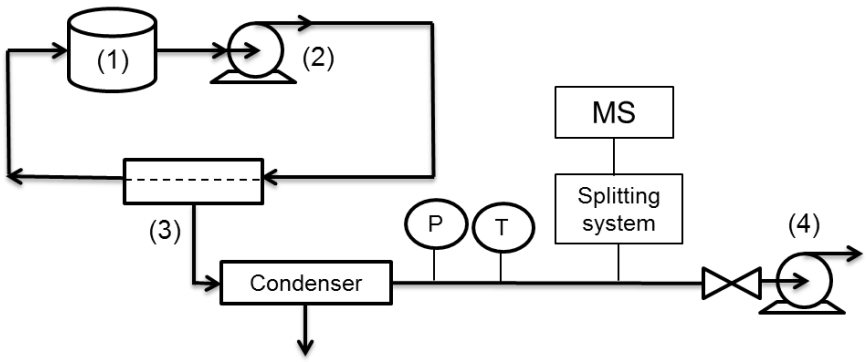

Figure 6.1: Representation of the pervaporation unit with online monitoring of the permeate stream through MS: (1) feed vessel, (2) recirculation pump, (3) pervaporation cell and (4) vacuum pump. The splitting system consists of a heated sapphire valve

The set-up for isopropanol dewatering includes a tubular stainless steel pervaporation cell (Pervatech, Netherlands) connected to a condenser. The feed vessel was a water jacketed vessel in which the temperature of water was controlled by a controlling bath (model CW 05G, JeioTech, Korea). The pervaporation module and the permeate circuit (to the condenser) was covered with a heating tape connected to a temperature controller (CB100, from RKC Instruments Inc., Japan). A rotary vane pump (DUO 2.5, Pfeiffer Vacuum, Germany) assured vacuum conditions in the permeate circuit and the downstream pressure was measured by a pressure gauge consisting of a capacitance manometer, model 600 Barocel, and a transducer power supply model 1575 (BOC Edwards, UK). The condenser was a glass U-shape trap immersed in liquid nitrogen (temperature of -196 ºC) which condensed all vapours permeating through the membrane. The splitting system to the MS consisted of a sapphire needle valve at 60ºC in order to avoid vapour condensation. The mass spectrometer (Prisma Plus QMG 220 M2, Pfeiffer Vacuum, Germany) was used with an axial beam ion source, emission current 1mA, electron energy 70 eV, single quadrupole, secondary electron multiplier SEM detection.

The pervaporation unit used for the recovery of ethyl acetate from water is described in detail in Brazinha *et al.* [40]. The rig includes a flat membrane test cell, which provides a radial flow over the membrane, and two condensers in series. The condensers were U-shaped traps: the first condenser was immersed in a refrigerated bath (FP500-MC model, Julabo, Germany) and the second one in liquid nitrogen. The feed water-jacketed vessel, the rotary pump and the devices for measuring pressure and temperature in the downstream circuit were the same as in the isopropanol dehydration system. The mass spectrometer (QMA125, Blazers, Germany) had the same features of the mass spectrometer of the previous system but with a Faraday Cup detection. The permeate was connected to the mass spectrometer through a splitting system with a needle valve installed in a tube line and adjusted according to the objective of each experiment.

6.3.3 Operating conditions

The feed compositions used in the pervaporation experiments were 5% wt of deionised water in isopropanol and 50 ppm of ethyl acetate in deionised water. In both systems the solutes were added in the beginning of the experiments and conditions were imposed in order to assure a constant feed composition during the experiments. The isopropanol dehydration unit was operated with a feed volume of 1 L and at linear feed stream velocity inside the membrane module of 2 m/s corresponding to a Reynolds number of approximately 4500. Temperature of the pervaporation module, the feed vessel and the permeate circuit was kept constant at 40 ºC. The permeate pressure, p_{perm} [Pa], was kept at 83 Pa. Regarding the ethyl acetate recovery, experiments were performed with a feed volume of 11L in order to ensure that the concentration of solute was constant throughout each experiment. The feed Reynolds number was maintained constant at 430 [143]. The temperature of the feed vessel and the permeate circuit was kept at 24±1 ºC and the permeate pressure was varied between 100 and 200 ± 10 Pa. The properties of

the feed solution are listed in Table 6.2. The Henry constant of compound *i*, H_i [Pa], is the product of its activity coefficient, γ_i [-], and its saturated vapour pressure, p_{vi} [Pa].

Table 6.2: Properties of the feed solution used in the pervaporation experiments at 40ºC

	molar fraction, x_i [-]	γ_i [-]	$p_{vi} \times 10^4$[Pa] [162]	$H_i \times 10^5$[Pa]
water,w	0.15	3.0[163]	0.74	0.21
isopropanol, IPA	0.85	1.0	1.4	0.14
ethyl acetate, eac	1.02×10^{-5}	50.0 [148]	1.2	5.8
water, w	~1.0	1.0	3.0	0.03

6.3.4 Sorption experiments

The sorption experiment of water in the HybSi® material was conducted at 40ºC starting with a binary mixture of 5%wt water in isopropanol (IPA), as in the pervaporation experiment performed to process this solution. The material was the active dense layer of the organic-inorganic hybrid silica-based hydrophilic membrane, HybSi®, provided by Pervatech. Small pieces of this active dense layer of HybSi® were placed in contact with the solution, in a mass ratio of solution to material of 3:1, in vials commonly used for headspace sampling in GC analysis, in order to assure a close system. A stirring and heating plate with a temperature controller was used. The vial was stirred with a magnetic stirrer for homogenising the mixture. The water content in the solution was periodically measured with a Karl-Fisher equipment (Model 756 KF Coulometer, Metrohm, Switzerland) after sampling with a gas tight syringe, from the beginning of the experiment until a stabilised value of water concentration was reached. Determination of sorption of ethyl acetate in the dense polymer POMS at 18ºC is described in Schäfer et al [150] using a similar method used for water, as described above.

6.3.5 Mass Spectrometry monitoring

A mass spectrometer characterises compounds according to their specific mass to charge ratio (m/z) and intensity of electric signal, providing a characteristic mass spectra of a specific compound. First the mass spectra are acquired in the scan mode in order to detect all mass fragments (m/z) for a defined compound. After the characteristic mass peaks are chosen, MS data is shown in the multiple ion detector (MID) mode. The selected mass fragments monitored were: m/z 18 for water, m/z 43 for ethyl acetate and m/z 43 also for isopropanol (ethyl acetate and isopropanol were not present in the same samples). The calibration procedure chosen is described in detail in [40]. Briefly, it converts the MS intensity of each individual compound in its corresponding pressure, assuring that each compound under study is the only specie in the circuit. The temperature is maintained constant as in the pervaporation experiments, measured

and controlled with a temperature controller (CB100, from RKC Instruments Inc., Japan) connected to a heating tape in the circuit. This calibration procedure allows for studying situations where a sudden and significant change in composition of the vapour stream occurs, since it can be performed in a wide range of partial pressures.

6.3.6 Off-line analysis

In order to confirm the concentrations provided by mass spectrometry, off-line analyses were performed to the condensate of the pervaporation experiments for both systems. The water content of the condensate was measured by a Refractive Index equipment. The concentration of ethyl acetate was measured by Gas Chromatography GC using a gas chromatograph CP-3800, Varian, USA, connected to an automatic sampler (Combi PAL, CTC Analytics, Switzerland) with a FFAP-CB capillary column Varian CP 7485. The method is described in [148]. Before injection, a previous dilution with water was performed, followed by a solvent extraction step with diethyl ether.

6.3.7 Calculation methods

Fittings to experimental data were performed using the TableCurve 2D® software. The model for characterising solute transient transport was developed using the Maple and the Wolfram Mathematica technical computing softwares, two different programs used in an independent way in order to assure confidence in the results.

6.4 Results and Discussion

6.4.1 Sorption experiments

At 40 ºC, the solution of water in isopropanol (5.0 % wt of water in isopropanol) in contact with the hybrid silica membrane, HybSi®, reached equilibrium conditions in less than two hours, as shown in Figure 6.2.

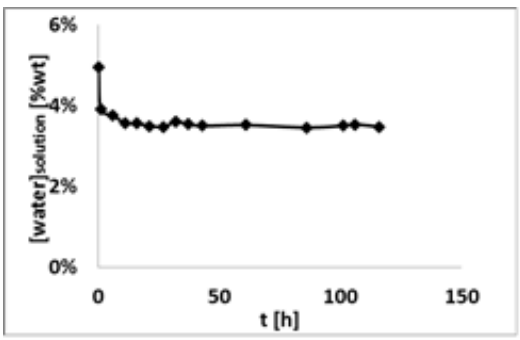

Figure 6.2: Sorption kinetics of water in hybrid silica, HybSi®, using a solution of water in isopropanol at 40ºC

The sorption coefficient obtained for water in hybrid silica, HybSi®, was found to be S_w=1.2, using equation (6.1)

$$S_w = \left[\frac{w_{w,membrane}}{w_{w,solution}} \right]_{equilibrium\ conditions} \quad (6.1)$$

where w [-] is the weight fraction. Sorption coefficient experiments were also performed for ethyl acetate in POMS, according to [150]. The sorption coefficient determined was 5.4, at 18 ºC, which was assumed to be very similar at 24±1 ºC (the temperature used in the pervaporation experiments). The sorption coefficients values for the two solutes under study in the respective membrane materials show that these solutes have a higher affinity towards the contacting membranes than to the solutions.

6.4.2 Characterisation of steady state transport properties

The length of each pervaporation test was enough to ensure that steady state was achieved (easily identified through the established MS online monitoring technique). The condensate from the steady period state was collected and characterised (using a Refractive Index measurement or by gas chromatography, according with the experiment) in terms of the solute molar fraction, partial fluxes (calculated from total fluxes and permeate composition), permeabilities, diffusion coefficients and selectivity (see Table 6.3). Composition of permeates, at steady state, determined off-line, was compared with the composition obtained on-line by MS measurement.

Table 6.3: Steady-state transport properties of pervaporation for the systems water in isopropanol and ethyl acetate in water using off-line analytical methods

	$y_{i,perm}$ [-]	J_i [m/s] .10^9	P_i [m^2/s] .10^{13}	D_i [m^2/s] .10^{13}	α_{i-j} [-]
water,w	0.99	316	377	3	391
isopropanol, IPA	0.01	5	0.96	-	-
ethyl acetate, eac	5.14E-03	0.05	655	121	602
water,w	0.995	10	1	2177	

Permeabilities, Pi [m^2/s] were calculated using the 1st Fick's law for systems at steady-state, using the sorption coefficient of solute i experimentally determined (water and ethyl acetate) and considering the gradient of partial pressure as the driving force of the process, through equation(6.2):

$$J_i = \frac{P_i}{L \cdot H_i} \cdot \left(p_{i,feed} - p_{i,perm} \right) \quad (6.2)$$

where $p_{i,feed}$ and $p_{i,perm}$ [Pa] are respectively the partial pressure of compound *i* in the feed and permeate compartments, which were calculated by the Raoult and Henry's laws.

$$J_i = \frac{P_i}{L \cdot H_i} \cdot \left(x_{i,feed} \cdot \gamma_{i,feed} \cdot p_{vi}\left(T_{feed}\right) - y_{i,perm} \cdot p_{perm} \right) \quad (6.2')$$

where L is the thickness of the active dense layer of film (m), T_{feed} is the temperature at the feed side and $y_{i,perm}$ [-] is the molar fraction of compound *i* in the permeate.

The solutes' diffusion coefficients in the steady state, D_i [m^2/s], were calculated through equation (6.3):

$$P_i = S_i \cdot D_i \quad (6.3)$$

and the solute selectivity in relation to the solvent, α_{i-j} [-], was defined as the ratio of the solute and solvent permeabilities. The ethyl acetate diffusion coefficient in the POMS membrane was found to be three orders of magnitude higher than the water diffusion coefficient in the hybrid silica membrane (see Table 6.3), even though ethyl acetate is a larger molecule (molecular mass of 88 g/mol) than water (molecular mass of 18 g/mol). This behaviour may be explained by the fact that the hybrid silica membrane, HybSi®, has a more rigid structure than the elastomeric POMS membrane.

6.5 Characterisation of solute permeation by on-line mass spectrometry

The transient period of pervaporation was characterised in terms of real-time permeate compositions and partial fluxes of the solutes (water and ethyl acetate), through on-line mass spectrometry monitoring, as shown in Figure 6.3.

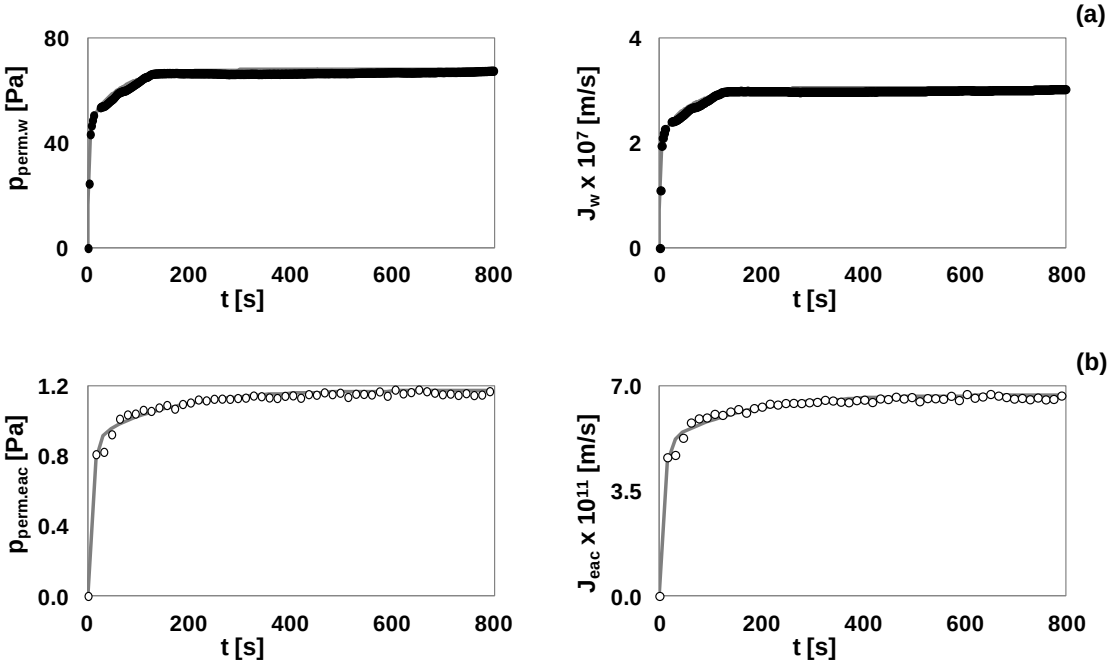

Figure 6.3: Experimental permeate partial pressures, pperm,i [Pa] and partial fluxes, Ji [m/s] obtained through on-line mass spectrometry (MS) monitoring (dots) for (a) the system of water in isopropanol and (b) the system of ethyl acetate in water and the respective fittings to the experimental data (lines)

Considering the linear relation between partial fluxes and corresponding intensities of electric signal of the characteristic mass peak, as shown in [39], the on-line partial fluxes, $J_i\ (t)$, were calculated using equation below.

$$J_i(t) = J_i(t=\infty) \cdot \frac{I_i(t)}{I_i(t=\infty)} \qquad (6.4)$$

The partial fluxes obtained using off-line methods (when the system is under steady state) were found to be similar to those obtained by mass spectrometry for the same period, as can be seen by comparing *Ji* values, shown in Table 6.3 and Figure 6.3. The values obtained by mass spectrometry in steady state were, therefore, validated when compared with those obtained by off-line measurement.

The partial pressures of each solute *i* in the permeate side, $p_{i,perm}$ [Pa], and its partial fluxes, J_i [m/s], were obtained by MS monitoring, enabling the acquisition of one data-point in every few seconds. This result is particularly remarkable and useful for monitoring fast transient periods. In this work it was possible to acquire one data point every two seconds, but this acquisition period may be additionally reduced.

The equation of transport (6.2'') and equations (6.5) and (6.6), obtained combining the equation of transport (6.2') with equations (6.3) and (6.4), were defined for the whole transient period, making possible to relate the flux and the diffusion coefficient of the solute:

$$J_i(t) = k_1 \cdot D_i(t) \cdot \left(k_2 - p_{i,perm}(t)\right) \qquad (6.2'')$$

$$k_1 = \frac{S_i}{L \cdot H_i} \qquad (6.5)$$

$$k_2 = p_{i,feed} \qquad (6.6)$$

where *L* [m] is the thickness of the membrane, *x* [m] is the space coordinate through which the mass transport occurs across the membrane, *x=0* corresponds to the membrane/feed interface and *x=L* corresponds to the membrane/permeate interface. k_1 [$Pa^{-1}.m^{-1}$] and k_2 [Pa] are constants. The partial permeate pressure of the solute pperm,i [Pa] and the solute partial fluxes J_i [m/s] evolve along time and were determined with a time interval as short as 2 seconds. The solute diffusion coefficient, D_i [m^2/s], is only dependent on time and is a spatial average for each short Δt. Consequently, solute diffusion coefficients through the whole transient period were calculated, from eq. (6.2'') - (6.6) (see Figure 6.4).

$$D(t) = \frac{J(t)}{k_1\left[k_2 - p(t)\right]} > 0; \quad t \geq 0 \qquad (6.7)$$

The evolvement of *D(t)* along time, presented in Figure 6.4 for the transport of water through the HybSi membrane and for ethyl acetate through the POMS membrane, offers extremely interesting information.

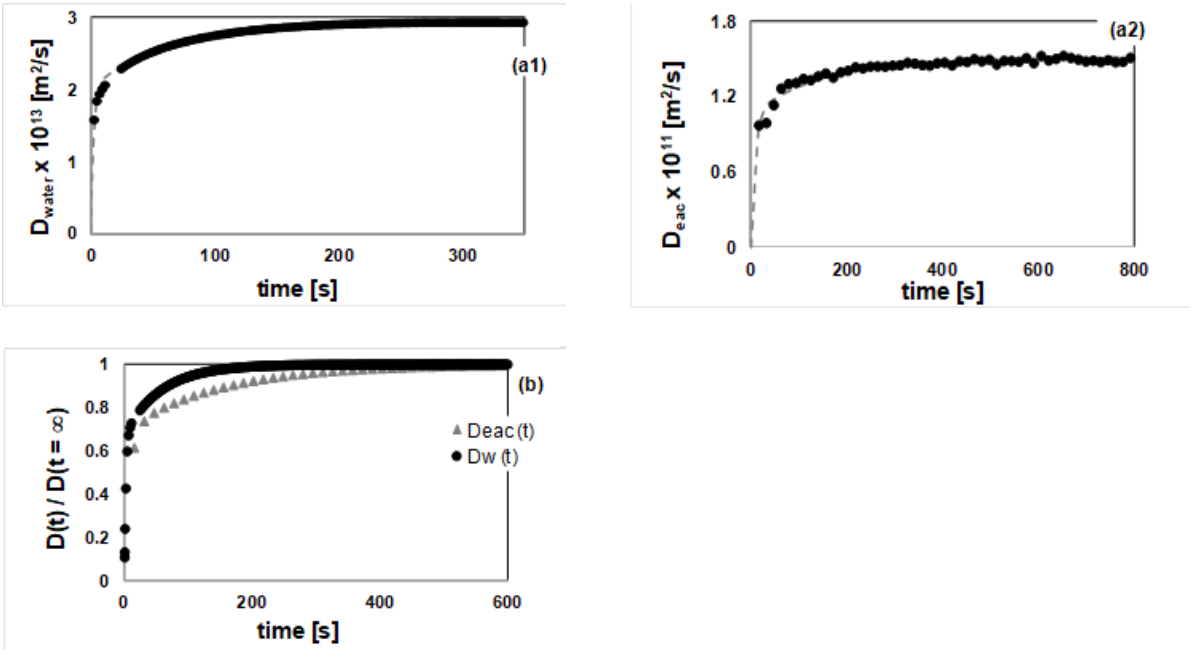

Figure 6.4: Solute diffusion coefficients, Di [m2/s], obtained through on-line mass spectrometry monitoring: (a) water diffusion coefficient in the system of water in isopropanol and (b) ethyl acetate diffusion coefficient in the system of ethyl acetate in water

In first place, it presents the actual values of the diffusion coefficients of target solutes and allows for comparing their absolute value. For the cases under study, it was interesting to find that the water diffusion coefficient through the HybSi membrane is smaller than the ethyl acetate diffusion coefficient through the POMS membrane. This behaviour results from the character of the HybSi membrane, which presents a more rigid structure, making difficult the diffusion of any permeant. In contrast, POMS is known as an elastomeric polymer that can easily accommodate permeant compounds, which can ultimately induce rearrangements in the polymer structure and lead to swelling effects. When comparing the evolvement of $D(t)/D\infty$ for both solutes it can be observed that the diffusion coefficient of water in the HybSi membrane reaches its steady state value, ($D\infty$), quicker than ethyl acetate in POMS, which is explained by the minor effect it induces in the structure of the more rigid membrane HybSi material. These curves, $D(t)/D\infty$, allow therefore to infer about the relevance of solute-membrane interactions and their relative importance.

It is interesting to mention that the transport of ethyl acetate through a POMS membrane can be studied using the time-lag method. The value found for the diffusion coefficient of ethyl acetate using this method is 1.2×10^{-12} m^2/s with a time-lag of 13.8s. This value is of the same order of magnitude of the average value of the experimental time-dependent diffusion coefficient of ethyl acetate (Figure 6.4b) between 0 s and 13.8 s (5.6×10^{-12} m^2/s, calculated from Figure 6.4b). However, the time-lag method does not allow to obtain a complete D(t) evolvement curve which can tell us a lot about the relevance of the solute-membrane interactions established.

6.5.1 Development of a mathematical model for solute transient transport through a dense membrane

Supported on the quality of the experimental data acquired by mass spectrometry, the next step was to derive the concentration profiles of the permeant solutes along the diffusion spatial coordinate (assuming a unidirectional flux). Using the on-line data obtained by mass spectrometry, the permeating solutes concentration profiles across the membrane were calculated along time.

In order to develop this mathematical model, fittings to the experimental values of solute permeate pressure (Figure 6.3) and solute flux were performed using the TableCurve 2D® software and were used in the model. Solutes sorption coefficients were also considered in the model, as well as other constants related with the solutes, namely their saturated vapour pressure at feed temperature, their Henry's constant and their molar fractions at the feed and permeate compartments (see eq.s. (6.2''), and (6.5) to (6.7)).

The analytical model proposed for the transient mass transport of a solute through a dense membrane material considered the following assumptions:

i. the fluid dynamic conditions used are sufficiently good to assure that the external mass transfer boundary layers (feed and permeate) are not relevant;

ii. the solute sorption is an extremely fast process that does not limit the process from a kinetic point of view;

iii. the active membrane layer is considered homogeneous for each short increment of time between measurements , and

iv. the diffusion of the solute is unidirectional, occurring only in the perpendicular direction to the membrane surface.

The first assumption was confirmed to be reasonable for the system of water in isopropanol considering the high value of feed Reynolds number used, which assures a turbulent flow. This assumption is also valid for the system of ethyl acetate in water according to study performed previously for ethyl acetate transport versus feed Reynolds number [143]. This assumption is also valid for the system of water in isopropanol considering the high value of feed Reynolds number of 4500, which clearly assures a turbulent flow, confirmed by the study of water transport *versus* feed Reynolds number as in [143]. The second assumption reflects the fact that interfacial phenomena are not the rate controlling steps in the penetrant transport from the external phase into the membrane material [27]. The third assumption is reasonable if we consider the extremely short time-interval achieved for data acquisition by mass spectrometry. The fourth assumption considers that the volume change of the polymer is small enough to assure a non-deformed coordinate system.

The change of concentration inside the membrane in the transient state can be given by the following expression:

$$\frac{\partial c}{\partial t} - \frac{\partial}{\partial x}\left(D(t) \cdot \frac{\partial c}{\partial x} \right) = 0; \quad 0 < x < L, t > 0 \tag{6.8}$$

where x=0 and x=L corresponds to the upstream and downstream interfaces of the membrane, respectively.

The initial condition of the model:

$$c(x, 0) = 0; \quad 0 < x < L \tag{6.9}$$

means that no solute is in the membrane at *t = 0*. The boundary conditions are:

$$c(0,t) = c_1; \quad t > 0 \tag{6.10}$$

$$-D(t)\frac{\partial c}{\partial x}(L,t) = J(t); \quad t > 0 \tag{6.11}$$

where *i* [-] is the solute concentration at the upstream surface of the membrane (*x=0*) (in weight fraction units) which considers the solubility of the solute in the membrane, and is given by the product of the solute concentration in the bulk feed solution (which was kept constant during the pervaporation experiment) and the solute sorption coefficient. The concentration at the downstream surface of the membrane (*x=L*) and for *t>0* is considered to be given by the partial pressure in the permeate circuit in each instant of time.

The output of the model is the concentration of the solute inside the membrane, which varies with the spatial coordinate *x* and time t, *c(x, t)*. The solution of the model is a concentration *c(x,t)* that is given as the sum of a transient *(u)* and of a quasi-stationary *(r)* component:

$$c(x,t) = u(x,t) + r(x,t); \quad 0 \le x \le L, \quad t \ge 0 \tag{6.12}$$

The transient component, function of *x* and *t*, was the product of orthogonal functions $X_n(x)$ and $T_n(t)$, unique solutions of the problem of Cauchy type solved numerically through the Euler method. The quasi-stationary component, function of *x* and *t*, were calculated with series of Fourier. When the diffusion coefficient was considered constant, the model was solved analytically. The detailed explanation of the solution of the model is given in Appendix A - 0.

Figure 6.5 shows the solutes' concentration profiles inside the membranes at different instants of time, considering time-dependent diffusion coefficients, for the systems water / HybSi and ethyl acetate / POMS-PEI. Time zero corresponds to the instant of time immediately before the solute started permeating the membrane, according to the initial condition of the model (eq.(6.9)).

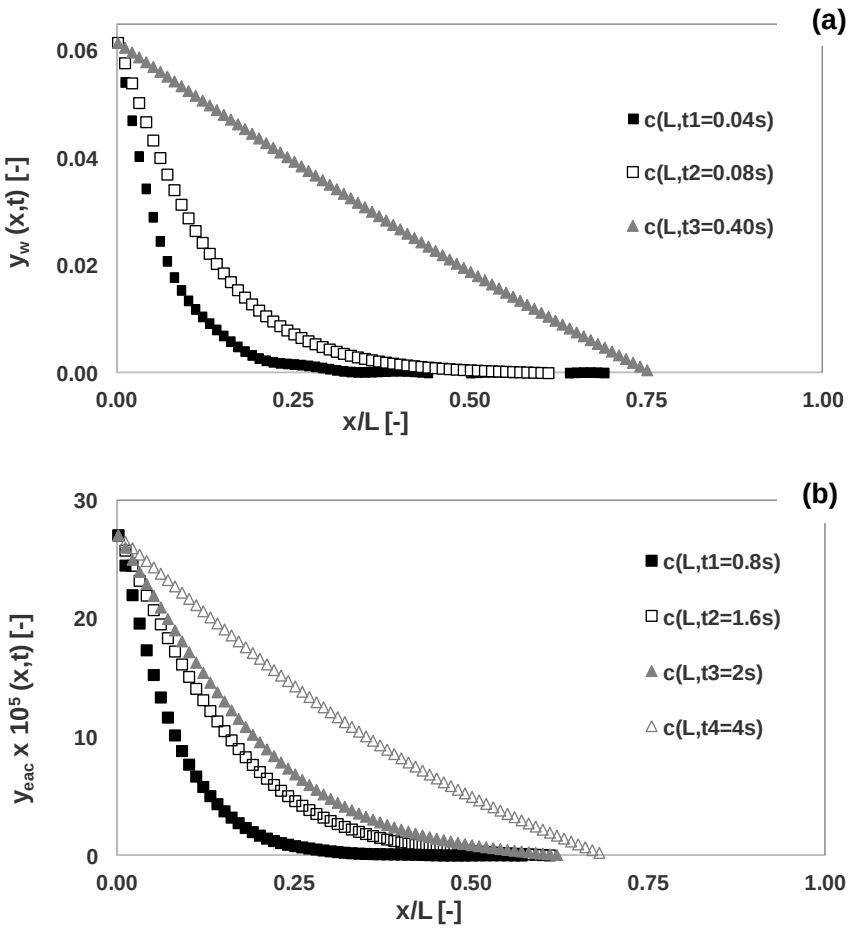

Figure 6.5: Time dependent solute weight fraction along the membrane for different periods of time (a) water concentration along HybSi® membrane and (b) ethyl acetate concentration along POMS-PEI membrane

The calculated concentrations profiles and their evolvement with time are extremely difficult to acquire experimentally, involving the use of sophisticated techniques, namely confocal methods such as confocal Raman. For the very short time span associated with transient periods it may be not possible to use these techniques and, under these circumstances it may not be possible to acquire solute concentration profiles inside dense membranes for the transient period. The concentration profiles presented in Figure 6.5 are non-linear and progressively approach a more linear profile. This behaviour reflects the evolvement of the membrane material as the penetrant solute starts by inducing rearrangements in the membrane structure until a more stable internal arrangement is achieved, as steady-state approaches. As expected, it can be seen the fast evolvement of the concentration profiles when water permeates the HybSi membrane (a shorter membrane rearrangement is induced), while this process takes longer when ethyl acetate is transported through the elastomeric POMS-PEI membrane.

In Figure 6.6, water and ethyl acetate concentrations inside the respective membranes, at the downstream interface of the membrane, are plotted as a function of time.

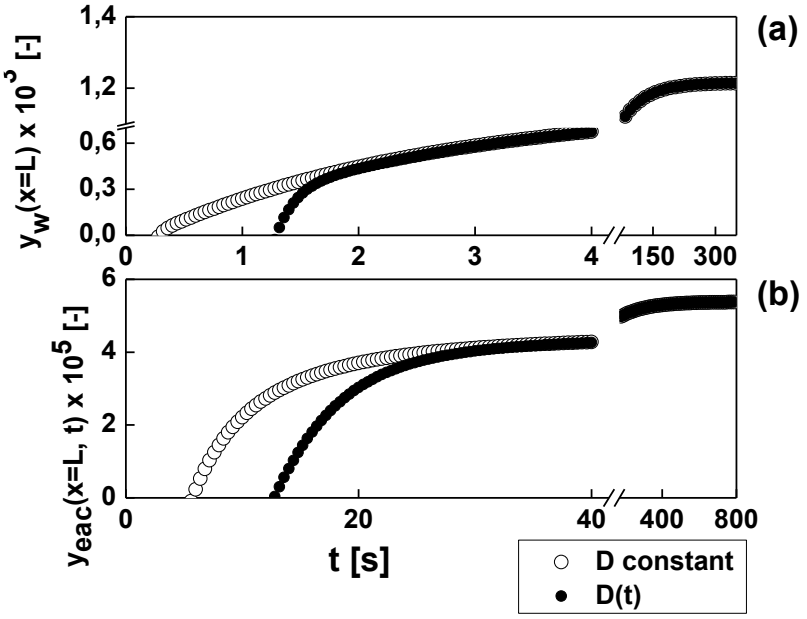

Figure 6.6: Solute weight fraction in the membrane at downstream side over time, calculated using (steady-state) constant and variable diffusion coefficients (a) for water in isopropanol using HybSi membrane and (b) ethyl acetate in water using POMS-PEI dense membrane.

Two different situations were considered: in one case, it was assumed that the solute transport process may be described by using a constant solute diffusion coefficient, calculated from steady-state conditions (D constant); in the other case, it was considered that a variable diffusion coefficient, *D(t)*, is required to properly describe the solute transport process. Obviously, at steady-state both approaches coincide. As it can be seen, the use of constant diffusion coefficients, estimated from steady-state conditions, leads to an overestimation of solute concentrations during the transient period, which are not correct, although expected since the $D_{constant}$ values were estimated when the membranes were already fully rearranged (steady-state) and transport occurs faster. This Figure shows clearly that the use of constant D values is, obviously, adequate for describing transport during steady-state; it also shows that they should not be used to describe transport during the transient period, where they predict wrongly the time required for permeation of the first molecules to the downstream compartment and the concentration of solute in the downstream interface during the transient period.

6.6 Conclusions

This work demonstrates that on-line monitoring of membrane processes by mass spectrometry offers a number of unique advantages for the understanding of membrane-solute interactions during mass transport. Since the composition of permeate streams can be acquired with time intervals as short as 2 seconds, and shorter, (see Figure 6.3) it is possible to follow the transport evolvement of multiple compounds through dense membranes from the onset of permeation. The way solute permeation evolves during the initial instants can tell us a lot about the nature of solute-

membrane interactions and how the membrane material adapts to the progressive penetration of target solutes.

Specifically this work shows that, using the on-line mass spectrometry technique and the adequate data analysis presented, it is possible to:

i. Determine the actual values of solute diffusion coefficients as a function of time elapsed since the onset of permeation, D(t) (see Figure 6.4a1 and Figure 6.4a2);

ii. Compare the absolute values of diffusion coefficient between solutes, for the same membrane or for different (or modified) membranes (see Figure 6.4a1 and Figure 6.4a2);

iii. Infer about membrane-solute interactions and their relative importance, i.e., the impact of solute penetration on membrane adaptation / rearrangement, by analysing and comparing the evolvement of *D(t)* curves for different solutes in different membranes (see Figure 6.4b);

iv. Infer solute concentration profiles inside the membrane as a function of time for different solutes in different membranes (see Figure 6.5);

v. Understand the limitations of describing a transient transport process using diffusion coefficients calculated from steady-state conditions (see Figure 6.6).

This methodology represents a fast and simple approach which can be used for guiding membrane development and better understanding of the impact of different membrane structures on solute transport. As an example that deserves to be studied, is the development of membranes starting from the same material but where different degrees of cross-linking are used [32]. Such membrane structures lead to different solute-membrane interactions and, therefore, different *c(L, t)* and *D(t)* profiles which can be obtained using the approach discussed. The same applies for situations where nanoparticles [164,165] or flakes are introduced within the membrane, either aiming to increase mass transport or hinder the permeation of given species.

7 General Conclusions And Future Work

7.1 General conclusions

The work presented in this thesis focused on developing a new methodology for characterising the multi-component solute transport through dense membranes, both in the transient and in the steady state of gas separation and pervaporation systems, using a Mass Spectrometer (MS) as an on-line, real-time, monitoring tool.

Different systems were characterised covering a wide variety of membranes and solutes worked under different operating conditions. A characterisation methodology was proposed aiming at studying systems that range from situations where the target solutes do not affect significantly the membrane structure to systems where the permeation of the solute may affect the transport properties, in particular the diffusion coefficient, along time.

In what concerns to gas permeation systems, two different approaches were used starting with the permeation of gases with low affinity to the membrane materials, where a single diffusion coefficient may be considered to the whole process (Chapter 2, using a time lag method for multicomponent systems), to gas permeation involving water vapour penetration with higher affinity to the membrane, causing modifications in its structure.

In relation to non-interacting solutes, a new method was developed to determine diffusion coefficients of individual components present in a gas mixture. The method, based on on-line Mass Spectrometry analysis of the permeate composition during the transient stage of permeation, is a powerful technique when compared with the traditional time lag method because of its unique capacity to quantify different gases simultaneously. There was a good agreement between individual gas diffusion coefficients obtained from the classical time lag method with pure gases and from the new time lag method with mixed gases, using the mass spectrometer as a monitoring analyser. The validation permeation experiments performed with ~~on~~ the polymer of intrinsic microporosity, PIM-EA-TB, not only demonstrated the potential of the method, but also showed the ability to perceive the concentration and pressure dependency of the transport parameters, and other “anomalous” phenomena related with CO_2-induced dilation.

Otherwise, several phenomena may occur inside the membrane in non-ideal processes, leading to a change of the diffusivity of the permeant with its own local concentration and, consequently, the change of its diffusivity with time. From the on-line MS monitoring technique, a method for calculating time-dependent diffusion coefficients in non-ideal systems was developed, both for gas separation, humidified gas streams, and pervaporation systems, where the solute presented a high affinity to the membrane. Time-dependent diffusion coefficients of a permeating solute

were calculated, where the membrane structure is potentially modified, due to solute-membrane interactions.

In this context, the potential of using the MS to monitor and characterise the permeation of gases under dry and humidified conditions was assessed. Aiming at studying the transient periods of the permeation processes, long transient periods were enforced to make possible the understanding of polymer rearrangements when penetrated by different solutes in multi-component systems and compare the behaviour exhibited by different materials. The methodology developed was also validated for pure gas permeation, with a general agreement with values reported in literature. Once validated, the methodology was implemented to monitor the permeation of water vapour, pure gases (CO_2, CH_4 and N_2) and gas mixtures containing 20 vol.% CO_2 + 80 vol.% N_2 and 70 vol.% CH_4 + 30 vol.% CO_2, at different conditions of relative humidity through a biopolymer membrane. This technique allowed also to monitor changes in gas permeation, in a binary gas mixture, potentially due to a coupling effect. Finally, on-line mass spectrometry was used to monitor the impact of water vapour in gas permeation, suggesting that membrane plasticisation may occur.

Two different pervaporation systems were also studied where the solutes presented affinity to the materials selected. In the first one, PDMS membranes were characterised by varying the degree of crosslinking in a pervaporation system coupled to a mass spectrometry (MS) for on-line monitoring. Using dilute aqueous solutions of ethyl acetate and hexyl acetate, it is shown how solutes with diverse nature and diverse partitioning into the membrane, determine the transport of solvent and solute by progressively modifying the membrane transport properties, namely during the transient permeation. It has been proved that solute solubilisation within the membrane polymer matrix induces internal rearrangements that impact not only on the transport of solutes themselves, but also on the transport of solvent. Moreover, solute transport evolves during the transient period during which the impact of solute solubilisation translates into a rearrangement of the membrane polymeric structure. It is worth mentioning that the impact is more relevant for bulky solutes, with a higher partitioning affinity, able to induce larger membrane rearrangements.

Finally, a mathematical model was developed in order to obtain solute concentration profiles inside the membrane and their evolvement along time. Two case-studies were selected, corresponding to different systems, using permeating solutes with different affinities towards the membranes under study. The transport properties of two different membrane materials were compared: a polymeric membrane, which may be prone to potential material reorganisation and a ceramic membrane with a rigid structure, where material rearrangements are not anticipated.

The model developed in this thesis constitutes a fast and simple approach, which can be used for guiding membrane development and better understanding of the impact of different membrane structures on solute transport. It has been proved that the way solute permeation evolves during the initial instants is related with the nature of solute–membrane interactions and how the membrane material adapts to the progressive penetration of target solutes.

It is important to mention that a reliable, easy and fast new calibration method was implemented to convert the electric signal of each compound into the volumetric concentrations (%vol/vol) or partial pressure. Through this calibration method, it was possible to quantify the mass transport permeating the membrane and, therefore, develop both the mixed gas time-lag and the time-dependent diffusion coefficient *D(t)* systems.

7.2 Future work

The tools developed in this PhD project for the study of solute transport through dense polymeric membranes, specifically the on-line Mass Spectrometry MS monitoring technique and the solute concentration model, should be used with complementary techniques, in order to gain a deeper understanding of this transport process.

In order to better understand solute-membrane interactions during solute permeation, the integration of complementary advanced and advanced characterisation techniques should be applied: Proton NMR Relaxometry, Thermogravimetric and Positron Annihilation Lifetime Spectroscopy (PALS). The results obtained will allow for understanding the relations between structural membrane properties and their functional behaviour.

Proton NMR Relaxometry techniques are particularly important if a non-destructive characterisation is required to explore the pore space of porous materials in contact with gases or liquid solutes. The information obtained through the combination of NMR Relaxometry with Thermogravimetry is extremely useful to infer about solute structuring inside the membrane polymer, which ultimately provides information about polymer arrangement. [166,167]

The Positron Annihilation Lifetime Spectroscopy technique allows to probe solid structures at an atomic scale. The information acquired may be particularly useful to determine the polymer free volume and interstitial cavity sizes. By measuring the lifetime of ortho-positronium prior to annihilation, the size of the free volume cavities can be determined [168]. The structural and morphological information acquired could be correlated with the most relevant functional properties aimed, including transport properties

Solute transport through dense membranes should also be studied at a molecular level, by combining on-line MS monitoring with molecular dynamics simulations, which will provide an opportunity for understanding molecular level mechanisms of solute transport through dense polymeric membranes.

The mathematical model developed in this work to obtain solute concentration profiles inside the membrane and their evolvement along time used experimental data obtained by the on-line MS. This model was validated through a very good agreement between the values of solute concentration at the downstream side of the membrane estimated by the model and obtained experimentally. In order to validate the model even further, other solute permeation systems

should be studied and other techniques that enable the determination of solute concentration inside the membrane along time, such as the Confocal Raman Microscopy or Fluorescence Spectroscopy, could be considered.

BIBLIOGRAPHY

[1] W.S.W. Ho, K. K.Sirkar, Membrane Handbook, Van Nostrand Reinhold, New york, 1992.

[2] K. Nath, Membrane Separation processes, Second Edi, Asoke K. Ghosh, Delhi, 2017.

[3] H. Strathmann, Membrane separation processes: Current relevance and future opportunities, AIChE J. 47 (2001) 1077–1087. doi:10.1002/aic.690470514.

[4] P. Shao, R.Y.M. Huang, Polymeric membrane pervaporation, J. Memb. Sci. 287 (2007) 162–179. doi:10.1016/j.memsci.2006.10.043.

[5] H. Lin, B.D. Freeman, Gas solubility, diffusivity and permeability in poly(ethylene oxide), J. Memb. Sci. 239 (2004) 105–117. doi:10.1016/j.memsci.2003.08.031.

[6]? ?lvaro A. Ram??rez-Santos, C. Castel, E. Favre, Utilization of blast furnace flue gas: Opportunities and challenges for polymeric membrane gas separation processes, J. Memb. Sci. 526 (2017) 191–204. doi:10.1016/j.memsci.2016.12.033.

[7] G.Q. Chen, C.A. Scholes, G.G. Qiao, S.E. Kentish, Water vapor permeation in polyimide membranes, J. Memb. Sci. 379 (2011) 479–487. doi:10.1016/j.memsci.2011.06.023.

[8] J. Potreck, K. Nijmeijer, T. Kosinski, M. Wessling, Mixed water vapor/gas transport through the rubbery polymer PEBAX® 1074, J. Memb. Sci. 338 (2009) 11–16. doi:10.1016/j.memsci.2009.03.051.

[9] M.R. Shah, R.D. Noble, D.E. Clough, Measurement of sorption and diffusion in nonporous membranes by transient permeation experiments, J. Memb. Sci. 287 (2007) 111–118. doi:10.1016/j.memsci.2006.10.026.

[10] J.G. Wijmans, R.W. Baker, The solution-diffusion model : a review, 107 (1995) 1–21. doi:10.1016/0376-7388(95)00102-I.

[11] M. Mulder, Basic Principles of Membrane Technology, Second Edi, Kluwer Academic Publishers, Netherlands, 2000.

[12] K. Tanaka, H. Kita, K.I. Okamoto, R.D. Noble, J.L. Falconer, Isotopic-transient permeation measurements in steady-state pervaporation through polymeric membranes, J. Memb. Sci. 197 (2002) 173–183. doi:10.1016/S0376-7388(01)00636-6.

[13] C.K. Yeom, B.S. Kim, J.M. Lee, Precise on-line measurements of permeation transients through dense polymeric membranes using a new permeation apparatus, 161 (1999) 55–66.

[14] H.A. Daynes, The process of diffusion through a rubber membrane, R. Soc. (1920).

[15] J. Crank, THE MATHEMATICS OF DIFFUSION, (1975).

[16] J. Crank, G.S. Park, Diffusion in Polymers, Academic Press, 1968.

[17] S.W. Rutherford, D.D. Do, Review of time lag permeation technique as a method for characterisation of porous media and membranes, Adsorption. 3 (1997) 283–312. doi:10.1007/BF01653631.

[18] E. Favre, N. Morliere, D. Roizard, Experimental evidence and implications of an imperfect upstream pressure step for the time-lag technique, J. Memb. Sci. 207 (2002) 59–72.

doi:10.1016/S0376-7388(02)00039-X.

[19] J.M. Watson, M.G. Baron, Precise static and dynamic permeation measurements using a continuous-flow vacuum cell, J. Memb. Sci. 106 (1995) 259–268. doi:10.1016/0376-7388(95)00090-Y.

[20] T. Schäfer, Recovery of wine-must aroma by pervaporation, 2002.

[21] P. Flory, Principles of Polymer Chemistry, Cornell University Press, Ithaca, New York, 1953.

[22] A. Heintz, W. Stephan, A generalized solution-diffusion model of the pervaporation process through composite membranes Part I. Prediction of mixture solubilities in the dense active layer using the UNIQUAC model, 89 (1994) 143–151.

[23] A. Jonquières, L. Perrin, S. Arnold, R. Clément, P. Lochon, From binary to ternary systems : general behaviour and modelling of membrane sorption in purely organic systems strongly deviating from ideality by UNIQUAC and related models, 174 (2000) 255–275.

[24] L. Perrin, Â. Arnold, P. Lochon, A. Jonquie, Comparison of UNIQUAC with related models for modelling vapour sorption in polar materials, 150 (1998).

[25] P. Iz??k, L. Bartovsk??, K. Friess, M. ????pek, P. Uchytil, Comparison of various models for transport of binary mixtures through dense polymer membrane, Polymer (Guildf). 44 (2003) 2679–2687. doi:10.1016/S0032-3861(03)00137-X.

[26] N. Follain, J.M. Valleton, L. Lebrun, B. Alexandre, P. Schaetzel, M. Metayer, S. Marais, Simulation of kinetic curves in mass transfer phenomena for a concentration-dependent diffusion coefficient in polymer membranes, J. Memb. Sci. 349 (2010) 195–207. doi:10.1016/j.memsci.2009.11.044.

[27] S. Marais, M. Metayer, Q.T. Nguyen, M. Labbe, D. Langevin, New methods for the determination of the parameters of a concentration-dependent diffusion law for molecular penetrants from transient permeation of sorption data, Macromol. Theory Simulations. 9 (2000) 207–214. doi:10.1002/(SICI)1521-3919(20000401)9:4<207::AID-MATS207>3.0.CO;2-Q.

[28] R.W. Baker, J.G. Wijmans, Y. Huang, Permeability, permeance and selectivity: A preferred way of reporting pervaporation performance data, J. Memb. Sci. 348 (2010) 346–352. doi:10.1016/j.memsci.2009.11.022.

[29] M. Fels, R.Y.M. Huang, Diffusion Coefficients of Liquids in Polymer Membranes by a Desorption Method, 14 (1970) 523–536.

[30] Q.T. Nguyen, E. Favre, Z.H. Ping, Clustering of solvents in membranes and its influence on membrane transport properties, 113 (1996) 137–150.

[31] P. Tremblay, M.M. Savard, J. Vermette, R. Paquin, Gas permeability, diffusivity and solubility of nitrogen, helium, methane, carbon dioxide and formaldehyde in dense polymeric membranes using a new on-line permeation apparatus, J. Memb. Sci. 282 (2006) 245–256. doi:10.1016/j.memsci.2006.05.030.

[32] C.R. Mason, L. Maynard-Atem, K.W.J. Heard, B. Satilmis, P.M. Budd, K. Friess, M. Lancì,

P. Bernardo, G. Clarizia, J.C. Jansen, Enhancement of CO2 affinity in a polymer of intrinsic microporosity by amine modification, Macromolecules. 47 (2014) 1021–1029. doi:10.1021/ma401869p.

[33] M. Macchione, J.C.J.C.J.C. Jansen, G. De Luca, E. Tocci, M. Longeri, E. Drioli, Experimental analysis and simulation of the gas transport in dense Hyflon?? AD60X membranes: Influence of residual solvent, Polymer (Guildf). 48 (2007) 2619–2635. doi:10.1016/j.polymer.2007.02.068.

[34] T.C. Bowen, J.C. Wyss, R.D. Noble, J.L. Falconer, Measurements of diffusion through a zeolite membrane using isotopic-transient pervaporation, Microporous Mesoporous Mater. 71 (2004) 199–210. doi:10.1016/j.micromeso.2004.03.032.

[35] M. Grazia, D. Angelis, G.C. Sarti, Mixed gas sorption in glassy polymeric membranes : I . CO 2 / CH 4 and n -C 4 / CH 4 mixtures sorption in poly (1-trimethylsilyl-1-propyne), 449 (2014) 97–108. doi:10.1016/j.memsci.2013.06.065.

[36] M. Grazia, D. Angelis, N. Du, N. Li, M.D. Guiver, G. Cesare, Mixed gas sorption in glassy polymeric membranes : II . CO 2 / CH 4 mixtures in a polymer of intrinsic microporosity (PIM-1), 459 (2014) 264–276. doi:10.1016/j.memsci.2014.02.003.

[37] I. Pinnau, Z. He, Pure- and mixed-gas permeation properties of polydimethylsiloxane for hydrocarbon/methane and hydrocarbon/hydrogen separation, J. Memb. Sci. 244 (2004) 227–233. doi:10.1016/j.memsci.2004.06.055.

[38] C.K. Yeom, S.H. Lee, J.M. Lee, Study of Transport of Pure and Mixed CO 2 / N 2 Gases through Polymeric Membranes, J. Appl. Phys. 78 (2000) 179–189. doi:10.1002/1097-4628(20001003)78:1<179::AID-APP220>3.0.CO;2-Z.

[39] T. Schäfer, J. Vital, J.G. Crespo, Coupled pervaporation/mass spectrometry for investigating membrane mass transport phenomena, J. Memb. Sci. 241 (2004) 197–205. doi:10.1016/j.memsci.2004.05.014.

[40] C. Brazinha, a. P.P. Fonseca, O.M.N.D.M.N.D. Teodoro, J.G. Crespo, On-line and real-time monitoring of organophilic pervaporation by mass spectrometry, J. Memb. Sci. 347 (2010) 83–92. doi:10.1016/j.memsci.2009.10.009.

[41] K.D. Cook, K.H. Bennett, M.L. Haddix, On-Line Mass Spectrometry : A Faster Route to Process Monitoring and Control, (1999) 1192–1204. doi:10.1021/ie9707984.

[42] W.J. Koros, A. Kratochvil, S. Shu, S. Husain, Energy and Environmental Issues and Impacts of Membranes in Industry, 2009. doi:10.1002/9783527626779.ch7.

[43] H.B. Park, J. Kamcev, L.M. Robeson, M. Elimelech, B.D. Freeman, Maximizing the right stuff: The trade-off between membrane permeability and selectivity, Science (80-.). 356 (2017) eaab0530. doi:10.1126/science.aab0530.

[44] I. Pinnau, L.G. Toy, Gas and vapor transport properties of amorphous perfluorinated copolymer membranes based on 2,2-bistrifluoromethyl-4,5-difluoro-1,3-dioxole/tetrafluoroethylene, J. Memb. Sci. 109 (1996) 125–133. doi:10.1016/0376-7388(95)00193-X.

[45] R.R. Tiwari, Z.P. Smith, H. Lin, B.D. Freeman, D.R. Paul, Gas permeation in thin films of

"high free-volume" glassy perfluoropolymers: Part I. Physical aging, Polym. (United Kingdom). 55 (2014) 5788–5800. doi:10.1016/j.polymer.2014.09.022.

[46] Z. Cui, E. Drioli, Y.M. Lee, Recent progress in fluoropolymers for membranes, Prog. Polym. Sci. 39 (2014) 164–198. doi:10.1016/j.progpolymsci.2013.07.008.

[47] N.B. McKeown, P.M. Budd, K.J. Msayib, B.S. Ghanem, H.J. Kingston, C.E. Tattershall, S. Makhseed, K.J. Reynolds, D. Fritsch, Polymers of intrinsic microporosity (PIMs): Bridging the void between microporous and polymeric materials, Chem. - A Eur. J. 11 (2005) 2610–2620. doi:10.1002/chem.200400860.

[48] N.B. McKeown, P.M. Budd, Polymers of intrinsic microporosity (PIMs): organic materials for membrane separations, heterogeneous catalysis and hydrogen storage., Chem. Soc. Rev. 35 (2006) 675–683. doi:10.1039/b600349d.

[49] I. Rose, C.G. Bezzu, M. Carta, B. Comesaña-Gándara, E. Lasseuguette, M.C.C. Ferrari, P. Bernardo, G. Clarizia, A. Fuoco, J.C. Jansen, K.E.E. Hart, T.P. Liyana-Arachchi, C.M. Colina, N.B. McKeown, Polymer ultrapermeability from the inefficient packing of 2D chains, Nat. Mater. 16 (2017) 932–937. doi:10.1038/nmat4939.

[50] S. Thomas, I. Pinnau, N. Du, M.D. Guiver, Pure- and mixed-gas permeation properties of a microporous spirobisindane-based ladder polymer (PIM-1), J. Memb. Sci. 333 (2009) 125–131. doi:10.1016/j.memsci.2009.02.003.

[51] N. Du, H.B. Park, G.P. Robertson, M.M. Dal-Cin, T. Visser, L. Scoles, M.D. Guiver, Polymer nanosieve membranes for CO2-capture applications., Nat. Mater. 10 (2011) 372–375. doi:10.1038/nmat2989.

[52] H.B. Park, C.H. Jung, Y.M. Lee, A.J. Hill, S.J. Pas, S.T. Mudie, E. Van Wagner, B.D. Freeman, D.J. Cookson, Polymers with cavities tuned for fast selective transport of small molecules and ions., Science. 318 (2007) 254–8. doi:10.1126/science.1146744.

[53] H.B. Park, S.H. Han, C.H. Jung, Y.M. Lee, A.J. Hill, Thermally rearranged (TR) polymer membranes for CO2 separation, J. Memb. Sci. 359 (2010) 11–24. doi:10.1016/j.memsci.2009.09.037.

[54] H. Shamsipur, B.A. Dawood, P.M. Budd, P. Bernardo, G. Clarizia, J.C. Jansen, Thermally Rearrangeable PIM-Polyimides for Gas Separation Membranes, Macromolecules. 47 (2014) 5595–5606. doi:10.1021/ma5011183.

[55] J.E. Bara, T.K. Carlisle, C.J. Gabriel, D. Camper, A. Finotello, D.L. Gin, R.D. Noble, Guide to CO 2 Separations in Imidazolium-Based Room-Temperature Ionic Liquids, Ind. Eng. Chem. Res. 48 (2009) 2739–2751. doi:10.1021/ie8016237.

[56] J.C. Jansen, K. Friess, G. Clarizia, J. Schauer, P. Izák, High Ionic Liquid Content Polymeric Gel Membranes: Preparation and Performance, Macromolecules. 44 (2011) 39–45. doi:10.1021/ma102438k.

[57] Z. Dai, R.D. Noble, D.L. Gin, X. Zhang, L. Deng, Combination of ionic liquids with membrane technology: A new approach for CO2 separation, J. Memb. Sci. 497 (2016) 1–20. doi:10.1016/j.memsci.2015.08.060.

[58] M.C. Villet, G.R. Gavalas, Measurement of concentration-dependent gas diffusion

coefficients in membranes from a psuedo-steady state permeation run, J. Memb. Sci. 297 (2007) 199–205. doi:10.1016/j.memsci.2007.03.045.

[59] N. Al-Qasas, J. Thibault, B. Kruczek, A new characterization method of membranes with nonlinear sorption isotherm systems based on continuous upstream and downstream time-lag measurements, J. Memb. Sci. 542 (2017) 91–101. doi:10.1016/j.memsci.2017.07.039.

[60] J.C. Jansen, K. Friess, E. Tocci, M. Macchione, Amorphous Glassy Perfluoropolymer Membranes of Hyflon AD ®: Free Volume Distribution by Photochromic Probing and Vapour Transport Properties, in: Y. Yampolskii, B. Freeman (Eds.), Membr. Gas Sep., John Wiley & Sons, Ltd, Chichester, UK, 2010: pp. 59–83. doi:10.1002/9780470665626.ch4.

[61] J.C. Jansen, K. Friess, E. Drioli, Organic vapour transport in glassy perfluoropolymer membranes: A simple semi-quantitative approach to analyze clustering phenomena by time lag measurements, J. Memb. Sci. 367 (2011) 141–151. doi:10.1016/j.memsci.2010.10.063.

[62] R.D. Raharjo, B.D. Freeman, E.S. Sanders, Pure and mixed gas CH<inf>4</inf> and n-C<inf>4</inf>H<inf>10</inf> sorption and dilation in poly(dimethylsiloxane), J. Memb. Sci. 292 (2007). doi:10.1016/j.memsci.2007.01.012.

[63] O. Vopička, M.G. De Angelis, G.C. Sarti, Mixed gas sorption in glassy polymeric membranes: I. CO2/CH4 and n-C4/CH4 mixtures sorption in poly(1-trimethylsilyl-1-propyne) (PTMSP), J. Memb. Sci. 449 (2014) 97–108. doi:10.1016/j.memsci.2013.06.065.

[64] O. Vopička, M.G.M.G. De Angelis, N. Du, N. Li, M.D.M.D. Guiver, G.C.G.C. Sarti, Mixed gas sorption in glassy polymeric membranes: II. CO2/CH4 mixtures in a polymer of intrinsic microporosity (PIM-1), J. Memb. Sci. 459 (2014) 264–276. doi:10.1016/j.memsci.2014.02.003.

[65] L. Garrido, C. García, M. López-González, B. Comesaña-Gándara, Á.E. Lozano, J. Guzmán, Determination of Gas Transport Coefficients of Mixed Gases in 6FDA-TMPDA Polyimide by NMR Spectroscopy, Macromolecules. 50 (2017) 3590–3597. doi:10.1021/acs.macromol.7b00384.

[66] S.L. Shannon, J.G. Goodwin, Characterization of Catalytic Surfaces, Chem. Rev. 95 (1995) 677–695. doi:10.1021/cr00035a011.

[67] R.C. Johnson, R.G. Cooks, T.M. Allen, M.E. Cisper, P.H. Hemberger, Membrane introduction mass spectrometry: trends and applications., Mass Spectrom. Rev. 19 (2000) 1–37. doi:10.1002/(SICI)1098-2787(2000)19:1<1::AID-MAS1>3.0.CO;2-Y.

[68] P.D. Tortell, OCEANOGRAPHY : METHODS Dissolved gas measurements in oceanic waters made by membrane inlet mass spectrometry, Limnol. Oceanogr. Methods. 2 (2005) 24–37. doi:10.4319/lom.2005.3.24.

[69] Z. Zhang, R. Chattot, L. Bonorand, K. Jetsrisuparb, Y. Buchmüller, A. Wokaun, L. Gubler, Mass spectrometry to quantify and compare the gas barrier properties of radiation grafted membranes and Nafion®, J. Memb. Sci. 472 (2014) 55–66.

doi:10.1016/j.memsci.2014.08.020.

[70] S.C.C. Fraga, L. Trabucho, C. Brazinha, J.G.G. Crespo, Characterisation and modelling of transient transport through dense membranes using on-line mass spectrometry, J. Memb. Sci. 479 (2015) 213–222. doi:10.1016/j.memsci.2014.12.016.

[71] S.C. Fraga, M.A. Azevedo, I.M. Coelhoso, C. Brazinha, G. Crespo, Steady-state and Transient Transport Studies of Gas Permeation Through Dense Membranes Using On-line Mass Spectrometry, Sep. Purif. Technol. (2017). doi:10.1016/j.seppur.2017.12.026.

[72] M. Carta, R. Malpass-Evans, M. Croad, Y. Rogan, J.C. Jansen, P. Bernardo, F. Bazzarelli, N.B. McKeown, An Efficient Polymer Molecular Sieve for Membrane Gas Separations, Science (80-.). 339 (2013) 303–307. doi:10.1126/science.1228032.

[73] M.R. Khdhayyer, E. Esposito, A. Fuoco, M. Monteleone, L. Giorno, J.C. Jansen, M.P. Attfield, P.M. Budd, Mixed matrix membranes based on UiO-66 MOFs in the polymer of intrinsic microporosity PIM-1, Sep. Purif. Technol. 173 (2017) 304–313. doi:10.1016/j.seppur.2016.09.036.

[74] E. Tocci, L. De Lorenzo, P. Bernardo, G. Clarizia, F. Bazzarelli, N.B. McKeown, M. Carta, R. Malpass-Evans, K. Friess, K. Pilnáček, M. Lanč, Y.P. Yampolskii, L. Strarannikova, V. Shantarovich, M. Mauri, J.C. Jansen, Molecular modeling and gas permeation properties of a polymer of intrinsic microporosity composed of ethanoanthracene and Tröger's base units, Macromolecules. 47 (2014) 7900–7916. doi:10.1021/ma501469m.

[75] J.C. Jansen, M. Macchione, E. Drioli, J. Carolus, M. Macchione, E. Drioli, On the unusual solvent retention and the effect on the gas transport in perfluorinated Hyflon AD ® membranes, J. Memb. Sci. 287 (2007) 132–137. doi:10.1016/j.memsci.2006.10.031.

[76] M. Macchione, J.C. Jansen, G. De Luca, E. Tocci, M. Longeri, E. Drioli, Experimental analysis and simulation of the gas transport in dense Hyflon® AD60X membranes: Influence of residual solvent, Polymer (Guildf). 48 (2007) 2619–2635. doi:10.1016/j.polymer.2007.02.068.

[77] P. Bernardo, J.C. Jansen, F. Bazzarelli, F. Tasselli, A. Fuoco, K. Friess, P. Izák, V. Jarmarová, M. Kačírková, G. Clarizia, Gas transport properties of Pebax®/room temperature ionic liquid gel membranes, Sep. Purif. Technol. 97 (2012) 73–82. doi:10.1016/j.seppur.2012.02.041.

[78] H. Ørsnes, S. Bohatka, H. Degn, Reaction of water at hot filament interferes with measurements of dissolved gases by membrane inlet mass spectrometry, Rapid Commun. Mass Spectrom. 11 (1997) 1736–1738. doi:10.1002/(SICI)1097-0231(19971015)11:15<1736::AID-RCM50>3.0.CO;2-J.

[79] C.R. Lieszkovszky, L.;Filippelli, A.R.;Tilford, Metrological characteristics of a group of quadrupole partial pressure analyzers, J. Vac. Sci. Technol. A Vacuum, Surfaces, Film. 8 (1990) 3838–3854. doi:10.1116/1.576458.

[80] J.A. Basford, M.D. Boeckmann, R.E. Ellefson, A.R. Filippelli, D.H. Holkeboer, L. Lieszkovsky, C.M. Stupak, Recommended Practice for the Calibration of Mass Spectrometers for Partial Pressure Analysis, J. Vac. Sci. Technol. A Vacuum, Surfaces,

Film. A11 (1993) A22. doi:10.1116/1.4755937.

[81] B. Flaconneche, J. Martin, M.H. Klopffer, Transport Properties of Gases in Polymers: Experimental Methods, Oil Gas Sci. Technol. 56 (2001) 245–259. doi:10.2516/ogst:2001022.

[82] J.H.H. Kim, S.Y.Y. Ha, Y.M.M. Lee, Gas permeation of poly(amide-6-b-ethylene oxide) copolymer, J. Memb. Sci. 190 (2001) 179–193. doi:10.1016/S0376-7388(01)00444-6.

[83] J. Marchese, E. Garis, M. Anson, N.A. Ochoa, C. Pagliero, Gas sorption, permeation and separation of ABS copolymer membrane, J. Memb. Sci. 221 (2003) 185–197. doi:10.1016/S0376-7388(03)00258-8.

[84] B. Bolto, M. Hoang, Z. Xie, A review of water recovery by vapour permeation through membranes, Water Res. 46 (2011) 259–266. doi:10.1016/j.watres.2011.10.052.

[85] S.J. Metz, W.J.C. Van De Ven, J. Potreck, M.H. V Mulder, M. Wessling, Transport of water vapor and inert gas mixtures through highly selective and highly permeable polymer membranes, 251 (2005) 29–41. doi:10.1016/j.memsci.2004.08.036.

[86] H. Sijbesma, K. Nymeijer, R. Van Marwijk, R. Heijboer, J. Potreck, M. Wessling, Flue gas dehydration using polymer membranes, 313 (2008) 263–276. doi:10.1016/j.memsci.2008.01.024.

[87] M. Shuangchen, C. Jin, J. Kunling, M. Lan, Z. Sijie, W. Kai, Environmental influence and countermeasures for high humidity flue gas discharging from power plants, Renew. Sustain. Energy Rev. 73 (2017) 225–235. doi:10.1016/j.rser.2017.01.143.

[88] E. Ryckebosch, M. Drouillon, H. Vervaeren, Techniques for transformation of biogas to biomethane, 5 (2011). doi:10.1016/j.biombioe.2011.02.033.

[89] B. Bharathiraja, T. Sudharsanaa, A. Bharghavi, J. Jayamuthunagai, R. Praveenkumar, Biohydrogen and Biogas – An overview on feedstocks and enhancement process, 185 (2016) 810–828.

[90] P. Scovazzo, A.J. Scovazzo, Isothermal dehumidification or gas drying using vacuum sweep dehumidification, Appl. Therm. Eng. 50 (2013) 225–233. doi:10.1016/j.applthermaleng.2012.05.019.

[91] P.G. Ingole, W.K. Choi, G.B. Lee, H.K. Lee, Thin-film-composite hollow-fiber membranes for water vapor separation, Desalination. 403 (2017) 12–23. doi:10.1016/j.desal.2016.06.003.

[92] K. Dalane, Z. Dai, G. Mogseth, M. Hillestad, L. Deng, Journal of Natural Gas Science and Engineering Potential applications of membrane separation for subsea natural gas processing : A review, 39 (2017) 101–117.

[93] P. Scovazzo, Testing and evaluation of room temperature ionic liquid (RTIL) membranes for gas dehumidification, J. Memb. Sci. 355 (2010) 7–17. doi:10.1016/j.memsci.2010.02.067.

[94] D. Thuan, A. Nida, K. Choon, K. Jon, Water vapor permeation and dehumidi fi cation performance of poly (vinyl alcohol)/ lithium chloride composite membranes, 498 (2016) 254–262.

[95] A. Figoli, T. Marino, S. Simone, E. Di Nicolò, X.-M. Li, T. He, S. Tornaghi, E. Drioli, Towards non-toxic solvents for membrane preparation: a review, Green Chem. 16 (2014) 4034. doi:10.1039/C4GC00613E.

[96] I.T. Meireles, R.M. Huertas, C.A.V. Torres, I.M. Coelhoso, J.G. Crespo, Development and Caracterization of Hybrid Polysaccharide Membranes for Dehydration Processes, Carbohydr. Polym. (2018).

[97] A. Woli, P. Kubica, A. Jankowski, M. Wójtowicz, Gas and water vapor transport properties of mixed matrix membranes containing 13X zeolite, 526 (2017) 334–347.

[98] X. Ren, M. Kanezashi, H. Nagasawa, T. Tsuru, Preparation of organosilica membranes on hydrophobic intermediate layers and evaluation of gas permeation in the presence of water vapor, 496 (2015) 156–164.

[99] S.C. Fraga, M.A. Azevedo, I.M. Coelhoso, C. Brazinha, J.G. Crespo, Steady-state and Transient Transport Studies of Gas Permeation trough Dense Membrane using On-line Mass Spectrometry, Sep. Purif. Technol. (2017) 0–31. doi:10.1016/j.healthpol.2016.12.009.

[100] S.C. Fraga, A. Kujawska, W. Kujawski, C. Brazinha, J.G. Crespo, Transport of dilute organics through dense membranes: Assessing impact on membrane-solute interactions, J. Memb. Sci. 523 (2017) 346–354. doi:10.1016/j.memsci.2016.10.013.

[101] R.D. Voyksner, G.W. Sovocool, M.M. Bursey, J.R. Hass, Comparison of Gas Chromatography/High-Resolution Mass Spectrometry and Mass Spectrometry/Mass Spectrometry for Detection of Polychlorinated Biphenyls and Tetrachlorodibenzofuran, Anal. Chem. 55 (1983) 744–749.

[102] Vaisala, HMI41 Indicator and HMP42 Probe Operating Manual, n.d.

[103] Y. Hasegawa, K. Kimura, Y. Nemoto, T. Nagase, Y. Kiyozumi, T. Nishide, F. Mizukami, Real-time monitoring of permeation properties through polycrystalline MFI-type zeolite membranes during pervaporation using mass-spectrometry, Sep. Purif. Technol. 58 (2008) 386–392. doi:10.1016/j.seppur.2007.05.014.

[104] J. Biscarat, C. Charmette, J. Sanchez, C. Pochat-bohatier, Gas permeability properties of gelatin / polyetheramine blend membranes made without organic solvent, 142 (2015) 33–39.

[105] P. Dole, C. Joly, E. Espuche, I. Alric, N. Gontard, Gas transport properties of starch based films, 58 (2004) 335–343. doi:10.1016/j.carbpol.2004.08.002.

[106] S. Nousir, N. Platon, K. Ghomari, A.S. Sergentu, T.C. Shiao, G. Hersant, J.Y. Bergeron, R. Roy, A. Azzouz, Correlation between the hydrophilic character and affinity towards carbon dioxide of montmorillonite-supported polyalcohols, J. Colloid Interface Sci. 402 (2013) 215–222. doi:10.1016/j.jcis.2013.03.050.

[107] N. Mehio, S. Dai, D. Jiang, Quantum Mechanical Basis for Kinetic Diameters of Small Gaseous Molecules, (2014) 1150–1154. doi:10.1021/jp412588f.

[108] C. Tsvigu, E. Pavesi, M.G. De Angelis, M.G. Baschetti, Effect of relative humidity and temperature on the gas transport properties of 6FDA – 6FpDA polyimide : Experimental

study and modelling, 485 (2015) 60–68.

[109] G.Q. Chen, S. Kanehashi, C.M. Doherty, A.J. Hill, S.E. Kentish, Water vapor permeation through cellulose acetate membranes and its impact upon membrane separation performance for natural gas puri fi cation, 487 (2015) 249–255.

[110] L.A. Neves, J.G. Crespo, I.M. Coelhoso, Gas permeation studies in supported ionic liquid membranes, J. Memb. Sci. 357 (2010) 160–170. doi:10.1016/j.memsci.2010.04.016.

[111] O. Aschenbrenner, P. Styring, Comparative study of solvent properties for carbon dioxide absorption, Energy Environ. Sci. 3 (2010) 1106–1113. doi:10.1039/C002915G.

[112] P. Scharlin, R. Battino, Solubility of CCl2F2, CClF3, CF4, and CH4 in Water and Seawater at 288.15-303.15 K and 101.325 kPa, J. Chem. Eng. Data. 40 (1) (1995) 167–169.

[113] S.R. Reijerkerk, R. Jordana, K. Nijmeijer, M. Wessling, Highly hydrophilic, rubbery membranes for CO2 capture and dehydration of flue gas, Int. J. Greenh. Gas Control. 5 (2011) 26–36. doi:10.1016/j.ijggc.2010.06.014.

[114] Kimberly Lynn Bothi, Characterization of Biogas from anaerobically digested dairy waste for energy use, New York, 2007.

[115] C.A. Scholes, B.D. Freeman, S.E. Kentish, Water vapor permeability and competitive sorption in thermally rearranged (TR) membranes, 470 (2014) 132–137.

[116] M. Irshad, P.G. Ingole, W. Kil, J. Jeon, B. Jang, J. Ho, H. Keun, Synthesis and characterization of thin film nanocomposite membranes incorporated with surface functionalized Silicon nanoparticles for improved water vapor permeation performance, 308 (2017) 27–39.

[117] R.W. Baker, K. Lokhandwala, Natural Gas Processing with Membranes : An Overview, (2008) 2109–2121.

[118] C.A. Scholes, G.Q. Chen, W.X. Tao, J. Bacus, C. Anderson, G.W. Stevens, S.E. Kentish, Energy Procedia The effects of minor components on the gas separation performance of membranes for carbon capture, Energy Procedia. 4 (2011) 681–687. doi:10.1016/j.egypro.2011.01.105.

[119] P.S. Tin, T.S. Chung, Y. Liu, R. Wang, S.L. Liu, K.P. Pramoda, Effects of cross-linking modification on gas separation performance of Matrimid membranes, 225 (2003) 77–90. doi:10.1016/j.memsci.2003.08.005.

[120] M. Miki, H. Horiuchi, Y. Yamada, Synthesis and Gas Transport Properties of Hyperbranched Polyimide–Silica Hybrid/Composite Membranes, (2013) 1362–1379. doi:10.3390/polym5041362.

[121] H. Lin, S.M. Thompson, A. Serbanescu-martin, J.G. Wijmans, K.D. Amo, K.A. Lokhandwala, B.T. Low, T.C. Merkel, Dehydration of natural gas using membranes . Part II : Sweep / countercurrent design and field test, J. Memb. Sci. 432 (2013) 106–114. doi:10.1016/j.memsci.2012.12.049.

[122] C.K. Yeom, J.M. Lee, Y.T. Hong, K.Y. Choi, S.C. Kim, Analysis of permeation transients of pure gases through dense polymeric membranes measured by a new permeation apparatus, J. Memb. Sci. 166 (2000) 71–83. doi:10.1016/S0376-7388(99)00252-5.

[123] M.W. Reij, J.T.. Keurentjes, S. Hartmans, Membrane bioreactors for waste gas treatment, J. Biotechnol. 59 (1998) 155–167. doi:10.1016/S0168-1656(97)00169-7.

[124] J. Vandewijngaarden, M. Murariu, P. Dubois, R. Carleer, J. Yperman, P. Adriaensens, S. Schreurs, N. Lepot, R. Peeters, M. Buntinx, Gas Permeability Properties of Poly(3-hydroxybutyrate-co-3-hydroxyhexanoate), J. Polym. Environ. 22 (2014) 501–507. doi:10.1007/s10924-014-0688-1.

[125] K. Nidhi, S. Indrajeet, M. Khushboo, K. Gauri, D.J. Sen, Hydrotropy: A promising tool for solubility enhancement: A review, Int. J. Drug Dev. Res. 3 (2011) 26–33. doi:10.1002/jps.

[126] F. Munarin, M.C. Tanzi, P. Petrini, Advances in biomedical applications of pectin gels, Int. J. Biol. Macromol. 51 (2012) 681–689. doi:10.1016/j.ijbiomac.2012.07.002.

[127] P.J.P. Espitia, W.X. Du, R. de J. Avena-Bustillos, N. de F.F. Soares, T.H. McHugh, Edible films from pectin: Physical-mechanical and antimicrobial properties - A review, Food Hydrocoll. 35 (2014) 287–296. doi:10.1016/j.foodhyd.2013.06.005.

[128] B.H.Gregory, Film Extrusion: A Process Manual, Edition 11, Trafford Publishing, USA., 2009.

[129] A. Jiménez, M.J. Fabra, P. Talens, A. Chiralt, Edible and Biodegradable Starch Films: A Review, Food Bioprocess Technol. 5 (2012) 2058–2076. doi:10.1007/s11947-012-0835-4.

[130] T.C. Merkel, V.I. Bondar, K. Nagai, B.D. Freeman, I. Pinnau, Gas sorption, diffusion, and permeation in poly(dimethylsiloxane), J. Polym. Sci. Part B Polym. Phys. 38 (2000) 415–434. doi:10.1002/(SICI)1099-0488(20000201)38:3<415::AID-POLB8>3.0.CO;2-Z.

[131] T.C. Merkel, R.P. Gupta, B.S. Turk, B.D. Freeman, Mixed-gas permeation of syngas components in poly (dimethylsiloxane) and poly (1-trimethylsilyl-1-propyne) at elevated temperatures, J. Memb. Sci. 191 (2001) 85–94. doi:10.1016/S0376-7388(01)00452-5.

[132] M.-B. Hägg, Membrane purification of Cl 2 gas I. Permeabilities as a function of temperature for Cl 2 , O 2 , N 2 , H 2 in two types of PDMS membranes, J. Memb. Sci. 170 (2000) 173–190.

[133] E. V. Perez, K.J. Balkus, J.P. Ferraris, I.H. Musselman, Mixed-matrix membranes containing MOF-5 for gas separations, J. Memb. Sci. 328 (2009) 165–173. doi:10.1016/j.memsci.2008.12.006.

[134] S.R. Reijerkerk, M.H. Knoef, K. Nijmeijer, M. Wessling, Poly(ethylene glycol) and poly(dimethyl siloxane): Combining their advantages into efficient CO2 gas separation membranes, J. Memb. Sci. 352 (2010) 126–135. doi:10.1016/j.memsci.2010.02.008.

[135] C. Tsvigu, E. Pavesi, M.G. De Angelis, M.G. Baschetti, M.G. De Angelis, M. Giacinti Baschetti, Effect of relative humidity and temperature on the gas transport properties of 6FDA-6FpDA polyimide: Experimental study and modelling, J. Memb. Sci. 485 (2015) 60–68. doi:10.1016/j.memsci.2015.02.032.

[136] Z. Wang, A.A. Volinsky, N.D. Gallant, Crosslinking effect on polydimethylsiloxane elastic modulus measured by custom-built compression instrument, J. Appl. Polym. Sci. 41050 (2014) 1–4. doi:10.1002/app.41050.

[137] Q.T. Nguyen, Z. Bendjama, R. Cle, M. Saint, A. Cedex, Poly (dimethylsiloxane) crosslinked in di † erent conditions Part I . Sorption properties in water – ethyl acetate mixtures, (1999) 2761–2766.

[138] J. Kujawski, A. Rozicka, M. Bryjak, W. Kujawski, Pervaporative removal of acetone, butanol and ethanol from binary and multicomponent aqueous mixtures, Sep. Purif. Technol. 132 (2014) 422–429. doi:10.1016/j.seppur.2014.05.047.

[139] T.A. Weschenfelder, P. Lantin, M.C. Viegas, F. De Castilhos, A.D.P. Scheer, Concentration of aroma compounds from an industrial solution of soluble coffee by pervaporation process, J. Food Eng. 159 (2015) 57–65. doi:10.1016/j.jfoodeng.2015.03.018.

[140] M. She, S.T. Hwang, Concentration of dilute flavor compounds by pervaporation: Permeate pressure effect and boundary layer resistance modeling, J. Memb. Sci. 236 (2004) 193–202. doi:10.1016/j.memsci.2004.03.014.

[141] A. Hasanoğlu, Y. Salt, S. Keleşer, S. Özkan, S. Dinçer, Pervaporation separation of ethyl acetate-ethanol binary mixtures using polydimethylsiloxane membranes, Chem. Eng. Process. Process Intensif. 44 (2005) 375–381. doi:10.1016/j.cep.2004.06.001.

[142] G.M. Shi, H. Chen, Y.C. Jean, T.S. Chung, Sorption, swelling, and free volume of polybenzimidazole (PBI) and PBI/zeolitic imidazolate framework (ZIF-8) nano-composite membranes for pervaporation, Polym. (United Kingdom). 54 (2013) 774–783. doi:10.1016/j.polymer.2012.11.056.

[143] T. Schäfer, J.G. Crespo, Study and optimization of the hydrodynamic upstream conditions during recovery of a complex aroma profile by pervaporation, J. Memb. Sci. 301 (2007) 46–56. doi:10.1016/j.memsci.2007.05.034.

[144] R.W. Baker, J.G. Wijmans, A.L. Athayde, R. Daniels, J.H. Ly, M. Le, The effect of concentration polarization on the separation of volatile organic compounds from water by pervaporation, J. Membr. Sci. Sci. 137 (1997) 159–172. doi:10.1016/S0376-7388(97)00189-0.

[145] A.M. Urtiaga, E.D. Gorri, I. Ortiz, Modeling of the concentration-polarization e ff ects in a pervaporation cell with radial flow, Sep. Purif. Technol. 17 (1999) 41–51.

[146] P. Gómez, R. Aldaco, R. Ibáñez, I. Ortiz, Modeling of pervaporation processes controlled by concentration polarization, Comput. Chem. Eng. 31 (2007) 1326–1335. doi:10.1016/j.compchemeng.2006.11.008.

[147] C. Wilke, P. Chang, Correlations of diffusion coefficients in dilute solutions, AICHE J. 1 (1955) 264–270.

[148] C. Brazinha, V.D. Alves, R.M.C. Viegas, J.G. Crespo, Aroma recovery by integration of sweeping gas pervaporation and liquid absorption in membrane contactors, Sep. Purif. Technol. 70 (2009) 103–111. doi:10.1016/j.seppur.2009.08.018.

[149] C. Brazinha, J.G. Crespo, Aroma recovery from hydro alcoholic solutions by organophilic pervaporation: Modelling of fractionation by condensation, J. Memb. Sci. 341 (2009) 109–121. doi:10.1016/j.memsci.2009.05.045.

[150] T. Schäfer, A. Heintz, J.G. Crespo, Sorption of aroma compounds in poly(octylmethylsiloxane) (POMS), J. Memb. Sci. 254 (2005) 259–265. doi:10.1016/j.memsci.2004.12.047.

[151] P. Ii, L.P.B.M. Umr, U. De Rouen, M. Saint, A. Cedex, Poly (dimethylsiloxane) crosslinked in di † erent conditions, (2000) 395–400.

[152] K. Pilnacek, J.C. Jansen, P. Bernardo, G. Clarizia, F. Bazzarelli, F. Tasselli, Determination of mixed gas permeability of high free volume polymers using direct mass spectrometric analysis of the gas compositions, Procedia Eng. 44 (2012) 1027–1029. doi:10.1016/j.proeng.2012.08.664.

[153] P. Silva, S. Han, A.G. Livingston, Solvent transport in organic solvent nanofiltration membranes, J. Memb. Sci. 262 (2005) 49–59. doi:10.1016/j.memsci.2005.03.052.

[154] P. Schaetzel, C. Vauclair, Q.T. Nguyen, R. Bouzerar, A simplified solution-diffusion theory in pervaporation: The total solvent volume fraction model, J. Memb. Sci. 244 (2004) 117–127. doi:10.1016/j.memsci.2004.06.060.

[155] M.R. Shah, R.D. Noble, D.E. Clough, Analysis of transient permeation as a technique for determination of sorption and diffusion in supported membranes, J. Memb. Sci. 280 (2006) 452–460. doi:10.1016/j.memsci.2006.01.051.

[156] O. Vopička, V. Hynek, V. Rabová, Measuring the transient diffusion of vapor mixtures through dense membranes, J. Memb. Sci. 350 (2010) 217–225. doi:10.1016/j.memsci.2009.12.031.

[157] A. Mafi, A. Raisi, A. Aroujalian, Computational fluid dynamics modeling of mass transfer for aroma compounds recovery from aqueous solutions by hydrophobic pervaporation, J. Food Eng. 119 (2013) 46–55. doi:10.1016/j.jfoodeng.2013.04.031.

[158] M. Moheb Shahrestani, A. Moheb, M. Ghiaci, High performance dehydration of ethyl acetate/water mixture by pervaporation using NaA zeolite membrane synthesized by vacuum seeding method, Vacuum. 92 (2013) 70–76. doi:10.1016/j.vacuum.2012.11.019.

[159] A. Buekenhoudt, F. Bisignano, G. De Luca, P. Vandezande, M. Wouters, K. Verhulst, Unravelling the solvent flux behaviour of ceramic nanofiltration and ultrafiltration membranes, J. Memb. Sci. 439 (2013) 36–47. doi:10.1016/j.memsci.2013.03.032.

[160] G.M. Shi, T.S. Chung, Thin film composite membranes on ceramic for pervaporation dehydration of isopropanol, J. Memb. Sci. 448 (2013) 34–43. doi:10.1016/j.memsci.2013.07.049.

[161] S.K. Mah, S.P. Chai, T.Y. Wu, Dehydration of glycerin solution using pervaporation: HybSi and polydimethylsiloxane membranes, J. Memb. Sci. 450 (2014) 440–446. doi:10.1016/j.memsci.2013.09.048.

[162] Site of National Institute of Standards and Technology, (n.d.). http://webbook.nist.gov.

[163] D.H.R. W.J. Lyman, W.F. Reehl, Chemical Property Estimation Methods, McGraw-Hill Book Company, 1982.

[164] L. Shao, J. Samseth, M.B. Hägg, Crosslinking and stabilization of nanoparticle filled PMP nanocomposite membranes for gas separations, J. Memb. Sci. 326 (2009) 285–292.

doi:10.1016/j.memsci.2008.09.053.

[165] J.E. Bara, A.K. Kaminski, R.D. Noble, D.L. Gin, Influence of nanostructure on light gas separations in cross-linked lyotropic liquid crystal membranes, J. Memb. Sci. 288 (2007) 13–19. doi:10.1016/j.memsci.2006.09.023.

[166] C. Horch, S. Schlayer, F. Stallmach, High-pressure low-field 1H NMR relaxometry in nanoporous materials, J. Magn. Reson. 240 (2014) 24–33. doi:10.1016/j.jmr.2014.01.002.

[167] D. Yang, J. Li, Z. Jiang, L. Lu, X. Chen, Chitosan/TiO2 nanocomposite pervaporation membranes for ethanol dehydration, Chem. Eng. Sci. 64 (2009) 3130–3137. doi:10.1016/j.ces.2009.03.042.

[168] S. Claes, P. Vandezande, S. Mullens, M.K. Van Bael, F.H.J. Maurer, Free Volume Expansion of Poly [1- (trimethylsilyl) -1-propyne] Treated in Supercritical Carbon Dioxide As Revealed by Positron Annihilation Lifetime Spectroscopy, Macromolecules. 44 (2011) 2766–2772. doi:10.1021/ma1029345.

[169] P. Taveira, A. Mendes, C. Costa, On the determination of diffusivity and sorption coefficients using different time-lag models, J. Memb. Sci. 221 (2003). doi:10.1016/S0376-7388(03)00252-7.

8 APPENDIX – SUPPORTING INFORMATION

A1 Description of the time-lag concept

The diffusion coefficient of the gases in the membranes was determined by the well-known time lag procedure, based on the penetration theory, and the instrument shown in Figure 2.2. If a penetrant-free membrane is exposed to the penetrant at the feed side at t=0 and the penetrant concentration is kept very low at the permeate side, then the total amount of penetrant, Q_t, passing through the membrane in time t is given by [16]:

$$\frac{Q_t}{l \cdot c_i} = \frac{D \cdot t}{l^2} - \frac{1}{6} - \frac{2}{\pi^2} \sum_1^\infty \frac{(-1)^n}{n^2} \exp\left(- \frac{D \cdot n^2 \cdot \pi^2 \cdot t}{l^2} \right) \qquad \text{(A1. 1)}$$

in which c_i is the penetrant concentration at the membrane interface at the feed side, l is the membrane thickness [m] and D is the diffusion coefficient [$m^2\ s^{-1}$]. For the fixed volume / pressure increase setup in the present work, eq (A1.1)becomes:

$$p_t = \frac{RT \cdot A \cdot l}{V_P \cdot V_m} \cdot p_f \cdot S \left(\frac{D \cdot t}{l^2} - \frac{1}{6} - \frac{2}{\pi^2} \sum_1^\infty \frac{(-1)^n}{n^2} \exp\left(- \frac{D \cdot n^2 \cdot \pi^2 \cdot t}{l^2} \right) \right) \text{(A1. 2)}$$

in which p_t is the permeate [bar] pressure at time t [s], R is the universal gas constant [$8.314 \cdot 10^{-5}$ m^3 bar $mol^{-1} \cdot K^{-1}$], T is the absolute temperature [K], A is the exposed membrane area [m^2], V_P is the permeate volume [m^3], V_m is the molar volume of a gas at standard temperature and pressure [$22.41 \cdot 10^{-3}$ m^3_{STP} mol^{-1} at 0 °C and 1 atm], p_f is the feed pressure [bar] and S is the gas solubility [m^3_{STP} m^{-3} bar^{-1}]. At long times, the exponential term approaches to zero and eq. (A1.2) reduces to:

$$p_t = \frac{RT \cdot A \cdot l}{V_P \cdot V_m} \cdot p_f \cdot S \left(\frac{D \cdot t}{l^2} - \frac{1}{6} \right) = \frac{RT \cdot A}{V_P \cdot V_m} \cdot \frac{p_f \cdot S \cdot D}{l} \left(t - \frac{l^2}{6D} \right) \qquad \text{(A1. 3)}$$

Thus, at long times a plot of p_t versus time describes a straight line which, upon extrapolation, intersects the time axis at $t = l^2/6D$, defined as the time lag, Θ [s].

$$\Theta = \frac{l^2}{6D} \qquad \text{(A1. 4)}$$

With this equation, the diffusion coefficient can simply be obtained by time lag measurements if the membrane thickness is known. More complex systems require numerical methods or Laplace transformation to solve for the diffusion coefficient.[169] The permeability is determined from the steady state pressure increase rate:

$$P = \frac{V_P \cdot V_m \cdot l}{RT \cdot A \cdot p_f} \cdot \frac{dp}{dt} \qquad \text{(A1. 5)}$$

In practice, for species with very low permeabilities the starting pressure and the baseline slope may not be completely negligible. The latter may be caused for instance by the formation of minor cracks in these rather brittle perfluoropolymers under the pressure of the sealing rings in the membrane cell. In that case eq. (A1.2) and eq. (A1.3) must be redefined as:

$$p_t = p_0 + \left(dp/dt\right)_0 \cdot t + \frac{RT \cdot A \cdot l}{V_P \cdot V_m} \cdot p_f \cdot S\left(\frac{D \cdot t}{l^2} - \frac{1}{6} - \frac{2}{\pi^2}\sum_1^\infty \frac{(-1)^n}{n^2} \exp\left(-\frac{D \cdot n^2 \cdot \pi^2 \cdot t}{l^2}\right)\right) \qquad \text{(A1. 6)}$$

$$p_t = p_0 + \left(dp/dt\right)_0 \cdot t + \frac{RT \cdot A}{V_P \cdot V_m} \cdot \frac{p_f \cdot S \cdot D}{l}\left(t - \frac{l^2}{6D}\right) \qquad \text{(A1. 7)}$$

in which p_0 is the starting pressure [bar] and $(dp/dt)_0$ is the baseline slope [bar s^{-1}]. Similar to what was described above, the time lag is then given by the intercept between the extrapolated baseline curve (p_0 + t·$(dp/dt)_0$) and the steady state pressure increase curve. Thus, (A1.6) and eq. (A1.7) allows for the correct calculation of the solution, diffusion and permeability coefficients of any membrane, even in the case of minor defects, giving rise to some Knudsen-type diffusion and an apparent baseline drift.

Assuming the validity of the solution-diffusion model, the solubility can be determined indirectly by the simple relation:

$$S = \frac{P}{D} \qquad \text{(A1. 8)}$$

A2 Contribution of the tubes to the instrumental time lag

The flow regime is cylindrical tubes is determined by the Reynolds number, Re:

$$\mathrm{Re} = \frac{\rho_i \cdot v \cdot d}{\eta_i} \qquad (A2.\ 1)$$

Where ρi is the density of the fluid [kg m ^{3}], v is the linear velocity [m s ^{1}], d is the tube diameter [m] and ηi is the fluid viscosity [Pa s]. For Re < 2000, the flow regime is laminar and the pressure drop, dp/dx [Pa m ^{1}], is a function of the flow rate Qi [m3 s ^{1}].and given by:

$$\frac{dp}{dx} = 128\frac{\eta_i \cdot Q_i}{\pi \cdot d^4} \qquad (A2.\ 2)$$

1/4"

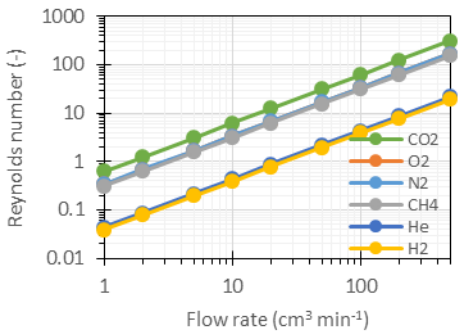

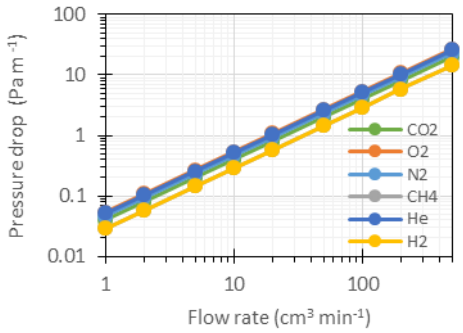

1/8"

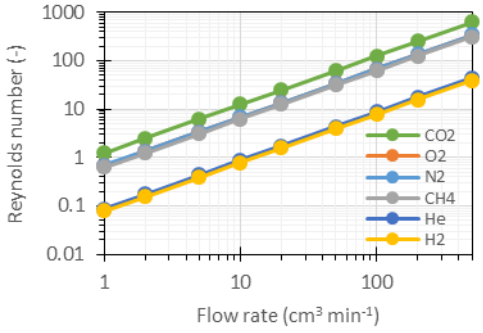

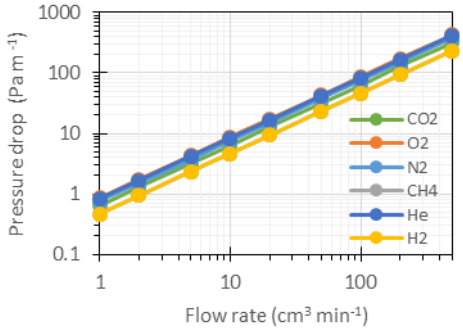

1/16”

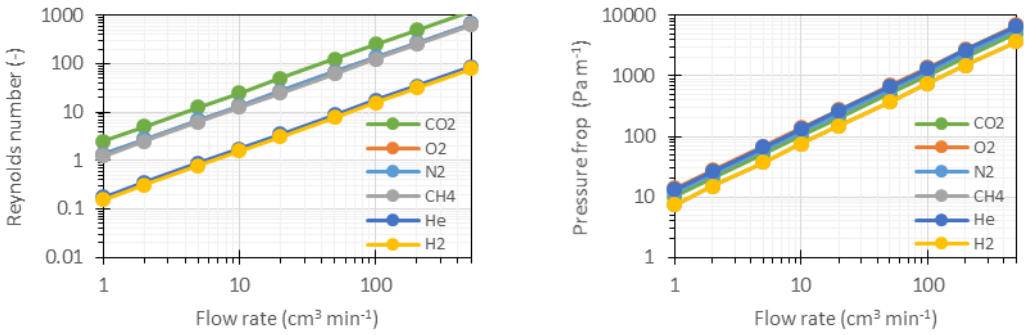

Figure A2. 1:Reynolds number (left) and pressure drop (right) in of tubes of different diameters for six light gases at typical flow rates in permeation experiments.

Under all conditions (Figure A2. 1), the Reynolds number remains below 2000, which means that the flow is always in the laminar regime. The pressure drop is similar for all gases and is always negligible (below 1 mbar m 1 = 100 Pa m 1) in tubes of 1/4", but it rapidly increases in smaller tubes, to ca. 100-200 Pa m 1 at 200 ml min 1 for 1/8” tubes and ca. 2000-3000 Pa m 1 at 200 ml min 1 for 1/16” tubes. At the typical flow rate for the Argon sweep gas (30-50 cm3 min 1), the average residence time in the order of 1-2 s m 1 in 1/16” tubes, and this time increases rapidly to 4-7 s m 1 in 1/8” tubes and 15-25 s m 1 in 1/4”tubes (Figure A2.2). This means that a suitable compromise must be sought between low pressure drop and acceptably low residence times, which do not contribute excessively to an instrumental time lag of the machine.

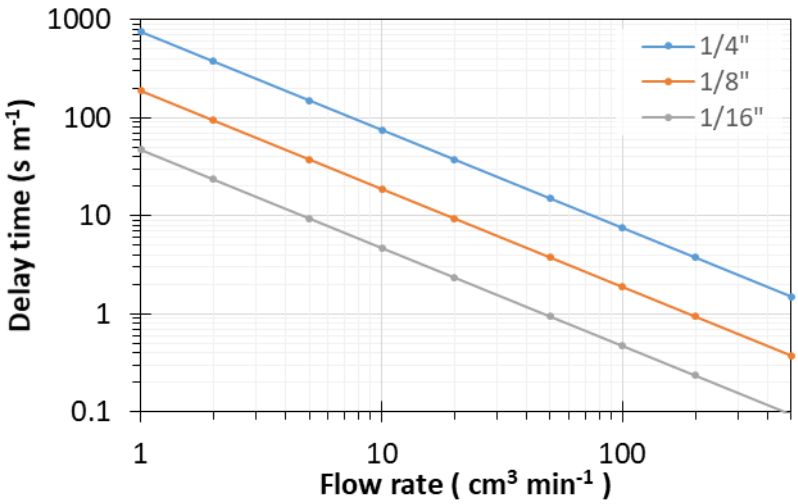

Figure A2.2: Approximate residence time of the gas as a function of the volumetric gas flow rate in tubes of different diameter.

Experimental analysis of the influence of the feed flow rate and the sweep flow rate in the system operated under sweeping gas conditions:

As discussed above and in section 2.4.1.1, each section of the instrument contributes to the overall time lag. An example of the importance of the individual contributions of the sweep flow in the setup with Argon sweep is shown in Figure A2.2. At the sweep flow rate of 30 cm^3 min 1, the downstream side of the setup contributes for approximately 6 seconds to the overall time lag. This contribution can be slightly reduced by setting the sweep flow rate higher, but this results in a lower permeate gas concentration. In any case, the sweep flow rate must be higher than the flow through the inlet capillary, which requires a minimum of approximately 11 cm^3 min 1 in the case of argon. As a compromise for optimum sensitivity and acceptably short residence times of the gas in the sweep line, the standard sweep flow rate is therefore set to 30 ml min 1.

A B

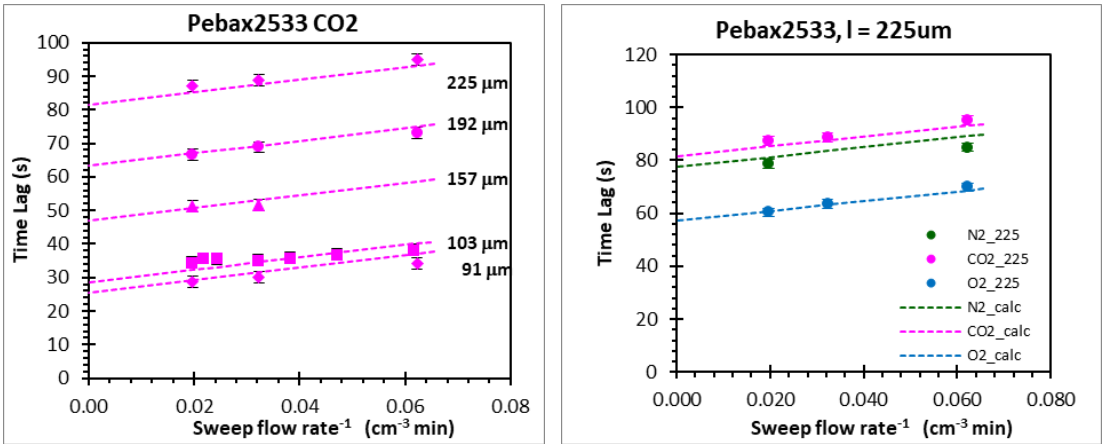

Figure A2.3: A) Typical examples of the dependence of the time lag on the reciprocal sweep flow rate 1/ϕSweep for CO2 in five membranes with different thickness, and B) the reciprocal sweep flow rate for the three gases in the 225 micron thick Pebax® 2533 membrane for the sweeping gas setup.

In contrast to the feed and sweep flow rates, which are set by the user, the gas flow entering the analyser, ϕ_{Inlet} , depends on the gas itself and on conditions of the instrument. It might decrease in time in the case of contamination of the capillary or of the molecular leak in the injection system. Thus, the instrumental time lag must be checked periodically. Since the inlet flow depends on the gas type, it is important to keep the composition of the gas to be analysed as constant as possible, i.e., the sweep flow rate should be much higher than the permeate flow rate.

The slope of the curves in Figure A2.2A and B corresponds to the dead volume of the permeate side. Simultaneous fitting of the data for different gases yields a volume of 2.2 cm3 for the feed side and 3.1 cm3 for the permeate side (Annex - A3). This means that at feed flow rate of 200 cm3 min^{-1} and a sweep flow rate of 30 cm3 min-1 they are responsible for 0.66 s and 6.1s of the instrumental time lag, respectively. This means that the remaining part of the instrumental time lag is due to the transport of the gas from the sampling point through the 6-valve port and the

capillary into the MS, which accounts for approximately 13 s and thus forms the largest contribution.

A3 Least squares fitting procedure with error analysis for simultaneous calculation of the diffusion coefficient from all measurements

Details of the method described in section 2.5.3.3 are as follows: for every given membrane with thickness *l*, and at a given feed flow rate ϕ_{Feed} and sweep flow rate ϕ_{Sweep}, the time lag was calculated as

$$\Theta_{i,calc} = \frac{V_{Feed,Fit}}{\phi_{Feed}} + \frac{V_{Perm,Fit}}{\phi_{Sweep}} + \left(\frac{V_{Inlet}}{\phi_{Inlet}}\right)_{Fit} + \frac{l^2}{6D_{i,Fit}} \qquad (A3.\ 1)$$

where $V_{Feed,Fit}$, $V_{Perm,Fit}$, $\left(\frac{V_{Inlet}}{\phi_{Inlet}}\right)_{Fit}$ and $D_{i,Fit}$ are estimated fit parameters. After a first estimation of these parameters, the sum of the squared error is calculated for all measurements *j (on a total of x)* and all gases *i* as:

$$\sum Err^2 = \sum_{j=1}^{x}\left(\sum_i \left(\Theta_{i,\mathrm{calc}} - \Theta_{i,\mathrm{exp}}\right)^2\right)_j \qquad (A3.\ 2)$$

Minimization of this term by a standard Excel routine gives the values for the time lag and the diffusion coefficient for all gases.

For a statistical analysis of the validity of this method, the absolute error, $\Delta\Theta_i$, in the determination of the time lag for each gas *i* in every measurement *j*, and the average absolute error for all measurements, $\delta\Theta_i$, were calculated as:

$$\Delta\Theta_i = \left|\Theta_{i,\mathrm{calc}} - \Theta_{i,\mathrm{exp}}\right| \qquad (A3.\ 3)$$

$$\delta\Theta_i = \frac{1}{n}\sum_{j=1}^{x}\sum_i \Delta\Theta_i = \frac{1}{n}\sum_{j=1}^{x}\sum_i \left|\Theta_{i,\mathrm{calc}} - \Theta_{i,\mathrm{exp}}\right|_j \qquad (A3.\ 4)$$

where *x* is the total number of analyses carried out and *n* is the total number of results. The standard error of the model (*i.e.* the standard error of the regression) for a line with slope and intercept, $\sigma\Theta_i$, is:

$$\sigma\Theta_i = \sqrt{\frac{1}{n-2}\sum Err^2} = \sqrt{\frac{1}{n-2}\sum_{j=1}^{x}\left(\sum_i \left(\Theta_{i,\text{calc}} - \Theta_{i,\text{exp}}\right)^2\right)_j} \qquad \text{(A3. 5)}$$

Where (n-2) represents the degrees of freedom of the model and 2 is the number of parameters (slope and intercept). For simultaneous fitting of multiple parameters, the degrees of freedom decrease accordingly. The correlation of the experimental and calculated data is shown in Figure A3. 1 The absolute average error in the time lag, $\delta\Theta_i$, calculated for Pebax® 2533 equals 1.36 s (standard error = 1.70 s) and for Hyflon® AD60X membranes it is 2.46 s (standard error = 3.13 s).

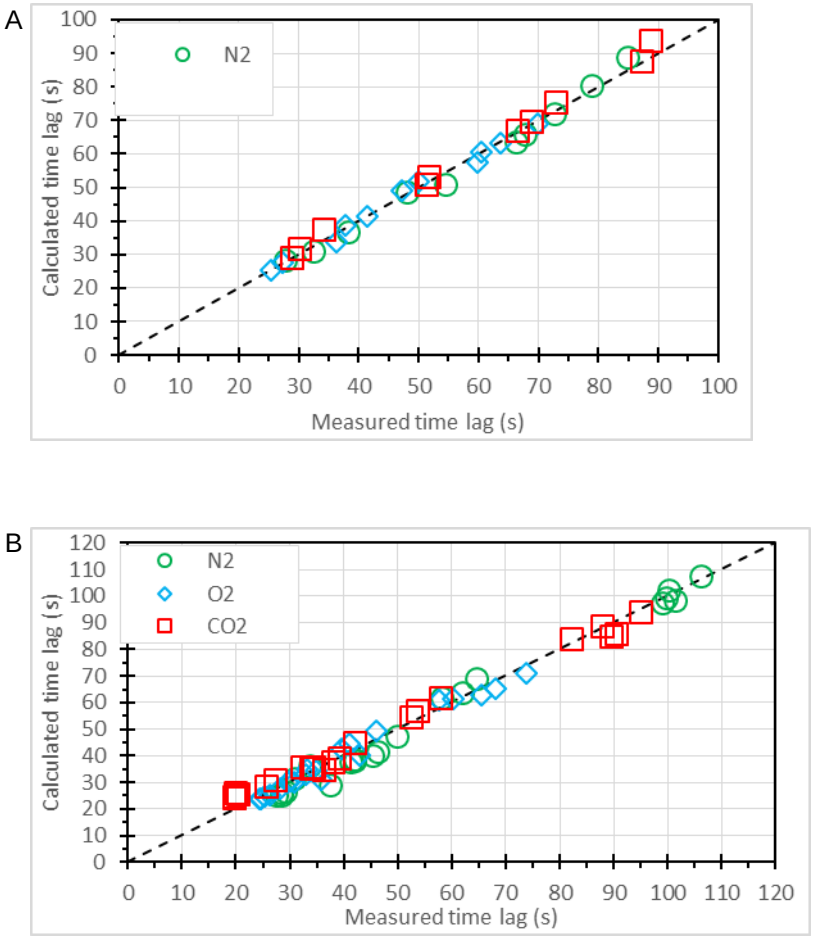

Figure A3. 1:Plot of the calculated time lag versus the experimental time lag for Pebax® 2533 (top) and for Hyflon® AD60X (bottom) for N2, O2 and CO2 in the mixture 80/10/10 vol%. The corresponding values of , were 1.46 s for Pebax®2533, and 2.46 s for Hyflon® AD60.

Given the average error in the instrumental time lag determined with the Pebax samples, the error in the determination of the diffusion coefficient becomes acceptably small if the membrane time lag is some tens of seconds or higher, resulting in less than 10% error in the analysis. The quantitative fitting parameters are given in Table A3. 1 and show that the dead volume at the permeate side of the membrane is approximately 3 cm^3, which contributes to approximately 6 seconds of the total instrumental time lag at 30 $cm^3\ min^{-1}$ sweep flow rate.

Pebax®2533			**Hyflon® AD60X**		
V_{perm_calc} =	3.03	cm^3	V_{perm_calc} =	2.72	cm^3
Θ_0 =	14.92	s	Θ_0 =	18.44	s
Θ_0 @ 30 $cm^3\ min^{-1}$ Ar =	20.99 ± 1.70*)	s	Θ_0 @ 30 $cm^3\ min^{-1}$ Ar =	23.88 ± 3.13*)	s
$D(O_2)$ =	199.0	$10^{-12}\ m^2\ s^{-1}$	$D(O_2)$ =	127.1	$10^{-12}\ m^2\ s^{-1}$
$D(N_2)$ =	135.7	$10^{-12}\ m^2\ s^{-1}$	$D(N_2)$ =	65.6	$10^{-12}\ m^2\ s^{-1}$
$D(CO_2)$ =	125.7	$10^{-12}\ m^2\ s^{-1}$	$D(CO_2)$ =	79.8	$10^{-12}\ m^2\ s^{-1}$

*) Standard error from calculated by Eq. (A.3.5)

Table A3. 1:Results of the simultaneous fitting procedure of the instrumental parameters and diffusion coefficients by the sweeping gas setup.

A4 MIXED CO2/CH4 PERMEATION IN THE MEMBRANE PIM-EA(ME)-TB

The figure below allows to see the kinetics cureves of different CO_2 composition in CH_4. As observed, the higher concentration of CH4 in the mixture composition, the higher time of the permeation process to achieve the stationarity (Θlag CH_4>Θlag CO_2).

Representing the results obtained in the Robbeson Plot, an increase in the real selectivity of $\alpha CO_2/CH_4$ can be observed when compared with the ideal selectivity. This result highlights the importance of using real values of permeabilities when mixed streams are used.

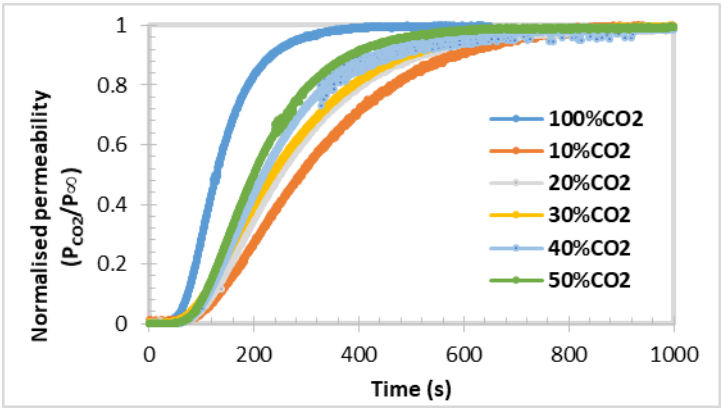

Figure A4. 1:Typical permeation curves of CO2 in the membrane PIM-EA(Me)-TB, showing normalized flux (Q_CO2/Q_∞) as a function of time for different CO2 concentrations in the CO2/CH4 mixture for the vacuum system.

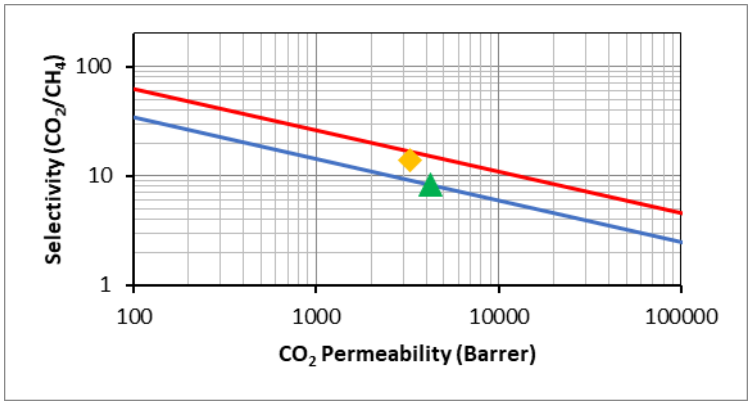

Figure A4. 2:Robeson of mixed gas CO2/CH4 in vacuum setup.

A5 Mathematical model to describe the concentration inside the membrane

The mathematical model aims at characterising the solute transport through dense membranes in the transient regime. The input of the model is the data obtained experimentally through mass spectrometry tool: flux, partial pressure and consequently diffusion coefficient over time. Using this data, the solute concentration profiles along the membrane thickness and at the downstream side were estimated. This information is essential to study the transient period and the changes that occurs in the membrane when in contact with different solutes, especially with high affinity to the membrane material.

A1.1. The analytical model

The following analytical model (equations (6.8) to (6.11) of the manuscript) describes the evolution of concentration c(x; t) inside the membrane at a point 0 < x< L and at time t > 0 during all the permeation process. The length of the membrane shall be denoted by L and the concentration, at a point x ∈ [0; L] and at time t ≥ 0, by c(x; t).

$$\frac{\partial c}{\partial t} - \frac{\partial}{\partial x}\left(D \frac{\partial c}{\partial x} \right) = 0 \qquad 0 < x < L \quad t > 0$$

$$c(x,0) = 0; \qquad 0 < x < L$$

$$c(0,t) = c_1(t) \qquad t > 0$$

$$-D(t)\frac{\partial c}{\partial x}(L,t) = J(t) \qquad t > 0 \qquad \text{(A5. 1)}$$

The second equation stands for the initial condition, which corresponds to zero concentration at all points in the membrane for $t = 0$. The last two equations are the boundary conditions. In the upstream side of the permeation process, the concentration is maintained constant since the feed solution does not change in terms of it composition during the process ($c_1(t)$) . The second

boundary condition, is associated with the flux which is permeating in the downstream surface of the membrane in each instant of time.

The data to the model

The flux J(t) is given by the experimental data following the equation at any time t ≥ 0 for the whole transient state:

$$J(t) = k_1 D(t)[k_2 - p(t)];\ t > 0 \qquad \text{(A5. 2)}$$

Where coefficients k_1 and k_2 are positive constants such that:

$$k_2 - p(t) > 0 \text{ for all } t \geq 0 \qquad \text{(A5. 3)}$$

The pressure, p(t), which is obtained experimentally through MS (Figure 3 of the manuscript), is automatically fit into a curve of the following form:

$$p(t) = B_p\left\{1 - e^{-C_p t} - \frac{D_p}{D_p + E_p}\left[1 + \frac{C_p e^{-(D_p + E_p)t} - (D_p - E_p)e^{-C_p t}}{(D_p - E_p) - C_p}\right]\right\};\ t \geq 0 \qquad \text{(A5. 4)}$$

where all the coefficients are equal or higher than zero. As a consequence, p(t) ≥0; for all t ≥ 0. We remark that $\lim_{t\to+\infty} p(t) = Bp \times Ep/(Dp + Ep)$.

The flux will also be given experimentally with the data obtained by the MS (equation 6.3 of the manuscript) and will be fit, into a curve of the same type (Figure 6.3), that is:

$$J(t) = B_f\left\{1 - e^{-C_f t} - \frac{D_f}{D_f + E_f}\left[1 + \frac{C_f e^{-(D_f + E_f)t} - (D_f - E_f)e^{-C_f t}}{(D_f - E_f) - C_f}\right]\right\};\ t \geq 0 \qquad \text{(A5. 5)}$$

where all the coefficients are non negative. As a consequence, J(t) ≥0; for all t ≥ 0. We remark that $\lim_{t\to+\infty} J(t) = Bf \times Ef/(Df + Ef)$.

From (A4.2), (A4.4) and (A4.5), the diffusion coefficient for each instant of time will be defined as:

$$D(t) = \frac{J(t)}{k_1[k_2 - p(t)]} \geq 0 \qquad t \geq 0 \qquad \text{(A5. 6)}$$

A1.2. Solution of the analytical model: Diffusion coefficient varying in the time

In order to solve (A5.1), we consider that the concentration c(x; t) is given as the sum of a transient (u) and of a quasi-stationary (r) components, that is:

$$c(x,t) = u(x,t) + r(x,t); \qquad 0 \le x \le L, \qquad t \ge 0 \tag{A5. 7}$$

The quasi-stationary component will be of the form r(x, t) = A(t) x + B(t) and will take care of the boundary conditions, that is, it has to verify:

$$r(0,t) = c_1(t) \qquad t > 0$$

$$-D(t)\frac{\partial r}{\partial x}(L,t) = J(t) \qquad t > 0 \tag{A5. 8}$$

As a consequence, it will be of the following form:

$$r(x,t) = -\frac{J(t)}{D(x)}x + c_1(t) = -k_1\left[k_2 - p(t)\right]x + c_1(t) \tag{A5. 9}$$

Since, from the data of the problem, the quasi-stationary component is known, it only remains to find the transient component u, which must solve the following problem, with homogeneous boundary conditions:

$$\frac{\partial u}{\partial t} - \frac{\partial}{\partial x}\left(D\frac{\partial u}{\partial x}\right) = -\frac{\partial r}{\partial t} \qquad 0 < x < L \qquad t > 0;$$

$$u(x,0) = -r(x,0) \qquad 0 < x < L;$$

$$u(0,t) = 0 \qquad t > 0;$$

$$-D(t)\frac{\partial u}{\partial x}(L,t) = 0 \qquad t > 0. \tag{A5. 10}$$

The solution of (A5.10) may be given by means of the Sturm-Liouville theory, combined with a Fourier series technique. The eigenvalues of the associated Sturm-Liouville problem, in the spatial variable, are of the form:

$$\lambda_n = \left[(2n-1)\frac{\pi}{2L}\right]^2; \quad n = 1,2,\ldots \tag{A5. 11}$$

The corresponding orthogonal set of eigenfunctions is given by:

$$\chi_n(x) = sin\left[(2n-1)\frac{\pi x}{2L}\right]; \quad 0 \le x \le L, \quad n = 1,2,\ldots \tag{A5. 12}$$

Therefore, the transient solution, u, governed by A5.10, is given by:

$$u(x,t) = \sum_{n=1}^{+\infty} T_n(t)\, sin\left[(2n-1)\frac{\pi x}{2L}\right] \qquad 0 \le x \le L, \quad t \ge 0, \; n = 1,2,\ldots \tag{A5. 13}$$

Where the functions Tn are the unique solutions of the following Cauchy type problems:

$$\frac{\partial T_n}{\partial t}(t) + \underbrace{\left[(2n+1)\frac{\pi}{2L}\right]^2}_{a_n(t)} D(t) T_n = -\frac{\partial r_n}{\partial t}(t) \quad t > 0$$

$$T_n(0) = -r_n(0) \tag{A5. 14}$$

And where functions r_n stand for Fourier coefficients of the quasi-stationary component are given by A5.9, that is:

$$r(x,t) = -\frac{J(t)}{D(t)}x + c_1(t) = \sum_{n=1}^{+\infty} r_n(t) \sin\left[(2n-1)\frac{\pi x}{2L}\right] \qquad 0 \le x \le L, \quad t \ge 0, \; n = 1,2,\ldots$$

With for t≥0 and n=1,2,… (A5. 15)

$$r(x,t) = \frac{2}{L}\left\{-\left[\frac{2L}{(2n-1)\pi}\right]^2 (-1)^n \left(-\frac{J(t)}{D(t)}\right) + \frac{2L}{(2n-1)\pi} c_1(t)\right\} = \varphi_n\left(-\frac{J(t)}{D(t)}\right) + \vartheta_n c_1(t) \tag{A5. 16}$$

Therefore, the solutions of the Cauchy problems (A5.14) are given by:

$$T_n(t) = e^{-\int_0^t \lambda_n D(s) ds}\left[T_n(0) + \int_0^t \left(-\frac{dr_n}{ds}(s)\right) e^{\int_0^s \lambda_n D(\xi) d\xi} ds\right]; \quad t \ge 0, \; n = 1,2,\ldots \tag{A5. 17}$$

The substitution of D(t) and of (A5.16) into these equations, leads to a closed form solution, rather complex in appearance, involving special functions and exponential integrals.

In order to solve the Cauchy type problems (A5.14) we shall consider a classical numerical implicit Euler scheme:

$$\frac{\partial T_n}{\partial t}(t) + \left[(2n-1)\frac{\pi}{2L}\right]^2 D(t) T_n = -\frac{\partial r_n}{\partial t}(t) \qquad t > 0$$

$$T_n(0) = -r_n(0) \tag{A4. 18}$$

Let $\Delta t \, \epsilon \, \mathbb{R}$ denote the time step and define $T_i = i\Delta t, (i = 0,1,..)$. Consider the first order approximation

$$\frac{\partial T_n}{\partial t}(t_i) \sim \frac{T_n(t_i) - T_n(t_{i-1})}{\Delta t}, i = 1,2,.. \quad \text{(A4. 19)}$$

Then the problem (A.14) is discretized as follows:

$$T_n(t_i) = \frac{1}{1 + \Delta T \, \lambda_n D(t_i)} [T_n(t_i) - \Delta T \, \dot{r}_n(t_i)], i = 1,2,... \quad \text{(A4. 20)}$$

$$T_n(0) = -r_n(0)$$

for all n=1,2,…and where

$$\dot{r_n}(t) = \varphi_n k_1 \dot{p}(t) = \varphi_n k_1 \, B_p \left\{ C_p e^{-C_p t} - \frac{D_p C_p}{D_p + E_p - C_p} \left[e^{-C_p t} - e^{-(D_p + E_p)t} \right] \right\} \quad \text{(A4. 21)}$$

A1.3. The Analytical Solution for a constant diffusion coefficient

The model was also developed for a constant concentration $c(0,t)$ and diffusion coefficient to compare the concentration inside the membrane when using the steady state and the time-dependent diffusion coefficient (see figure 6a and 6b).

$$D(t) = d \in \mathbb{R}^+, c(0,t) = c_1 \in \mathbb{R}^+, \; t \geq 0, \quad \text{(A4. 22)}$$

the integrals, in equation (A.19), simplify and one gets, for t ≥ 0 and all n=1,2,…

$$T_n(t) = [\varphi_n k_1 k_2 - \vartheta_n c_1] e^{-a_n t} + \varphi_n k_1 B_p \frac{C_p (C_p - E_p)}{(a_n - C_p)(D_p + E_p - C_p)} e^{-C_p t} -$$

$$\varphi_n k_1 B_p \frac{D_p C_p}{(a_n - (D_p + E_p))(D_p + E_p - C_p)} e^{-(D_p + E_p)t} + \varphi_n k_1 B_p \frac{C_p (a_n - E_p)}{(a_n - C_p)[a_n - (D_p + E_p)]} e^{-a_n t}.$$

Where $a_n = \lambda_n d$ (A4. 22)